HYDROLOGIC BEHAVIOR OF A FORESTED MOUNTAIN SLOPE IN COASTAL BRITISH COLUMBIA

by

EVELYN TISCHER

B.Sc. (Meteorology), McGill University, 1974

M.Sc. (Meterology), Reading University (U.K.), 1975

A THESIS SUBMITTED IN PARTIAL FULFILLMENT OF THE

REQUIREMENTS FOR THE DEGREE OF

MASTER OF SCIENCE

in

THE FACULTY OF GRADUATE STUDIES

(INTERDISCIPLINARY STUDIES)

We accept this thesis as conforming

to the required standard

THE UNIVERSITY OF BRITISH COLUMBIA

In presenting this thesis in partial fulfilment of the requirements for an advanced degree at the University of British Columbia, I agree that the Library shall make it freely available for reference and study. I further agree that permission for extensive copying of this thesis for scholarly purposes may be granted by the head of my department or by his or her representatives. It is understood that copying or publication of this thesis for financial gain shall not be allowed without my written permission.

Department of Soil Science

The University of British Columbia
1956 Main Mall
Vancouver, Canada
V6T 1Y3

Date September 20, 1986

ABSTRACT

This is a study of the hydrologic behavior of a forested west coast mountain slope soil.

Flow mechanisms were investigated using experimental results, mainly outflow hydrographs, and a simple model of saturated flow over a steep bed, described in the second chapter and called the kinematic wave model.

The main experiments consisted of subjecting the forest plot to both concentrated and uniform irrigation. The rationale for using concentrated irrigation was that it was expected it would enhance flow in low resistance paths or as fingers in the unsaturated zone, also called short-circuiting.

It was concluded that the soil-water system behaves as if short-circuiting were not enhanced by concentration of irrigation.

The fact that both the observed hydrograph and the kinematic wave model hydrograph display a straight line rise was the rationale for using the kinematic wave model. It indicates that the system behaves as if the kinematic wave model were valid. Readily verified assumptions are a steep bed slope and a high hydraulic conductivity due to concentration of low resistance paths on top of the bed.

As for other assumptions, it can only be said that the system behaves as if they were satisfied. In particular it behaves as if no short-circuiting occurred.

Using the kinematic wave model, an effective hydraulic conductivity of 1.6×10^{-4} to 3.2×10^{-4} ms^{-1} was obtained for the saturated zone.

Finally, it was shown that nonlinear flow, if it occurs at all, is probably uncommon in the unsaturated zone of the Forest plot and its vicinity. It is not certain whether it can occur in the saturated zone of the Forest plot.

TABLE OF CONTENTS

Page

LIST OF TABLES

LIST OF FIGURES

LIST OF SYMBOLS

Note: Units given indicate the dimensions. They are not always the units used for the given symbol. For instance, mm are sometimes used in place of m.

a	Constant determined by the properties of the fluid and of the porous medium (or possibly of the porous medium only), appearing in Forchheimer's equation (Eq. 3.2.1). $(s^2\ m^{-3})$
a'	$a' = ga$. (m^{-2})
a_d	Constant determined by the properties of the porous medium and of the fluid (or possibly of the porous medium only), appearing in Eq. I-1. (m^{-2})
b	Constant determined by the properties of the fluid and of the porous medium (or possibly of the porous medium only), appearing in Forchheimer's equation (Eq. 3.2.1.). $(s^2\ m^{-2})$
b'	$b' = \frac{\rho g}{\mu} b$. (sm^{-3})
C	A constant in a friction factor definition (ms^{-2}). See Eq. 3.3.6.
c	Wave velocity in the kinematic wave model. (ms^{-1}) $c = \frac{dx}{dt}$.
c_{re}	Wave velocity during the recession. (ms^{-1})
c_{ri}	Wave velocity during the rise. (ms^{-1})

D	Width of the hillslope. For the Forest plot it is taken as the length of the channel measured perpendicular to the slope. (m)
d	Some measurement related to the size of the pores. (m)
e	Constant determined by the properties of the porous medium and of the fluid (or possibly of the porous medium only), appearing in Eq. I-1. (Dimensionless)
f	Friction factor. See Eqs. 3.3.6, 3.3.8 and 3.3.9 for definitions. (Dimensionless)
g	Gravitational acceleration. (ms^{-2})
h	Hydraulic head. (m)
$\frac{dh}{ds}$ or $\frac{dh}{dx}$	Rate of change of h with s or x. Since in the present work, q is in the main flow direction and the porous media are considered to be isotropic and homogenous, $\frac{dh}{ds}$ or $\frac{dh}{dx}$ is the (macroscopic) hydraulic gradient. It is not clear whether homogeneity is actually required for $\frac{dh}{ds}$ or $\frac{dh}{dx}$ to be the macroscopic hydraulic gradient. (Dimensionless).
i	Recharge rate per unit area parallel to the bed. Can vary with time and be zero. (ms^{-1})
i_o	Recharge rate per unit area parallel to the bed during rise and steady state. i_o is a constant. (ms^{-1})
K	Satiated hydraulic conductivity. Will be referred to as hydraulic conductivity for simplicity. Satiated hydraulic conductivity is defined in Section 1.2. (ms^{-1})
K_{eff}	Effective hydraulic conductivity obtained by the kinematic wave model. See eq. 2.4.1. (ms^{-1})

K_{gen} General conductivity (ms^{-1}). The term is used for both the linear and nonlinear range and K_{gen} depends on q.

$$K_{gen} = q \left(\frac{dh}{ds}\right)^{-1}$$

k Permeability (m^2). k is defined by

$$K = \frac{k\rho g}{\mu}.$$

L Length of the saturated zone. (m)

L_{ch} A characteristic (or representative) length. (m). When a number is given for the Reynolds number characterizing flow in a porous medium, the diameter of the particles forming the porous medium will be used for L.

n Effective porosity ($m^3\ m^{-3}$). See Appendix G for definition.

n_a Porosity ($m^3\ m^{-3}$). See Appendix G for details.

n_{re} Effective porosity for the recession. ($m^3\ m^{-3}$)

n_{ri} Effective porosity during the rise. ($m^3\ m^{-3}$)

Q Outflow rate or discharge (volume per unit time). ($m^3\ s^{-1}$)

q Discharge per unit area or macroscopic flow velocity (ms^{-1}). In the present work, q is in the main flow direction.

q_{cr} Critical macroscopic flow velocity, that is, the velocity at which flow becomes nonlinear. (ms^{-1})

r Impermeability. (m^{-2}) The r used by de Vries (1979) is defined by

$$r \equiv \frac{\rho g}{\mu} \frac{\frac{dh}{ds}}{q}$$

R_{ap} Time average pooled irrigation rate. (ms^{-1})

R_p Pooled irrigation rate (ms^{-1})

Re — Reynolds number (Dimensionless).

In the present work, the following definition is used unless otherwise specified:

$$Re = \frac{v_{ch} L_{ch}}{\nu}$$

Re_{cr} — Critical Reynolds number (Dimensionless). It is the Reynolds number at which flow becomes nonlinar. For the discussion of the behavior of the f versus Re relationships, Re_{cr} has been defined as $Re_{cr} = \frac{q_{cr} d}{\nu}$

s — Distance (m)

T — Thickness of the saturated zone (measured perpendicular to the bed). (m)

T_o — Saturated zone thickness seen by the observer at x_o and t_o (m). Used in the solution of the kinematic wave equation by the method of characteristics, Note 1, Appendix H.

t — Time. (s)

t' — Time from start of recession. (s)

t* — Time from start of the recharge. (s)

t_o — Time at which the observer left from x_o (measured from the start of recharge) (s). Used in the solution of the kinematic wave equation by the method of characteristics, Note 1, Appendix H.

t_r — Time at which recharge stopped. (s)

v_{ch} — A characteristic flow velocity, generally taken to be q.

x — Downslope distance from the highest point on the bed where recharge occurs. (m)

x_o	An observer leaves from $x = x_o$. x_o is used in the solution of the kinematic wave equation.
z	Axis perpendicular to the bed and upward (along T; see Fig. 2.3.1.).
α_{lin}	$\alpha_{lin} = \frac{1}{\nu K}$. $(s^2\ m^{-3})$
α_{nonlin}	$\alpha_{nonlin} = a$. $(s^2\ m^{-3})$
β_o	$\beta_o = b$. $(s^2\ m^{-2})$
ε_1, ε_2	Variable coefficients of q and q^2 respectively in the extension of Forchheimer's equation, eq. 3.2.7. ε_1 has units sm^{-1}, ε_2 has units $s^2\ m^{-2}$.
θ	Soil water content. $(m^3\ m^{-3})$
θ_{in}	Soil water content measured by the neutron probe before the start of irrigation. $(m^3\ m^{-3})$
$\theta_{in\ s.z.}$	Water content of the soil just before the water table rises in it. $(m^3\ m^{-3})$. Used to calculate K_{eff} by the kinematic wave model.
$\theta_{st.st.}$	Soil water content measured by the neutron probe during steady state. $(m^3\ m^{-3})$. Used to calculate K_{eff} by the kinematic wave model.
μ	Dynamic viscosity of the fluid. $(kg\ s^{-1}\ m^{-1})$
ν	Kinematic viscocity of the fluid. $(m^2\ s^{-1})$ $\nu = \frac{\mu}{\rho}$.
ρ	Fluid density. $(kg\ m^{-3})$
ψ	Pressure head. (m)
ω	Angle that the bed makes with the horizontal. (Degrees)

ACKNOWLEDGEMENTS

I wish to thank my supervisor, Dr. Jan de Vries, for guidance, assistance and friendship. Dr. de Vries provided many of the ideas found in this thesis and helped greatly with fieldwork.

Thanks are also due to the members of my committee, Drs. O. Slaymaker, A. Freeze and M. Quick for advice and suggestions. Dr. Quick's assistance with a number of technical problems was especially appreciated.

I am very grateful to Dr. T.A. Black whose door was always open when I was in need of help or encouragement.

Encouragement from my colleagues, Messrs Compton Paul, John Heinonen, Trevor Murrie and Mensah Bonsu, and from T.D. Nguyen has been a great help during the completion of this thesis.

I also wish to thank Jeeva Jonahs for patient and expert typing.

Finally, thanks are expressed to the Natural Science and Engineering Research Council for a research assistantship and to the University of British Columbia for a Killam pre-doctoral fellowship.

INTRODUCTION

The purpose of this work is to shed some light on the hydrologic behavior of an open and permeable forested mountain slope soil such as is found in the University of British Columbia Research Forest. A major feature of this soil is the presence of low resistance paths due to root material. Special emphasis will be placed on these features in relation to the shape of the outflow hydrograph.

One hypothesis of the present work is that fast flow occurring in the unsaturated zone is due to the combination of the existence of low resistance paths and of concentrating elements found at or above the soil surface, as suggested by Whipkey (1968) and de Vries and Chow (1978). In order to test this hypothesis, experimental data obtained from uniform and concentrated irrigation were compared.

In the first chapter, the results of three experiments conducted on a small hillslope plot in the University of British Columbia Research Forest are discussed. The experiments consisted of irrigating the plot and monitoring the outflow rate, the height of the water table and the soil water content. For the second experiment, plastic sheets were laid on the ground in order to concentrate the irrigation. Experimental results, mainly the outflow hydrograph, will be used to infer flow mechanisms both in the unsaturated and the saturated zones. One tool used for this purpose will be a model for saturated flow over a steep bed which will be called kinematic wave model and presented in Chapter II. The conclusions drawn will lead to a descriptive flow model.

In the second chapter, the kinematic wave model will be presented. While recognizing that the term "kinematic wave model" may be used for a multitude of models using a kinematic wave equation, in the present work, the term will denote exclusively the model presented in Chapter II. The kinematic wave model will be used to calculate an effective hydraulic conductivity for the saturated zone of the plot.

A search of the literature showed that this is the first time the kinematic wave model has been used as a tool to infer flow mechanisms and to obtain an effective hydraulic conductivity from the outflow hydrograph.

A major assumption of the kinematic wave model is the presence of a thin saturated zone which represents a water table approximately parallel to the bed. One of the requirements for a thin saturated zone is fast flow. If however, flow is so fast that it is nonlinear, the kinematic wave model fails due to failure of Darcy's law.

In this respect Chapter III starts where Chapter II ends since nonlinear flow is the topic of Chapter III. In Chapter III, a brief theoretical discussion based on the literature is offerred. Then, using experimental results obtained by de Vries (1979), the possibilities of nonlinear flow in both the unsaturated and the saturated zones are investigated.

CHAPTER I

THE INFERENCE OF FLOW MECHANISMS FROM THE OUTFLOW HYDROGRAPH

1.1 Introduction

The shape of the outflow hydrograph for a hillslope in part depends on the integrated effect of the travel of infiltrated rainwater from the ground surface to the stream bank. While it is not possible to infer every detail about flow mechanisms and pathways from the outflow hydrograph, some salient features of underground flow can affect the outflow hydrograph in a noticeable manner. Indeed, Nagpal and de Vries (1976) state that "one of the objectives of research in soil hydrology is to obtain a better understanding of the relationship between rainstorm characteristics, soil hydrologic behavior, and streamflow characteristics." Also, Chamberlin (1972), in a qualitative fashion, relates stream behavior to the nature of the soil when he states "an open soil explains the very flashy response of coastal streams to precipitation events."

Thus, the focus of this chapter is the inference of water flow mechanisms from the outflow hydrographs measured for an experimental plot located on a mountain slope. This plot is situated in the University of British Columbia Research Forest (hereafter called the Forest for simplicity).

At most locations in the Forest, a permeable and open B horizon rests on a bed of compacted and therefore slowly permeable till. One meter is a representative depth for the B horizon.

A major soil feature contributing to the open and permeable nature of the B horizon of the Forest soil is the presence of low resistance paths. Some low resistance paths found in the B horizon are long and continuous. They will be called pipelike low resistance paths, even though they do not necessarily have a cylindrical shape. Pipelike low resistance paths are due mainly to root material. Other low resistance paths are short and are associated with the presence of stones.

In low resistance paths, water moves at zero or near zero pressure head. A number cannot be assigned to the pressure, especially because some of the pipelike low resistance paths are filled with a high conductivity organic material.

The rapid flow of water in these paths, by-passing the soil matrix in the unsaturated zone, is called short-circuiting. Finger flow will be included in the term. One of the hypotheses that will be tested in this chapter is that short-circuiting is an important mechanism of water flow in the Forest soil. Finger flow is discussed in Section 1.2, point (iii).

Low resistance paths at the interface between the B horizon and the bed contribute to quick saturated flow parallel to the bed.

A particular subject of investigation was flow in low resistance paths within the unsaturated zone. Water cannot enter a low resistance path unless it is at a near zero pressure head. It is thus expected that an increased supply of free water would facilitate flow of water in low resistance paths. This hypothesis was tested by concentrating irrigation water and determining whether concentration had any effect on the behavior of the water table and on the shape of the outflow

hydrograph. Concentration was achieved by laying plastic sheets on the ground. The rationale for supplying free water in this fashion was the fact that Whipkey (1968) and de Vries and Chow (1978) observed that free water is supplied by natural concentrating elements such as the tree canopy and logs.

The experimental plot was located in the UBC Research Forest. It was equipped with standpipes and irrigated with sprinklers. A channel was dug at the bottom of the plot and outflow was measured using a tipping bucket.

The site was irrigated three times during the summer of 1979. Each irrigation lasted three days. These three experiments will be denoted by EX1, EX2 and EX3. For Ex2, plastic sheets were laid on the ground.

In the present chapter, the outflow hydrograph is used to infer flow mechanisms in both the unsaturated and the saturated zones. Direct observation of the hydrograph is one approach that will be used in order to achieve this goal. Another approach that will be used is the comparison of the observed hydrograph with the hydrograph obtained by the kinematic wave model presented in Chapter II. Visual observation of flow and of the soil will be used to complement conclusions.

1.2 Literature Review

In this section, previous work on the concept of relating the shape of the hydrograph to flow mechanisms will be presented. Beven's (1982) model will be briefly discussed because it integrates a model of flow in the saturated zone, similar to the one used for the present work, with a

model of flow in the unsaturated zone. Finally, literature on nonuniform flow, and in particular on flow in low resistance paths will be reviewed.

(i) Linking the Hydrograph Shape to Basin Properties and Flow Mechanisms

An early example of attempts to link physical characteristics of a watershed to geometric aspects of the unit hydrograph is the synthetic unit hydrograph (see for example Gray, 1970). In unit hydrograph synthesis, the shape of the unit hydrograph is obtained from physical characteristics of the watershed like the length of the main stream.

In certain cases, authors have associated the shape of the hydrograph with flow processes. A number of authors have interpreted the shape of the recession curve in terms of physical processes involved.

According to Anderson and Burt (1980), Barnes (1939) was able to distinguish between the parts of the recession due to overland flow, subsurface stormflow and baseflow by plotting the outflow hydrograph on semilogarithmic graph paper. The same authors mention that using the recession curve, Ineson and Downing (1964) subdivided baseflow recession into discharge from areas close to the stream and discharge from areas further away from the stream. Finally, Hewlett and Hibbert (1963) associated the first major limb observed for the recession on a double logarithmic graph with saturated flow and the second with unsaturated flow. This interpretation was substantiated by piezometers and tensiometers readings.

However, Anderson and Burt caution that changes in the shape of the recession curves can be due to the method of plotting and thus be spurious. They also caution that changes in physical processes may not necessarily show in recession curves. They conclude that "runoff processes generating recession flow cannot be inferred from graphical plotting techniques."

Dunne and Black (1970) inferred the importance of channel precipitation by noticing how sensitive the outflow hydrograph was to fluctuations in rainfall intensity and by comparing the observed outflow volume with the amount of precipitation falling onto the stream's channel.

In a site close to the one chosen for the present study, and situated on the same hillslope, Nagpal and de Vries (1976) connected the sharp rise of the hydrograph with start of outflow from root channel outlets along the streambanks. For further reference, the site used by these authors will be called "Nagpal and de Vries' site."

(ii) Beven's (1982) Model: A Simple Physically Based Model for Unsaturated and Saturated Flow in Soil Over a Steeply Sloping Bed

Beven (1982) obtained a simple flow model by coupling flow in the unsaturated zone with flow in the saturated zone. The model of flow for the saturated zone is similar to the kinematic wave model presented in Chapter II and which is used in the present chapter, except that in Beven's (1982) work, the satiated hydraulic conductivity and the

porosity decrease with depth. The term "satiated hydraulic conductivity, used by Miller and Bresler (1977) designates the proportionality factor between the flow velocity and the hydraulic gradient in Darcy's law (Eq. 1.3.1.1), under conditions such that the porous medium has the highest possible water content given entrapped air. It will often be referred to as hydraulic conductivity for simplicity. Beven (1982) also compares the outflow hydrograph thus obtained with the outflow hydrograph obtained experimentally by Weyman (1970, 1973) for a slope segment. He states that the model reproduces the observed hydrograph very well. In Section 1.5.3, Beven's work will be discussed in relation to the present work.

(iii) Nonuniform Flow

Two kinds of nonuniform flow have been observed by various authors: finger flow and flow in low resistance paths.

Whereas finger flow is confined to the unsaturated zone, flow in low resistance paths can occur in both the saturated and unsaturated zones.

The term "short-circuiting" was introduced by Bouma and Dekker (1978) to describe flow occurring through vertical interpedal voids (> 2 mm) in a clay soil, thus bypassing the soil matrix. In the present work, the term will be extended to include finger flow in addition to flow in low resistance paths within the unsaturated zone. The reason for doing so is that finger flow, although it does occur within the soil matrix, is concentrated in such a way that it bypasses a significant part of the matrix.

The term "finger" was used by Hill and Parlange (1972) to describe concentrated flow in sands as a result of wetting front instability. In the present work, fingers will be due to concentrated inflow, not to wetting front instability. Fingers are approximately cylindrical regions of concentrated infiltration originating from a point source of water. The water content within fingers is much higher than at locations where uniform infiltration occurs. In fact, soil within a finger may be saturated.

When irrigation occurs as point irrigation, fingers may occur. Smith (1967) observed infiltration in sand due to a point source. He obtained "filaments" or fingers of water formed in an initially dry sand by drops of water applied to the soil surface with a burette.

A finger can in some way be considered as a low resistance path that water created for itself since a higher water content means a higher hydraulic conductivity. For clarity, the term "low resistance path" will, however, be used only in the sense of a structural feature.

An extensive literature review of flow in low resistance paths is found in Beven and Germann (1980). It is interesting to note that the earliest reference on low resistance paths they quote is more than one century old; Schumacher (1864) states that "the permeability of a soil during infiltration is mainly controlled by big pores. . . ."

Both Whipkey (1968) and Aubertin (1971) conducted experiments in plots of coarse textured and of medium to fine textured soil in the Allegheny Plateau (USA). Low resistance paths were "roots, root channels, small animal and earthworm burrows, and structural cracks" (Whipkey, 1968). Their results agree on several points, namely:

i. flow in low resistance paths is more important in the medium to fine textured soil that in the coarse textured soil.

ii. outflow from a uniformly wetted zone is more important in the coarse textured soil.

iii. outflow from the medium to fine textured soil occurs earlier.

iv. the soil matrix in the case of the medium to fine textured soil wets little and/or late. Also, from Whipkey's results, outflow from medium to fine textured soil ends much earlier.

As Whipkey (1968) pointed out, all these results are consistent with flow in low resistance paths occurring in the medium to fine textured soil but not in the coarse textured soil. One reason may be that in the finer material it is easier to obtain free water due to the low conductivity of the soil matrix. (Water must be at zero or low pressure head in order to enter low resistance paths since these have a zero or low water entry pressure head.) Both Aubertin and Whipkey suggest that water concentrates on top of the mineral surface and enters low resistance paths there.

Beasley (1976) also observed flow in low resistance paths (decayed roots) in a forested region in northern Mississipi. In addition to visual observations, evidence was offered by

i. A subsurface flow velocity estimated to be 9.3×10^{-3} ms^{-1}.

ii. "Timing of subsurface flow peaks (. . .) unrelated to antecedent soil moisture". From Beasley's findings, it appears that flow in low resistance paths probably occurred within the unsaturated zone.

Chamberlin (1972) studied water flow in a forested area in the Seymour watershed near Vancouver. There was extensive root development and the average soil depth was 1 m. He also obtained some evidence of flow in root channels in both the unsaturated and the saturated zones. Evidence was

i. For the saturated zone:

   - A hydraulic conductivity of 9.7×10^{-5} ms^{-1}.

ii. For the unsaturated zone:

   - Tensiometers located at a depth of 1 m sometimes responded before tensiometers at a depth of 0.70 m.
   - Tensiometers at 0.70 m and at 1 m responded either very slowly or very rapidly.

   Note however that flow may have occurred along the tensiometer access tubes, invalidating the data.

de Vries and Chow (1978), in a plot located in the Seymour watershed (Greater Vancouver Water District) noticed irregular patterns of pressure head during irrigation of a forest soil equipped with tensiometers. These authors suggest that these patterns are due to flow through root channels. The patterns could also be due to localized hydrophobicity.

In their site Nagpal and de Vries (1976) noticed flow out of root channels at the streambank. In particular, they calculated a Reynold's number larger than 2000 for flow out of one root channel. They point out that "assuming the nature of flow in the rootchannel to be similar to that in a pipe", this number indicates "the existence of turbulent flow conditions within the rootchannel."

Mosley (1979), in a beech-podocarp-hardwood forest in New Zealand observed various low resistance paths.

Among the works discussed above, the one that offers the strongest evidence that flow in low resistance paths can occur within the unsaturated zone is the work of Whipkey. The difference between time to outflow in the medium to fine textured soil and in the coarse textured soil is so large that in the medium to fine textured soil the flow must have occurred in low resistance paths throughout the major part of its travel in the soil. At least part of the flow in low resistance paths must have occurred in the unsaturated zone.

A high hydraulic conductivity layer within the soil profile can be another kind of low resistance path. Mosley observed flow of dyes in the forest mentioned earlier. At some places, he observed that "a large proportion [of the dye] runs downslope above the surface of the A-horizon [which is the top of the mineral soil] and within its top 1-2 cm, which is more loosely aggregated and more porous than the rest of the mineral soil."

Utting (1978), in Nagpal and de Vries' site noted the presence of a rootmat on top of the till and root channels in the B horizon. He stated these organic zones to have a very high satiated hydraulic conductivity.

Natural pipes are a form of low resistance paths observed by Pond (1971). According to Atkinson (1978), Pond (1971) reported that in the grass-covered Nant Gerig watershed (U.K.), natural pipes were located less than 0.30 m below the surface. Water flowing in pipes could be

heard gurgling beneath the surface after a storm. A natural pipe in the technical sense is formed by "piping", a "process of continued backward erosion" (Sowers and Sowers, 1970). It is not certain if the pipes referred to by Atkinson have been formed by this process. Atkinson also stated that "the hydrographs from upland pipes are often flashy."

In the Seymour watershed (near Vancouver, B.C.), Chamberlin (1972) noticed "small (. . .) ephemeral channels (. . .), controlled by bedrock morphology, large trees, and rock outcrops." He noted that these channels were "at times exposed and at times underground."

1.3 Material and Methods

1.3.1 Site Description

Figure 1.3.1.1 shows the experimental plot with the location of the instruments set-up. The plot (49° 18' N, 122° 35'W) was located in the University of British Columbia Research Forest which is 45 km east of Vancouver, B.C., Canada. It is about 350 m above sea level.

The climate is Pacific Marine Humid with 2 to 3 m of precipitation annually. More than 85% of the precipitation occurs as rain. Vegetation consists of mature western hemlock, balsam fir, Douglas-fir, and red cedar.

The average slope of the plot is 30°. The plot area is 50 m^2. The soil is a humo-ferric podzol. The B horizon is underlain partly by compacted till and partly by bedrock. This low conductivity layer forms the bed. The forest floor depth varies between 0.05 and 0.20 m.

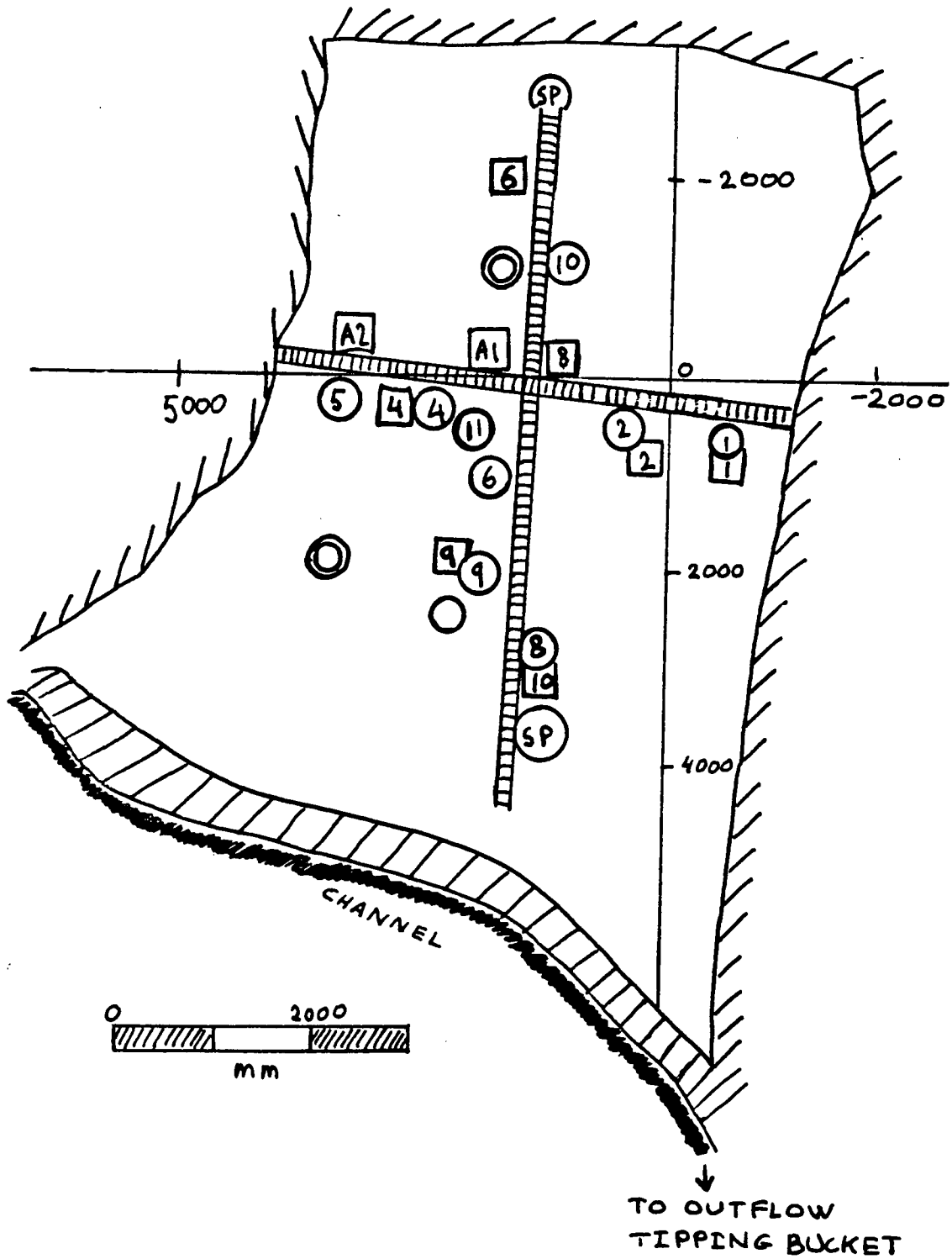

Fig. 1.3.1.1 Site layout. See p. 15 for explanation.

Sprinkler

Automatic Raingage

Funnel raingage

Standpipe

Neutron probe access tube

Walking board

Plastic frame

There is no ground cover vegetation. Six logs or groups of logs in various states of decay are present on the soil surface. They cover an area of about 3 m^2 which represents 6% of the plot area. Some of these logs may have acted as natural concentrating elements. There are also seven live trees.

The top of the forest floor (L horizon) consists mainly of needles. The F horizon consists of stratified organic material (from recognizable twigs to amorphous decayed material). The bottom layer of the forest floor (H or humified layer) and the top layer of the mineral soil (Ae or eluviated or leached layer) together form a layer of lower conductivity (de Vries and Chow 1978). Pieces of wood create barriers to flow in the forest floor.

Soil depth (including the forest floor) varies from 0 to 1.65 m. A minimum depth of 0 was found at the south tip of the channel at the location of a rock outcrop, and a maximum depth of 1.65 m in the middle of the upper part of the plot.

The outcrop occurs at the channel's bank which was not irrigated. In the irrigated region, minimum soil depth may have been greater.

The texture of the B horizon at Nagpal and de Vries' site has been determined to be sandy loam (Nagpal and de Vries, 1976) and is considered to be the same for the plot used for the present study. The B horizon is very strongly structured with many live and decayed roots, as well as with stones and cemented aggregates. Its structure is very stable. A larger amount of root material is found at the interface of the B horizon with the bed than in the rest of the B horizon.

At the top of the B horizon, the ratio of stones to bulk soil by volume was found to be 0.14. Also, the porosity of the top part of the B horizon is 0.63. (Calculations are shown in Appendix A. For the definitions and symbols used for porosity and effective porosity, see Appendix G).

Studies on two in situ cores gave a satiated hydraulic conductivity of 8×10^{-4} ms^{-1} (Heinonen, pers. comm.) for the upper part of the soil profile, including the forest floor. The cores had a diameter of about 0.25 m and a length of about 0.30 m. The method is described in Baker and Bouma (1976). Later mention of "in situ cores" will refer to these measurements.

The lower part of the forest floor may have a satiated hydraulic conductivity smaller than the one of the upper part of the B horizon, as was noticed by de Vries and Chow (1978) in the Seymour Watershed of the Greater Vancouver Water District. Therefore the upper part of the B horizon may have a satiated hydraulic conductivity larger than 8×10^{-4} ms^{-1}.

A similar value of 10^{-3} ms^{-1} was found by Harr (1977) at 0.10 m depth in the soil of a Douglas-fir and western hemlock forest in western Oregon. The similarity of these values is interesting in view of the similarity in vegetation and climate of the two places.

Figs. 1.3.1.2 a to c show the characteristic flow curves obtained by Nagpal and de Vries (1976) on their site. The forest floor was 0.15 m deep. In the present work, K designates the satiated hydraulic conductivity whereas $K(\psi)$ and $K(\theta)$ designate the unsaturated conductivity as a function of the pressure head ψ and of the soil water content θ respectively. For simplicity, the satiated hydraulic

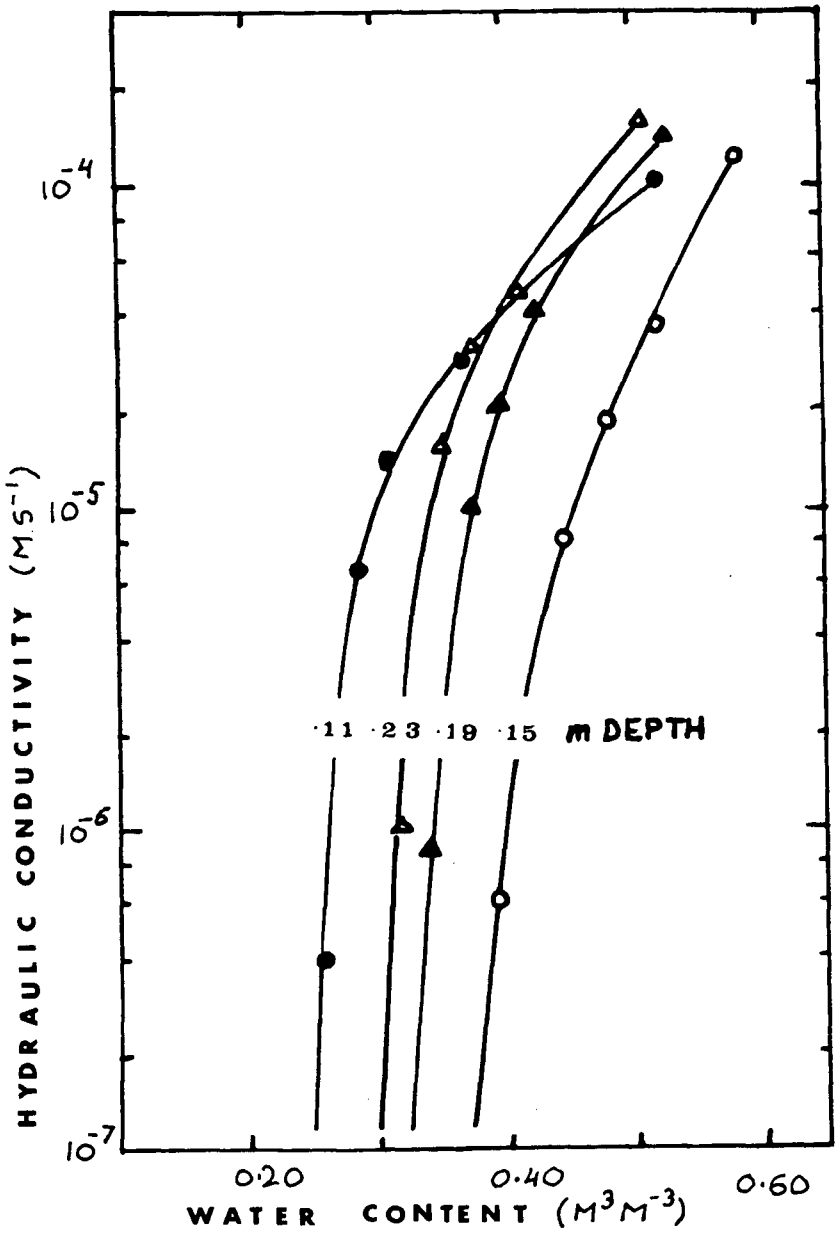

Fig. 1.3.1.2a Partial hydraulic conductivity curve for the 0.11, 0.15, 0.19 and 0.23 m depths on Nagpal and de Vries' site. Adapted from Nagpal and de Vries (1976). (Forest floor was 0.15 m deep.)

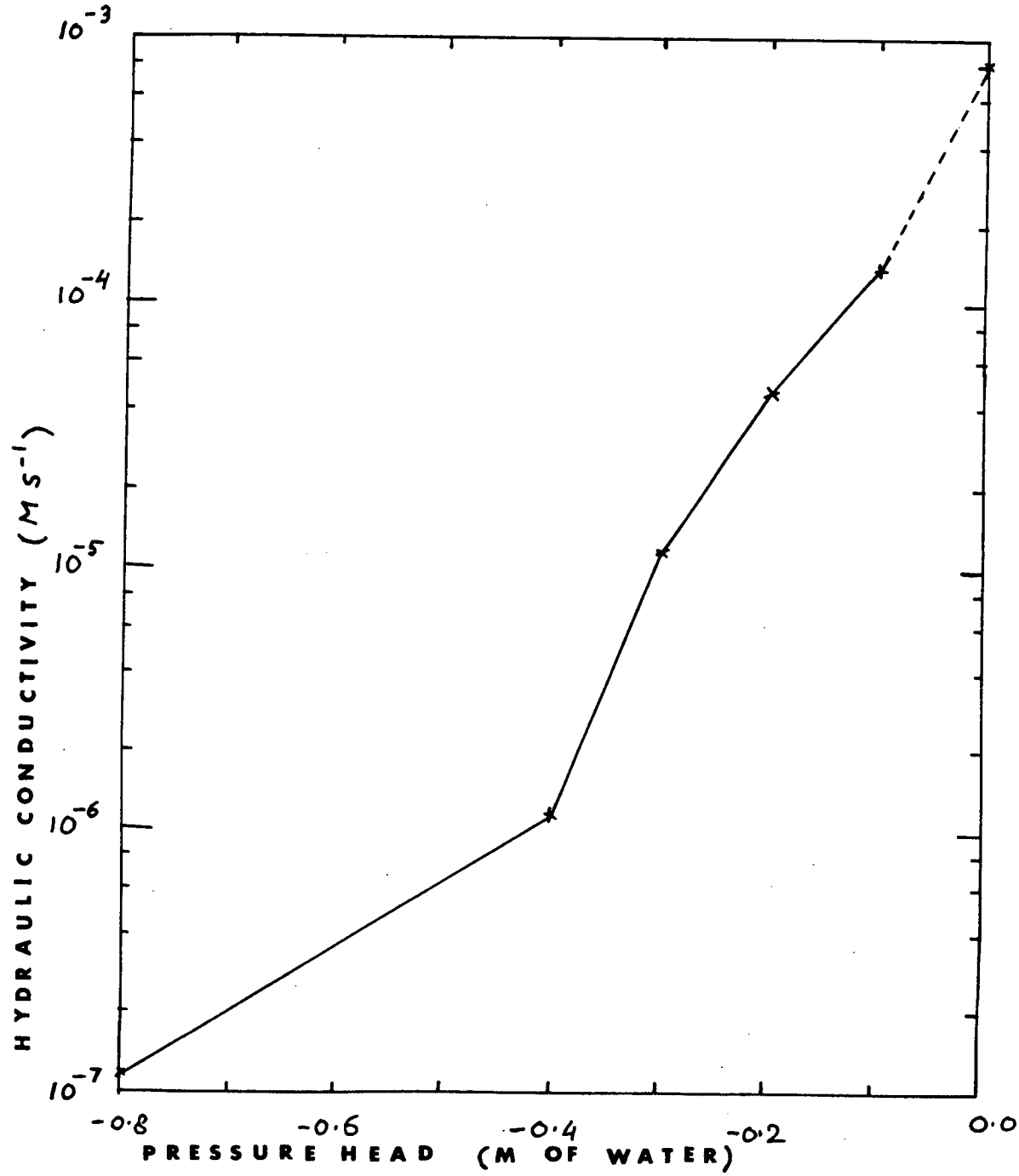

Fig. 1.3.1.2b $K(\psi)$ for Nagpal and de Vries' site at 0.23 m depth obtained from Nagpal and de Vries' (1976) $K(\theta)$ and $\theta(\psi)$ curves.

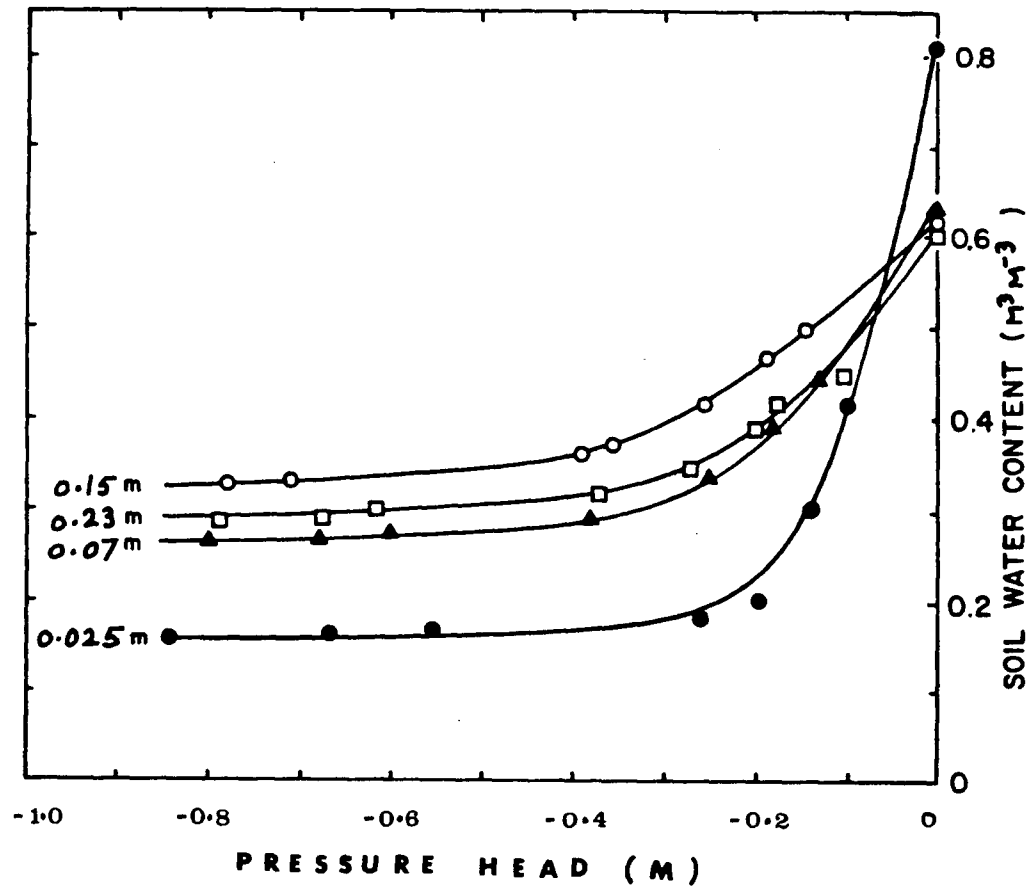

Fig. 1.3.1.2c Partial retention curves for the 0.025, 0.07, 0.15 and 0.23 m depths for Nagpal and de Vries' site. Reproduced from Nagpal and de Vries (1976). (Forest floor was 0.15 m deep.)

conductivity will be referred to as hydraulic conductivity. Porous media will be considered to be isotropic and homogeneous whenever Darcy's law is used. When the uniformity of K is in question, the value of K can be considered to be an overall value. The assumption of isotropy is not good for the forest plot but has been considered to be a necessary simplification.

Also, flow is assumed to be linear whenever the phrase "satiated hydraulic conductivity" or "hydraulic conductivity" or the symbol "K" is used. Otherwise the phrase "general hydraulic conductivity" or the symbol "K_{gen}" is used (see Chapter III).

The $K(\psi)$ curve (Fig. 1.3.1.2b) has been obtained from Nagpal and de Vries' $K(\theta)$ and $\theta(\psi)$ curves. The satiated conductivity point on the $K(\psi)$ curve comes from the value obtained in the present work. This is why a dotted line has been used to join the last 2 points. The lower part of the $K(\theta)$ curves for 0.19 m and 0.23 m are so steep that small differences in θ yield large differences in K. This suggests that extrapolation of the curves to another site and even from one place to another within a site is questionable. However, the curves parallel each other, suggesting that their general shape is similar. Because the soil at Nagpal and de Vries' site is similar to the one at the present site, it is suggested that the general shape of the characteristic curves for the present site is similar to the general shape of the characteristic curves obtained by Nagpal and de Vries.

It is interesting to compare the value of the satiated hydraulic conductivity obtained for the Forest plot with values obtained for an agricultural watershed.

Betson et al. (1968) obtained satiated hydraulic conductivities of 7×10^{-6} to 2×10^{-5} ms^{-1} for a clay loam A horizon in a North Carolina agricultural watershed.

Table 1.3.1.1 shows results of measurements of satiated hydraulic conductivities at two outflow points along the channel. Outflow was from a natural storm event. These outflow points were in the zone rich in root material found at the interface of the B horizon with the bed. It was observed that the outflow points themselves coincided with an accumulation of root material. Hydraulic conductivity values were obtained by measuring the outflow rate and the area of outflow at these points. The water table was assumed to be parallel to the bed (see Chapter II) and the slope of the bed was assumed to be the same as the surface slope of the plot.

It will be shown in Chapter II that for this case, Darcy's law for homogeneous isotropic porous media,

$$q = K \frac{dh}{ds} \qquad 1.3.1.1$$

becomes approximately

$$q = K \sin\omega \qquad 1.3.1.2$$

where

q = Discharge per unit area or macroscopic flow velocity, often called Darcy's velocity. In the present work, q is in the main flow direction.

h = hydraulic head

s = distance

$\frac{dh}{ds}$ = rate of change of h with s. Since in the present work, q is in the main flow direction, and the porous media are considered to be isotropic and homogeneous, $\frac{dh}{ds}$ is the macroscopic hydraulic gradient

K = satiated hydraulic conductivity

ω = angle that the bed makes with the horizontal

It is not certain homogeneity is actually required for Eq. 1.3.1.1 to hold and for $\frac{dh}{ds}$ to be the macroscopic hydraulic gradient.

Table 1.3.1.1 shows the results. The area of outflow was difficult to measure and for this reason, two values per outflow point are given corresponding to a maximum and a minimum area. K is found to vary from about 5×10^{-4} to about 5×10^{-3} ms^{-1}. Because possibly too small an outflow area was used for the higher number, this number may be an upper limit. On the other hand, the smaller K, being smaller than the K found with the in situ core method may be too small. Indeed, if it is assumed that at least a major proportion of the water flowing out of an outflow point has been travelling through a low resistance path, it is surprising that the K measured at the outflow point is smaller than the K found by <u>in situ</u> cores. It is thus possible that the actual two K's that should be obtained at the two outflow points are bracketed by the two values given here.

Table 1.3.1.1 Estimate of satiated hydraulic conductivity K at two outflow points.

	Discharge $m^3\ s^{-1}$	Estimated area of ouflow m^2	q = discharge per unit area ms^{-1}	$K = \frac{q}{\sin\omega} = \frac{q}{.5}$ ms^{-1}
Outflow Point 1	4.7×10^{-6}	0.18×0.03	8.7×10^{-4}	2×10^{-3}
		0.18×0.01	2.6×10^{-3}	5×10^{-3}
Outflow Point 2	2.7×10^{-6}	0.01 (1)	2.7×10^{-4}	5×10^{-4}
		0.26×0.01	1.1×10^{-3}	2.1×10^{-3}

[1] 0.26 m x a varying height.

Note that it is shown in Chapter III that there is a possibility that flow at these outflow points may have been nonlinear, in which case Darcy's law should not be used. For the above calculations of K, it has been necessary to assume that the nonlinearity, if existant, is negligible.

Figure 1.3.1.3 shows the topography of bedrock or compacted till obtained from standpipe depths. Values are vertical distances from a datum to the tip of the pipes. Soil sampling with a tube indicated the tip of standpipes 2, 4, 5, 6 and 10 to be resting on the low conductivity layer. It is not certain what the other pipes are resting on (see Section 1.3.5).

At Nagpal and de Vries' site, Utting (1978) found the satiated hydraulic conductivity of the compacted till to be 10^{-7} ms^{-1} to 10^{-6} ms^{-1}.

The plot used for the present work (see Fig. 1.3.1.1.) was about 8 x 7 m^2. In order to irrigate a definite area, the plot was surrounded with plastic. Water falling onto the plastic was routed away from the plot. Some walking took place on the plot but very early during the phase of instruments installation boards were placed a few cm above the ground surface in order to avoid compaction.

Irrigation was provided by 2 impact sprinklers. Sprinkling rates were measured by 2 tipping bucket raingages and 11 funnel raingages. Water table elevation was measured with 10 standpipes, 2 of which were automatically recording. The outflow collection and measurement system consisted of a channel dug at the foot of the plot which was connected to a tipping bucket flow meter with metal troughs. The collection channel was covered with plastic.

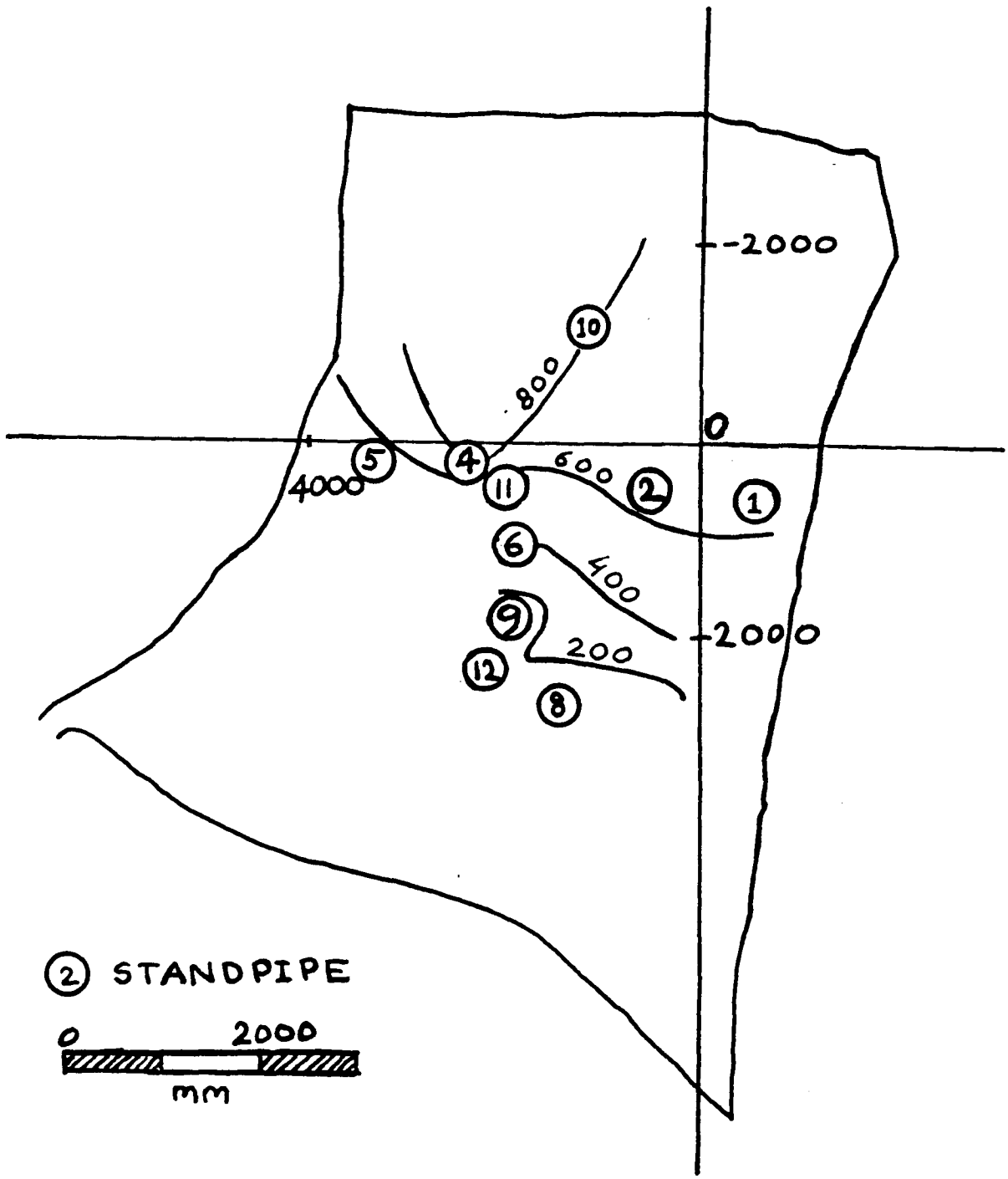

Fig. 1.3.1.3 Contours of the bed (bedrock or compacted till) obtained from pipes depth. Values in mm. Values are vertical distances from a datum situated below the tip of the pipes to the tip of the pipes.

1.3.2 Sprinklers

The 2 impact sprinklers were installed at a spacing of 6.25 m. They were adjusted to sweep approximately half a circle and their ranges overlapped. Range was adjusted for uniformity according to visual observation at the beginning of Ex1 and no further adjustments were made.

1.3.3 Raingages, Pooled Irrigation and Time Averaged Pooled Irrigation

Two tipping bucket raingages (denoted by A1 and A2) were placed at about 0.40 m (A2) and 0.50 m (A1) above ground level. The diameter of their collection area was 0.20 m. The volume of one tipping bucket was approximately 15.5×10^{-6} m^3. These raingages were connected to an event recorder. The variance of the time between tips was zero for constant inflow. This shows that unsteadiness during the experiments was not due to raingage malfunction but to actual unsteadiness in irrigation rate.

The 11 funnel raingages (individually denoted by RG1, RG2 etc.) were constructed from 1 liter plastic bottles. A hole in the lid accommodated a plastic funnel. The diameter of the collection area was about 0.10 m. Funnel raingages were usually read when they were more than half full. Readings were made every 3 to 6 hours or more.

Pooled irrigation rates for every .1 hour were calculated using Thiessen polygons and then plotted. For the third experiment RG11 had been removed from the plot and this resulted in a pooled irrigation rate apparently higher for Ex3 than for Ex1 and Ex2.

The pooled irrigation rate for Ex3 has been computed by using the remaining raingages on the smaller area covered by these raingages, the area covered by RG11 being left out. Each remaining raingage was covering the same area as during Ex1 and Ex2. A similar method was used to obtain irrigation rates without RG11 for Ex1 and Ex2.

Some of the funnel raingages data were accidentally lost. When this happened, the average rate measured at a given raingage during a given experiment was used to replace the missing values of this raingage for this experiment.

For the water balance, a time average of the pooled irrigation rate was needed. Irrigation rate is not constant with time so that, when an average is taken for a certain period, it depends upon the period's duration. An effort was made to choose the period in a rational way (see Section 1.4.6).

Time averages of the pooled irrigation rates were obtained by positioning a thread on the irrigation graphs (Figs. 1.4.2.3 to 1.4.2.5) in such a manner that the area between R_p and the thread above the thread looked approximately equal to the area between R_p and the thread below the thread, R_p being the pooled irrigation rate. Time average values of pooled irrigation rates showed the ratio irrigation rate with RG11 to irrigation rate without RG11 to be approximately 0.8 for Ex1 and Ex2 (see Table 1.4.6.1). Pooled irrigation rates for Ex3 were corrected by multiplying them by 0.8 for the water balance, since it was desired to estimate the irrigation rate that would have been obtained had RG11 been available.

Errors in the irrigation rate are due to nonuniformity of irrigation and to an insufficient number of raingages, especially in the

plot's fringes. A lower irrigation rate on the fringes of the plot was especially responsible for nonuniformity. This can be appreciated by the fact that when irrigation is obtained without the area covered by RG11, a time average pooled irrigation rate 1/0.8 larger is obtained, as shown in Table 1.4.6.1. The Thiessen polygon covered by RG11 has a size equal to 1/4 the size of the plot and is the bottom fringe of the plot.

The difference in pooled irrigation rate due to the absence of this polygon thus gives an indication of the importance of recording correctly the irrigation rate in the fringes of the plot. Part of the reason why the Thiessen polygon covered by RG11 is so important for the overall irrigation rate is that it represents such a large proportion of the total area.

1.3.4 Neutron Probe Access Tubes

Two neutron probe access tubes were installed in the same way as the standpipes (see Section 1.3.5). Readings were made at depths of 0.15, 0.30, 0.50, 0.70, 0.90 and 1.10 m for the upper neutron probe access tube, and 0.15, 0.30, 0.50 and 0.63 m for the lower neutron probe access tube. There may be a systematic error due to the fact that the manufacturer's calibration and not a calibration specific for the places where measurements were taken was used. This error does not affect soil water content differences at a given point.

1.3.5 Standpipes

Eight small (I.D. 16 mm) and 3 large (I.D. 40 mm) standpipes were installed. (They will be called pipes for short). They were

constructed from galvanized steel conduit pipes. The end of the small pipes was pinched shut to prevent clogging and slits 2 mm wide were cut at their base. The end of the large pipes was left open. The small pipes were numbered 1 to 9 (7 missing). The large ones were numbered 10 to 12. Pipes 10 and 11 were equipped with Stevens water level automatic recorders. There may be large time errors associated with these two pipes, therefore only their steady state readings were used.

The standpipes were installed in the following manner: a hole was made by hammering down a metal rod (25 mm diameter for the small ones, 50 mm for the large ones) using a sledge hammer. Because of stones it was not always possible to reach the compacted till or bedrock and it is possible that some standpipes rest on stones instead. The metal rod was then removed with a jack-all. This was sometimes a difficult operation. A gravel filter was used to prevent clogging of the pipe inlet. Small pipes were used because they were easier to install. They also responded faster but were subject to larger measurement errors as will be discussed later on. The tip of the pipes reached depths varying from 0.50 m (pipe 8) to 1.66 m (pipe 10). Pipes 1, 11, and 12 rested on bedrock or on a stone. Pipes 2, 4, 5, 6 and 10 rested on till. What the remaining pipes rested on is unknown.

The pipes were not sealed because the soil was vented down to the bottom of the B horizon. During Ex1, the elevations of the water levels in the pipes were measured with a plastic tube (9.5 mm O.D., 6.3 mm I.D.) holding a float. In Ex2 and Ex3 an electric water level detector was used. This detector consisted of a 1.5 m long, 9.5 mm O.D. plastic

tube with two bare wire ends mounted at the tip. Contact of the wire ends with the water in the standpipe resulted in closure of an electrical circuit and the lighting up of an indicator light.

The main problem that arose with the data collection was lack of reproducibility. For instance, the water level in pipe 1 climbed about 50 mm during a continual series of readings while the general trend given by the graph was a rise of at most 12 mm in 2 hours.

Lack of reproducibility could be traced to 3 causes: extraneous inflow of water into the pipes, clogging of the pipes, and displacement of water inside the pipes when the float tube was used.

At least part of the variation can be explained by water flowing along the measuring tube into the pipe. This problem arose from the fact that the sprinkler jet had a significant horizontal component. It presumably was aggravated by clogging of some pipes. It was found that in a closed small pipe water rose at a rate of 3.3×10^{-5} to 27×10^{-5} ms^{-1} while the measuring tube was held in the same way as for a measurement. This source of error is more important for small pipes than for large ones.

In May 1981 "slug tests" were performed to check the pipes for clogging. These tests consisted of pouring water into the pipes and then measuring the water level as a function of time. They indicated that pipes 4, 12 and 6 responded well and pipes 10 and 11 responded slowly. The slow response of pipes 10 and 11 does not matter since these pipes are used only at steady state. The response times of pipes 2, 8, 5 and 1 were intermediate.

Clogging is probably responsible for the fact that pipe recessions for Ex2 are slower than for Ex1. Although rainfall occurred during the recession of Ex2, several pipes show a slower recession rate before rain starts.

It is unlikely that rainfall is responsible for a slower recession of the pipes for Ex2 and Ex3 since the outflow recessions of the 3 experiments are remarkably parallel.

Gradual clogging is also supported by the behavior of pipes 3 and 9. Accordingly, these pipes are not used.

It is true that clogging seems unlikely for such a stable soil, and also given the fact that a gravel filter was used but that is the only possible explanation for the observed pipe behavior.

When the float tube was used, an additional cause of error was introduced. Due to displacement, the water level inside the pipe was higher than outside the pipe. Water thus would flow out of the pipe and the water level in the pipe would be lower for the next reading. This error is also more important for small pipes than for large ones. One series of measurements during EX2 and one during EX3 were taken with both the electric detector and the float in order to determine whether results agreed. Differences are less than 0.04 m except for pipes 5 and 8 where they reach 0.10 m. For these large differences, the height given by the electric detector is higher than the one given by the float, as is the case for most of the other differences. For these tests, readings with the float detector were made after readings made with the electric detector, so that the displacement due to the float would not influence the electric detector reading.

For the data analysis, the first reading in a series of readings of water level was used because it was considered that it was the least affected by the extraneous inflow of water mentioned above and by displacement. Water level was often obtained in a continual series of readings. In most cases time was recorded at the end of the series. Since the first reading of the series was used there is a time error estimated to be < 10 minutes.

1.3.6 Collecting Channel and Outflow Tipping Bucket

The collecting channel intercepted subsurface flow over a length of 7 meters measured perpendicular to the slope. Its depth varied from 0 to 1.10 m.

The channel bottom consisted of compacted till in the north reach and bedrock in the south reach. A cement trough was constructed on top of the bedrock. The compacted till reach was not cemented because its conductivity was judged low enough. A plastic cover prevented irrigation water from entering the channel.

Outflow rates were measured with a tipping bucket unit (Chow, 1976) having a maximum capacity of 2.2×10^{-3} m^3.

The following problems should be kept in mind when considering results obtained from the outflow tipping bucket.

1. There was some antecedent outflow for Ex2 and Ex3.

2. Spurious inflow (overland flow over the hydrophobic forest floor) may have reached the channel; this happened mainly during Ex1. Flow from water falling onto the plastic plot boundaries may also have

reached the channel. This latter inflow was assumed negligible except for an extra 1.4×10^{-5} m^3 s^{-1} during the rerise of Ex3 till 7:35 a.m., August 23. This part has been suppressed on the outflow graphs. Also, some water collected on the plastic plot boundaries and routed out of the plot may have subsequently reached the channel via an underground route. Such a mechanism was observed while using a hose. The fact that the channel outflow point where outflow started during the experiments was not the same one as the one noted to yield outflow while the mechanism just described was operating indicates that the amount of water (if any) using this route during the experiment did not influence the time to start of outflow.

3. Water escaping collection because the channel had not been dug far enough.

4. There is some uncertainty as to whether the correct tipping bucket calibrations were used for Ex1 and Ex2. Details are given under point 4, Appendix E.

5. The tipping bucket, initially adjusted to fill to a certain mark and calibrated for this mark would gradually fill more and even overflow at times. The ratio of the volume contained by the tipping bucket when it is full to when it is filled to the mark is 4/3. Thus errors of more than 30% may have occurred since theoretically, errors of at least 30% could have occurred when the tipping bucket overflowed. This may have happened for Ex1 at least once, around t = 61 hours. For Ex2, overflowing possibly occurred around t = 19.25 hours and occurred around t = 38.1 hours. This problem was corrected when noticed. No overflow occurred during Ex3.

6. There is an inconsistency between irrigation, water table height, and outflow hydrograph results. This will be discussed in Section 1.4.6.

7. For Ex3, the tipping bucket had been prefilled with one liter. For Ex1 and Ex2, there is doubt as to whether it had been prefilled or not.

From the above, one sees that the error in accuracy can, theoretically, be larger than 30%. There is, however, no way of knowing what the accuracy is. Therefore the problem of error will be approached from the point of view of whether the conclusions drawn from the data are reliable or not. For this purpose, a detailed error analysis is given in Appendix E.

1.3.7 Experimental Procedure

All 3 experiments were conducted in the same manner: the plot was irrigated for two days in order to ensure that steady state was reached. Irrigation was then stopped for about 2 hours and resumed for about 21 hours. The purpose of stopping the irrigation in the middle of an experiment was to determine the response of the water table and of the outflow to a "dry pulse". Irrigation times for the 3 experiments are shown in Table 1.3.7.1 a). Being performed after two weeks of dry weather, Ex1 has dry antecedent conditions. Being performed after Ex1, Ex2 has wet antecedent conditions. Ex3 follows Ex2 and has antecedent conditions slightly wetter than Ex2.

For Ex2, concentrated inflow of free water was supplied by placing plastic sheets on the ground. Their location is shown in

Table 1.3.7.1 Field experiments (summer 1979)

a) Irrigation times

	Irrigation starts	Irrigation stops	Irrigation restarts	Irrigation stops
Ex1	13:41 July 31	14:00 August 2	15:21 August 2	13:40 August 3
Ex2	11:45 August 11	15:31 August 13	17:23 August 13	14:09 August 14
Ex3	11:55 August 20	13:54 August 22	15:56 August 22	12:40 August 23

b) Main features

	Irrigation	Antecedent conditions
Ex1	Uniform	dry
Ex2	Concentrated	wet
Ex3	Uniform	Slightly wetter than Ex2

Figure 1.3.7.1. The sheets were approximately rectangular and ranged in size from about 0.55 x 0.75 m^2 to 0.80 x 1.40 m^2. The number of outflow points per sheet ranged from 1 to 4. There were 16 sheets covering 20% of the plot area. Concentration of irrigation for the area covered by plastic sheets, calculated as

$$\frac{\text{area of plastic}}{\text{area of inflow from plastic}}$$

is at least 100, as shown in Appendix B. Irrigation type and antecedent conditions are summarized in Table 1.3.7.1 b.

Figure 1.3.7.2 shows the occurrence of natural rainfall during the experiments' period. Rainfall records were obtained from the climatological station 4.8 km from and about 240 m below the site. Values are from 08:00 of one day to 08:00 of the next day. From what could be observed, rainfall at the climatological station could be quite different from rainfall at the site. It is expected that this is particularly so for rainfall before and during EX3, which was of the convective kind. It must be noted that, for the same rate, rainfall has more effect than irrigation applied to the plot only, because the plot receives subsurface flow originating from rain that fell uphill.

It is impossible to know the magnitude of this subsurface flow. It will therefore be neglected, keeping in mind that in the summer, rainfall events of the magnitude commonly observed, and occurring after a long dry spell are less likely to generate subsurface flow.

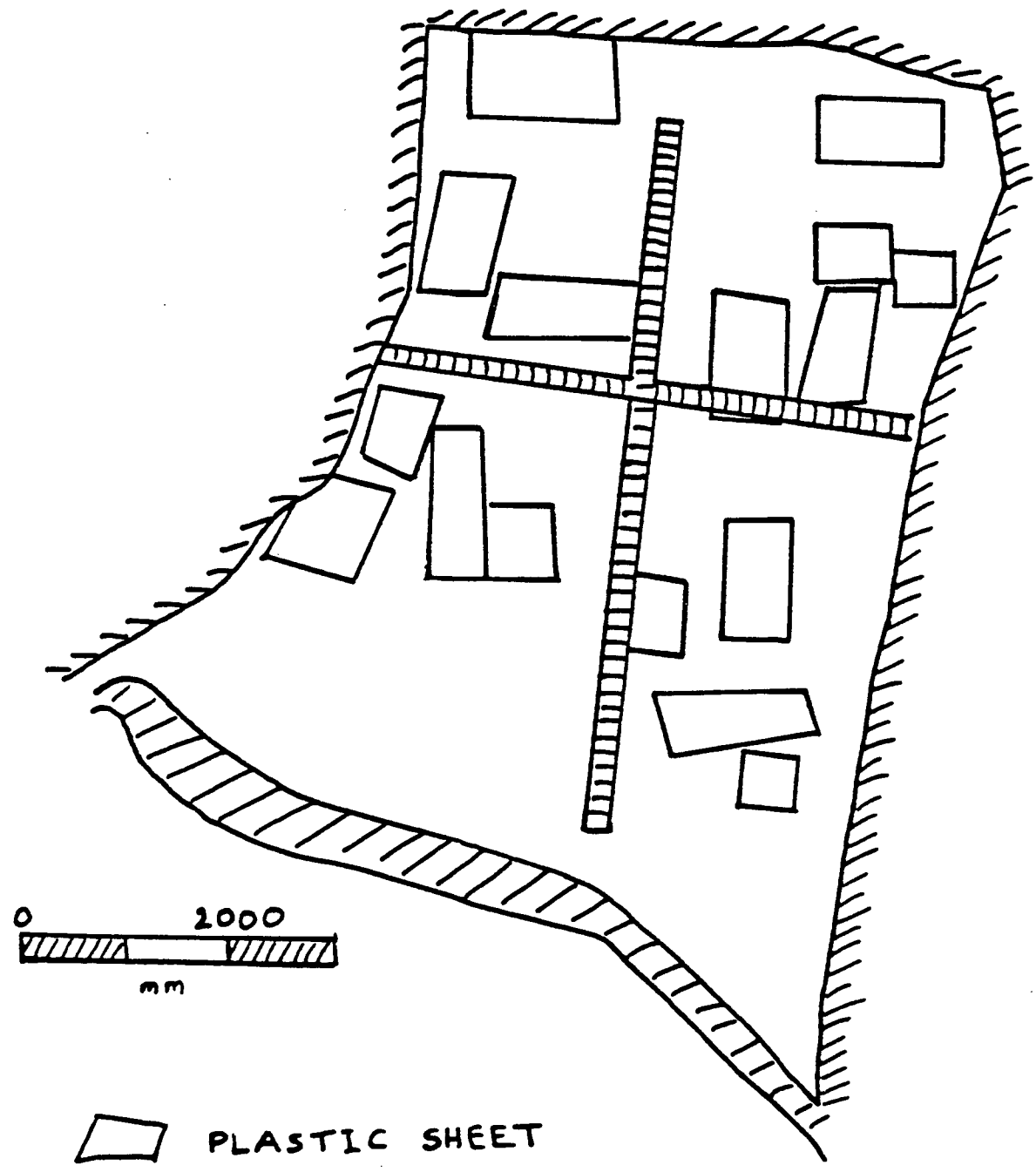

Fig. 1.3.7.1 Plastic sheets lay-out.

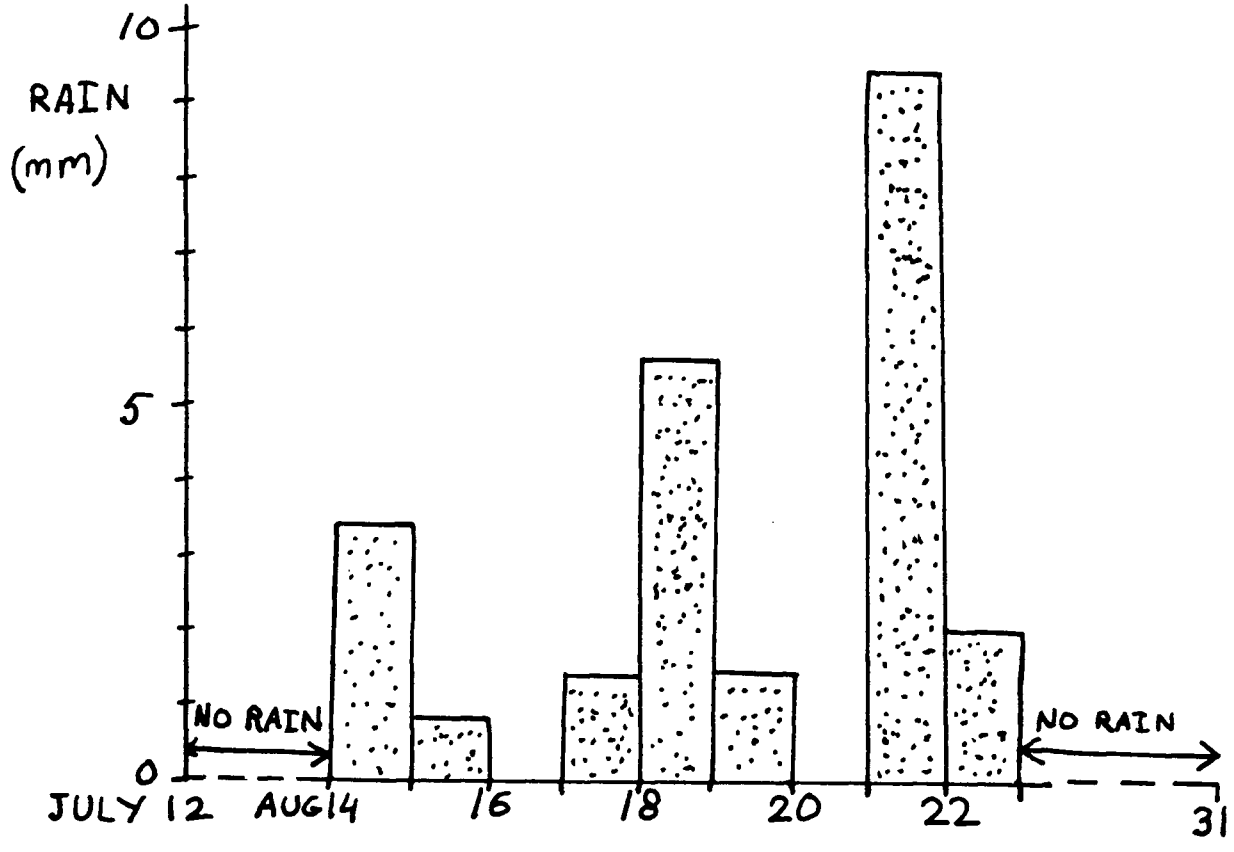

Fig. 1.3.7.2 Natural rain from climatological station 4.8 km away. Rain is in mm from 0800 to 0800 the next day.

1.4 Results

In this section, results are presented. Special emphasis is placed on the effect of initial soil water content and irrigation concentration on the outflow hydrograph and on the behavior of the water table. In addition, recession rates obtained in the present work are compared with results reported in the literature. Visual observations carried out on low resistance paths are also presented.

1.4.1 Soil Water Content, θ

Figures 1.4.1.1 and 1.4.1.2 show the profiles of θ obtained with the neutron probe.

The neutron probe itself never reached free water, either because the access tubes did not reach the bed, or because of the bed topography. However, some of the readings at the lowest levels may have been influenced by a saturated zone existing below the probe (See Note 2, Appendix H).

Because another initial soil water content will be introduced in Section 2.4, the symbol $\theta_{initial}$, or θ_{in} and the phrase "initial soil water content" will mean specifically "soil water content measured by the neutron probe before the start of irrigation." The symbol $\theta_{steady\ state}$ or $\theta_{st.st.}$ will mean "soil water content measured by the neutron probe during steady state."

Initial water content for Ex1 is not known exactly because it was measured before 1.5 hours of preliminary irrigation that took place on July 29, prior to Ex1.

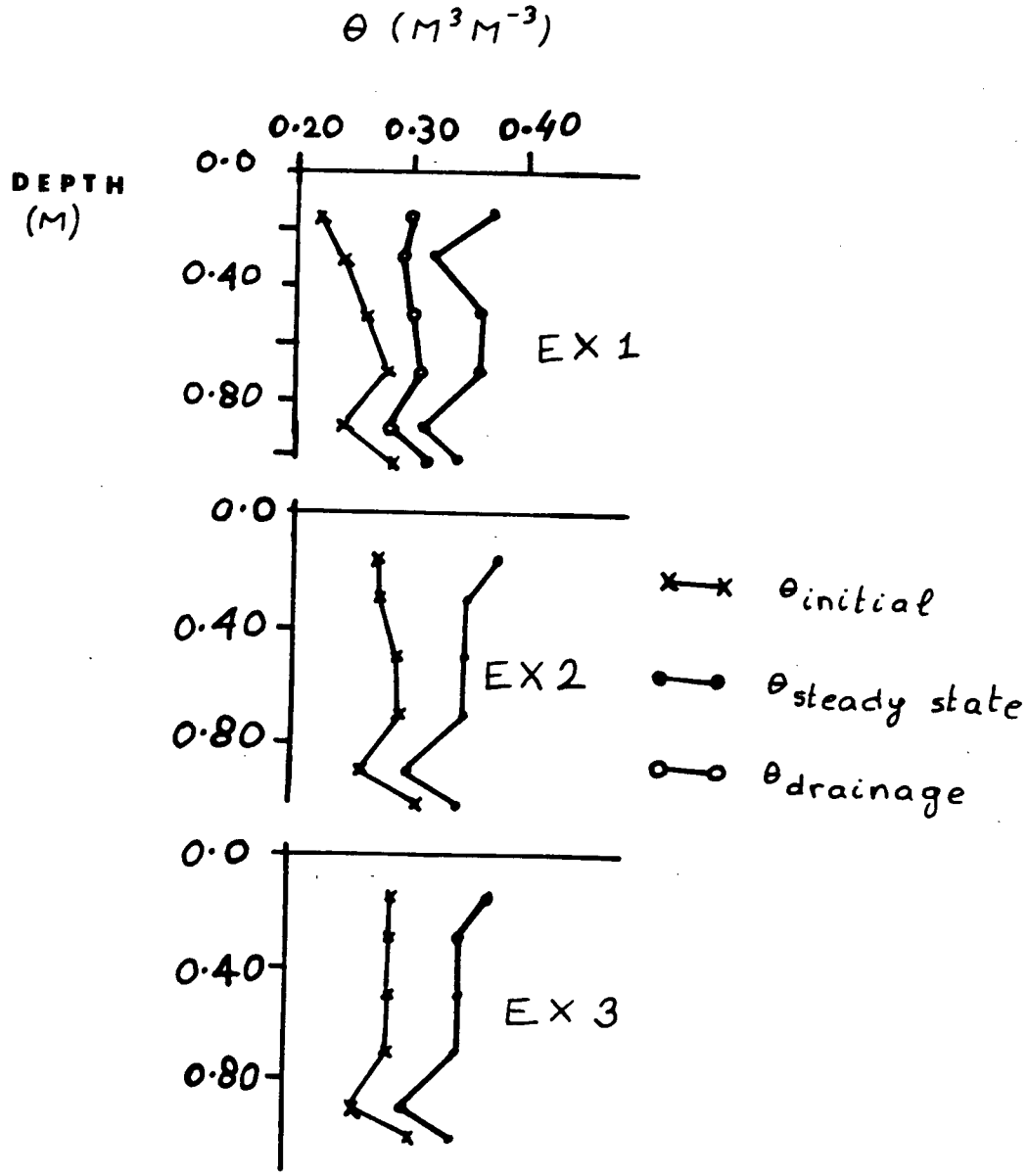

Fig. 1.4.1.1 Water content from the neutron probe readings at the upper neutron probe access tube. See p. 42 for details.

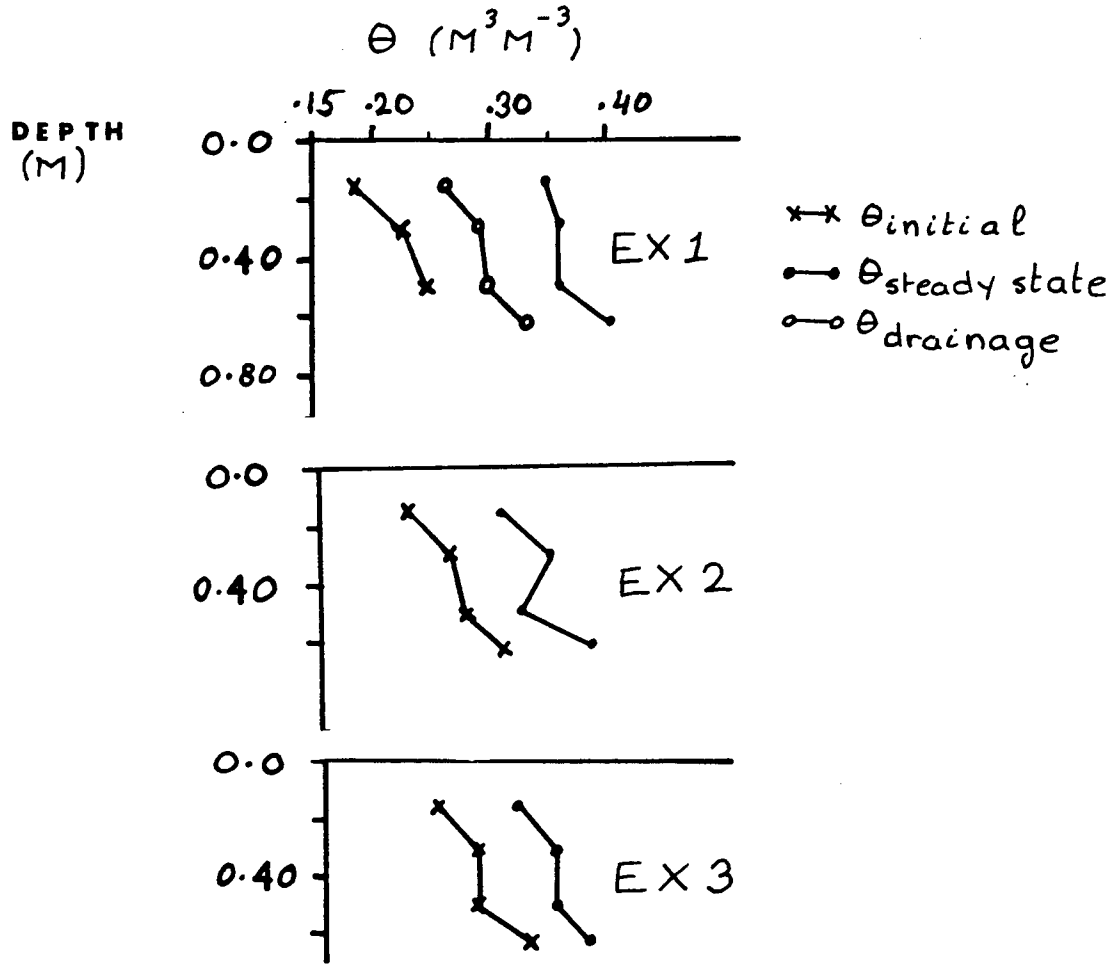

Fig. 1.4.1.2 Water content from the neutron probe readings at the lower neutron probe access tube. See p. 42 for details.

Details for Figs. 1.4.1.1 and 1.4.1.2

$\theta_{initial}$

EX1: July 28, before a preliminary irrigation.
EX2: August 10, at 1630
EX3: August 19, at 1100

$\theta_{steady\ state}$

EX1: August 2, at 1100
EX2: August 13, at 1130
EX3: August 22, at 1145

$\theta_{drainage}$

EX1: August 5, at 1000, 44 hours after irrigation stopped.

The θ profiles of Figures 1.4.1.1 and 1.4.1.2 show that θ_{in} was lower for Ex1 than for Ex2 and Ex3, and about the same for Ex2 and Ex3. They also indicate that $\theta_{st.st.}$ was nearly the same for all three experiments.

More specifically, θ_{in} differences between Ex1 and Ex2 range from 2 to 5.5% at the 0.90 and 0.30 m depths respectively. Both these values were obtained at the upper neutron probe access tube. Differences in θ_{in} between Ex2 and Ex3 range from 0% at the 0.50 to 1.10 m depths at the upper neutron probe access tube to 2% at the 0.30 m depth at the lower neutron probe access tube. Finally, differences in θ_{in} between Ex1 and Ex3 range from 2 to 7% at the 0.90 and 0.15 m depths respectively. Both these values were obtained at the lower neutron probe access tube. The reasons for these differences are that Ex1 was carried out after a dry period, and that Ex3 followed Ex2 more closely than Ex2 followed Ex1. For Ex2 and Ex3, data obtained at the upper neutron probe access tube during steady state indicate the presence of a θ straight of 0.35 m^3m^{-3} over the 0.30 to 0.70 m depth interval. For unknown reasons, the corresponding θ values for Ex1 are more variable.

These water content data indicate that over the 0.30 to 0.70 m depth interval, water that was in transit during the simulated rainfall event of average intensity 3.1×10^{-6} ms^{-1} caused θ to increase from 0.28 to 0.35 in Ex2 and from 0.29 to 0.35 in Ex3. Figure 1.4.1.2 indicates that θ data for the lower neutron probe access tube follow the same trend.

Finally, it is of interest to note that these θ straight values of 0.35 m^3m^{-3} are well below 0.63 m^3m^{-3}, which is the porosity of the upper

part of the B horizon.

1.4.2 Outflow

Before proceeding with the presentation of the outflow results, definitions of the terms used to describe the hydrograph are given. Fig. 1.4.2.1 shows that a hydrograph rise can be schematically broken down into three parts: the early part of the rise, the main limb of rise and the late part of the rise.

Figure 1.4.2.2 shows the superposition of the three hyetographs obtained without raingage 11 for Ex1, Ex2 and Ex3. It also shows the three hydrographs superposed. Figures 1.4.2.3 to 1.4.2.5 show the rainfall hyetographs obtained with RG11 for Ex1 and Ex2 but without RG11 for Ex3 together with the outflow hydrographs for the three experiments. RG11 had been removed from the site for Ex3.

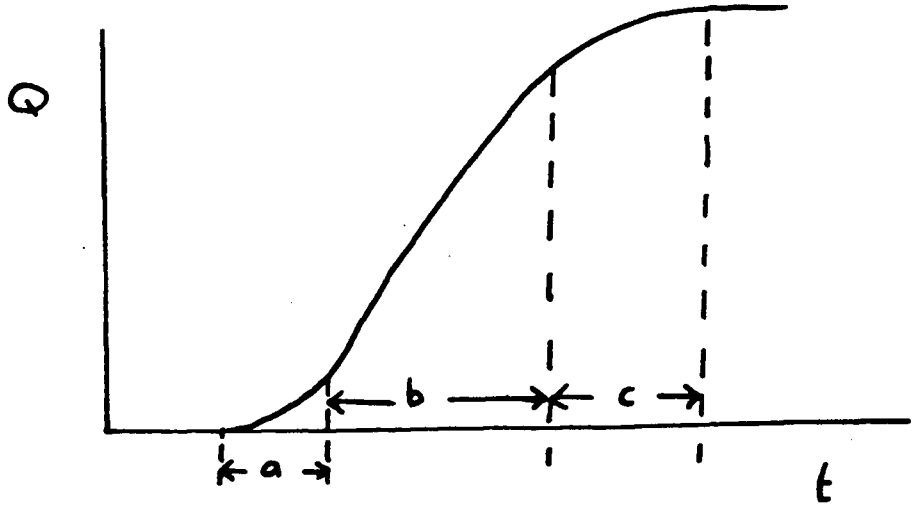

Fig. 1.4.2.1 The three parts of the hydrograph rise: (a) early part of the rise; (b) main limb of rise; (c) late part of the rise.

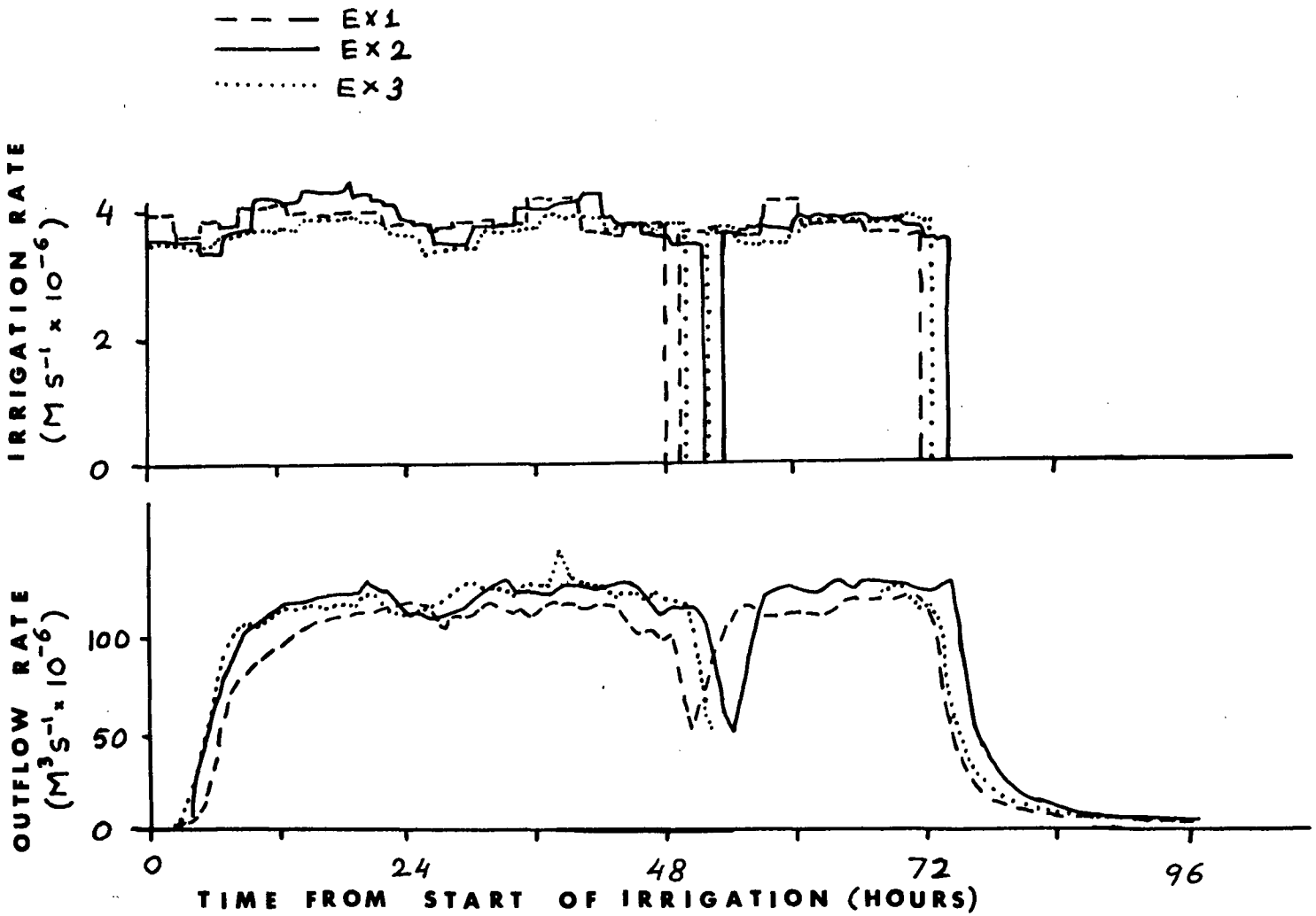

Fig. 1.4.2.2 Superposition of the 3 hyetographs (pooled irrigation rates calculated without RG11) and of the 3 outflow hydrographs.

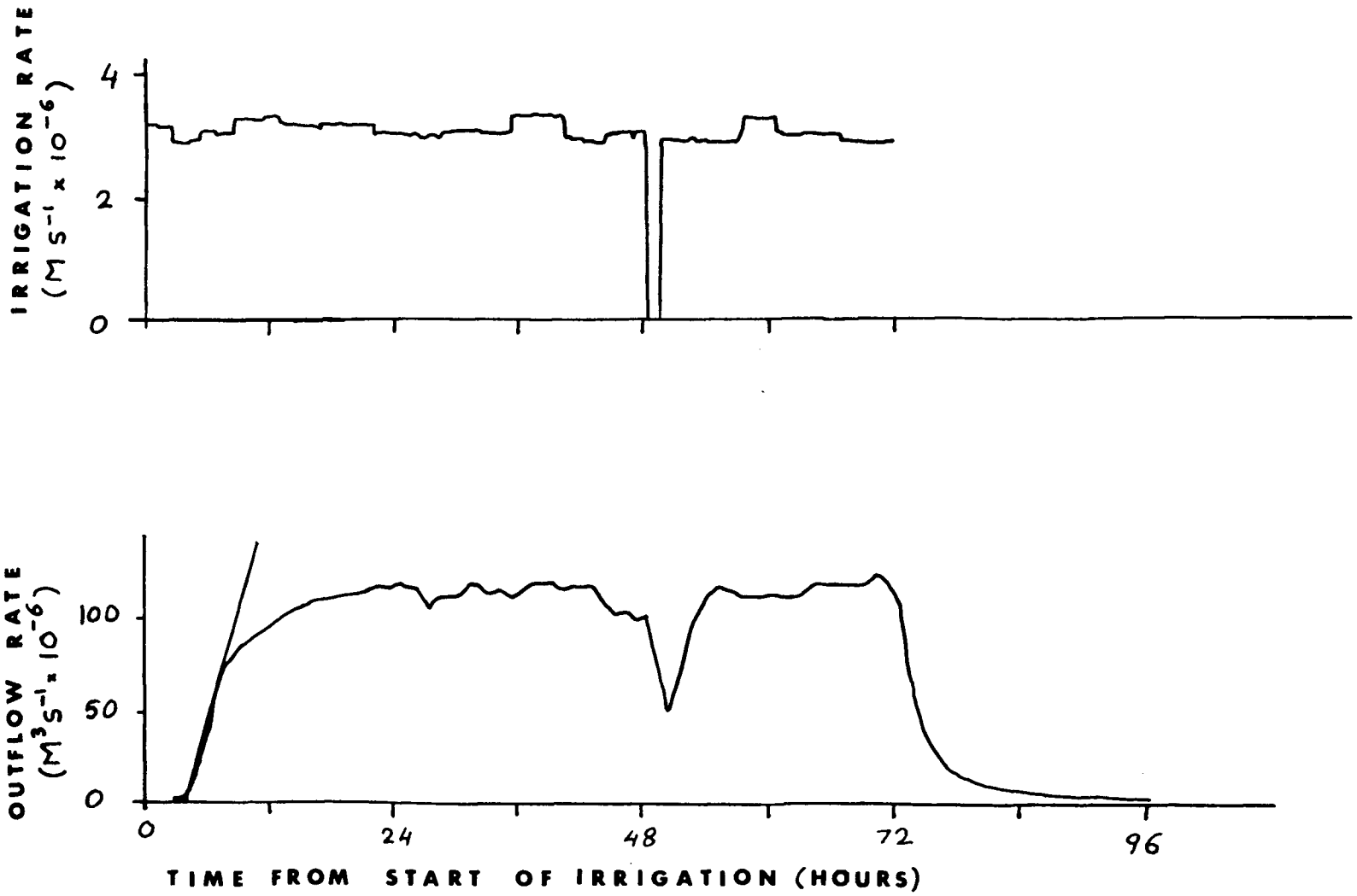

Fig. 1.4.2.3 Pooled irrigation and outflow rate for EX1.

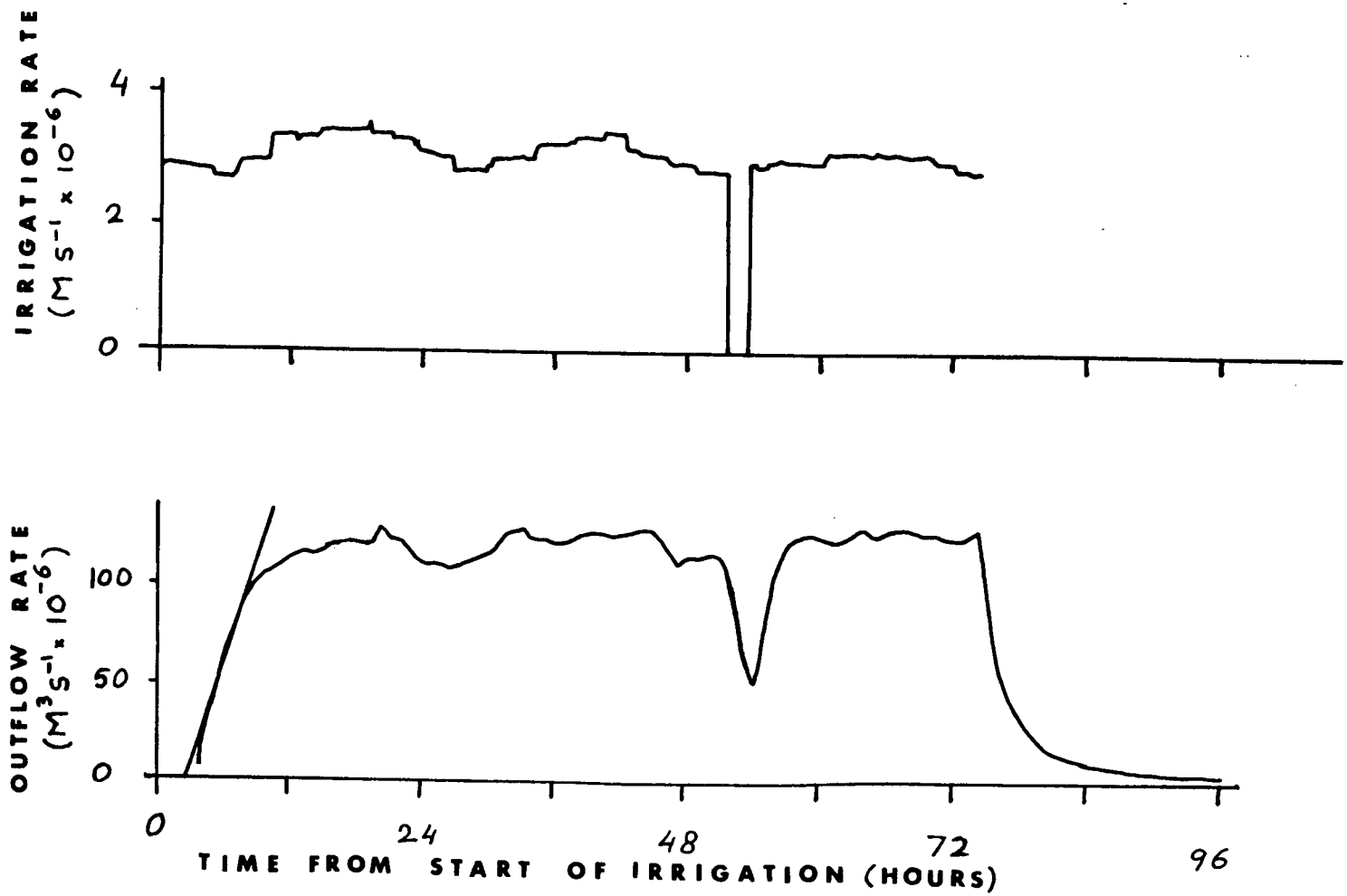

Fig. 1.4.2.4 Pooled irrigation and outflow rate for EX2.

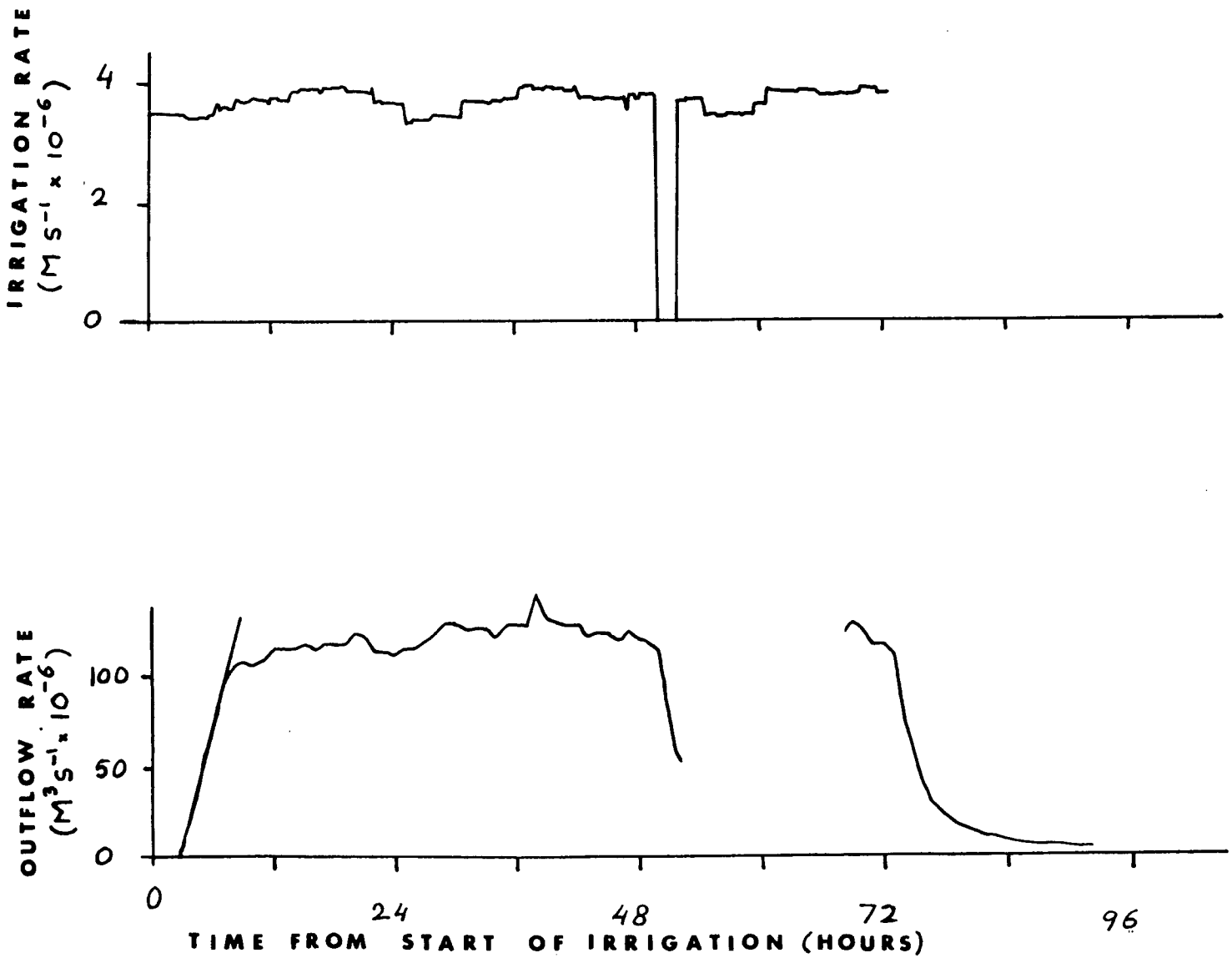

Fig. 1.4.2.5 Pooled irrigation and outflow rate for EX3.

On Figs. 1.4.2.2 and 1.4.2.5, the rerise of the outflow for Ex3 till 7:35 a.m. August 23 has been omitted because of error, as explained under point 2, Section 1.3.6.

Figure 1.4.2.6 shows the detailed rises. The method used to arrive at the data of Fig. 1.4.2.6 is described in Appendix D.

The effect of errors on the outflow hydrographs is discussed in Appendix E. The effect of natural rain on the hydrograph rises is discussed in the same Appendix.

Examination of Figs. 1.4.2.2 to 1.4.2.5 shows the outflow hydrographs present the following main features:

(i) The main limbs of rise start after little preliminary outflow.

(ii) The main limbs of rise are straight lines.

(iii) The main limbs of rise are steep and approximately parallel.

(iv) The recession limbs are steep and parallel.

Examination of the detailed rises of Fig. 1.4.2.6 shows that there is a small initial step for Ex1 and Ex3 but none for Ex2.

In order to determine the effect of initial conditions, Ex1 must be compared with Ex3. As mentioned in Section 1.4.1, the initial water content is lower for Ex1 than for Ex2 and Ex3. Initial conditions are also in part expressed by antecedent outflow rates. The latter was zero for Ex1, smaller than 2.78×10^{-8} $m^3 s^{-1}$ for Ex2, and 1.5×10^{-7} $m^3 s^{-1}$ nine hours before the start of irrigation for Ex3. From Figure 1.4.2.2, one can observe that the main limb of rise for Ex1 lags behind the one for Ex3.

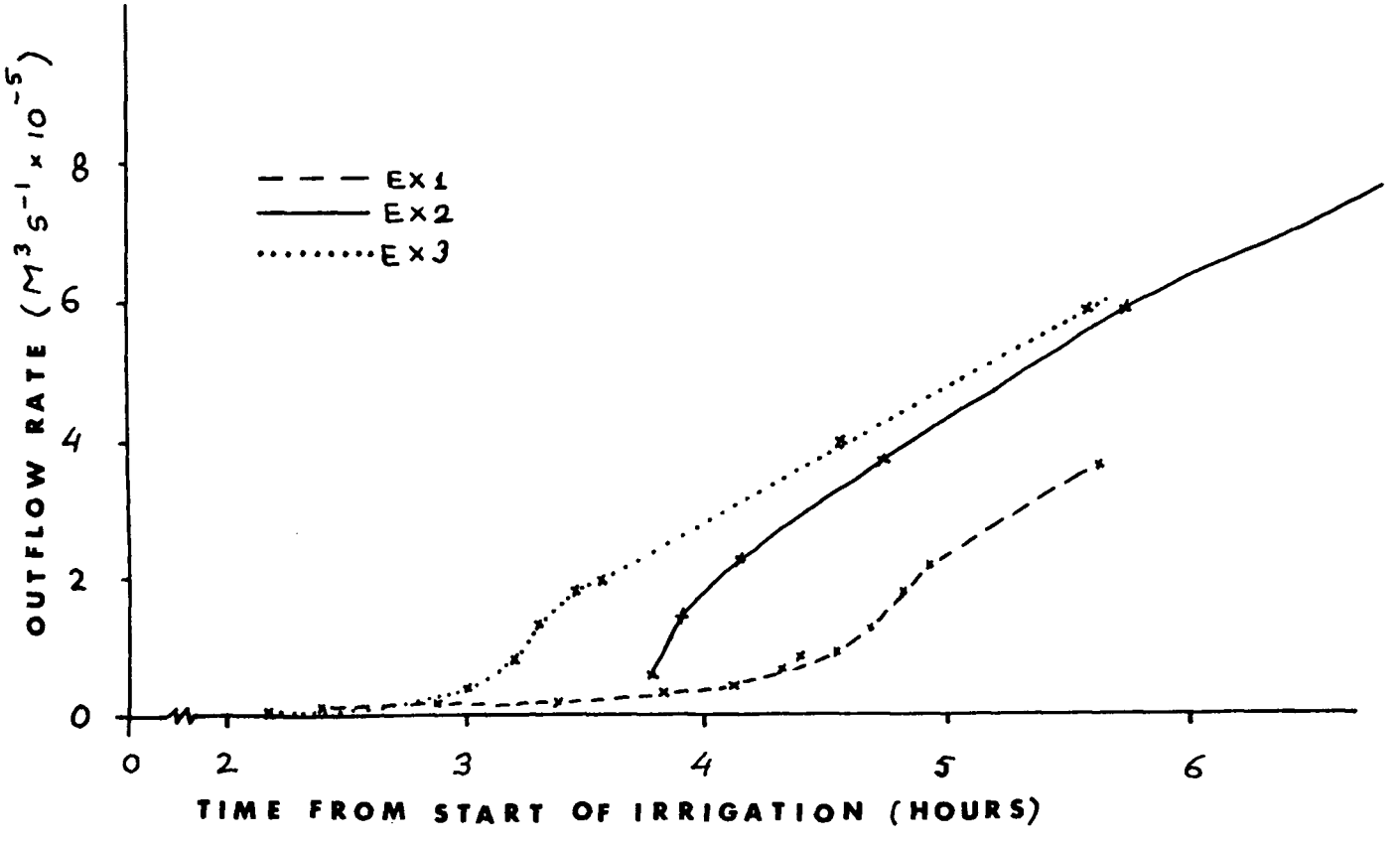

Fig. 1.4.2.6 Detail of the three hydrograph rises.

Hydrophobicity on the surface of the forest floor is an extreme example of the effect of initial conditions. Overland flow due to hydrophobicity was observed during the preliminary irrigation prior to Ex1 and during the beginning of Ex1. Overland flow was observed in an area where the soil was kept dry under the plastic covering the channel. It is not certain whether hydrophobicity-related overland flow can take place on soil not protected from the rain and how significant it can be under natural conditions.

In order to determine the effect of concentration on irrigation, Ex2 must be compared with Ex3. Fig. 1.4.2.2 shows that the main limb of rise for Ex2 is approximately parallel to the one of Ex3 and coincides with it or lags behind it by at most one hour.

To summarize, steep and linear main limbs of rise start after little preliminary outflow and are approximately parallel. Drier initial conditions resulted in a later main limb of rise. Concentration of irrigation did not change the general shape of the hydrograph rise and did not decrease the time lag to the main limb of rise. Neither did it enhance the initial step observed for Ex1 and Ex3.

1.4.3 Water Table

The behavior of the water table can be studied from the water levels measured at the standpipes.

Table 1.4.3.1. shows the standpipes depths and indicates whether the pipes are resting on till, or on bedrock or a stone.

Figures 1.4.3.1 to 1.4.3.7 show the water table behavior at the 7 pipes superimposed for the three experiments. Figures 1.4.3.8 and

Table 1.4.3.1 Standpipes depth

Pipe	depth (m)	Resting on
1	0.88	stone or bedrock
2	0.98	till
4	0.97	till
5	1.41	till
6	1.08	till
8	0.50	?
12	0.58	stone or bedrock
10	1.66	till
11	1.19	stone or bedrock

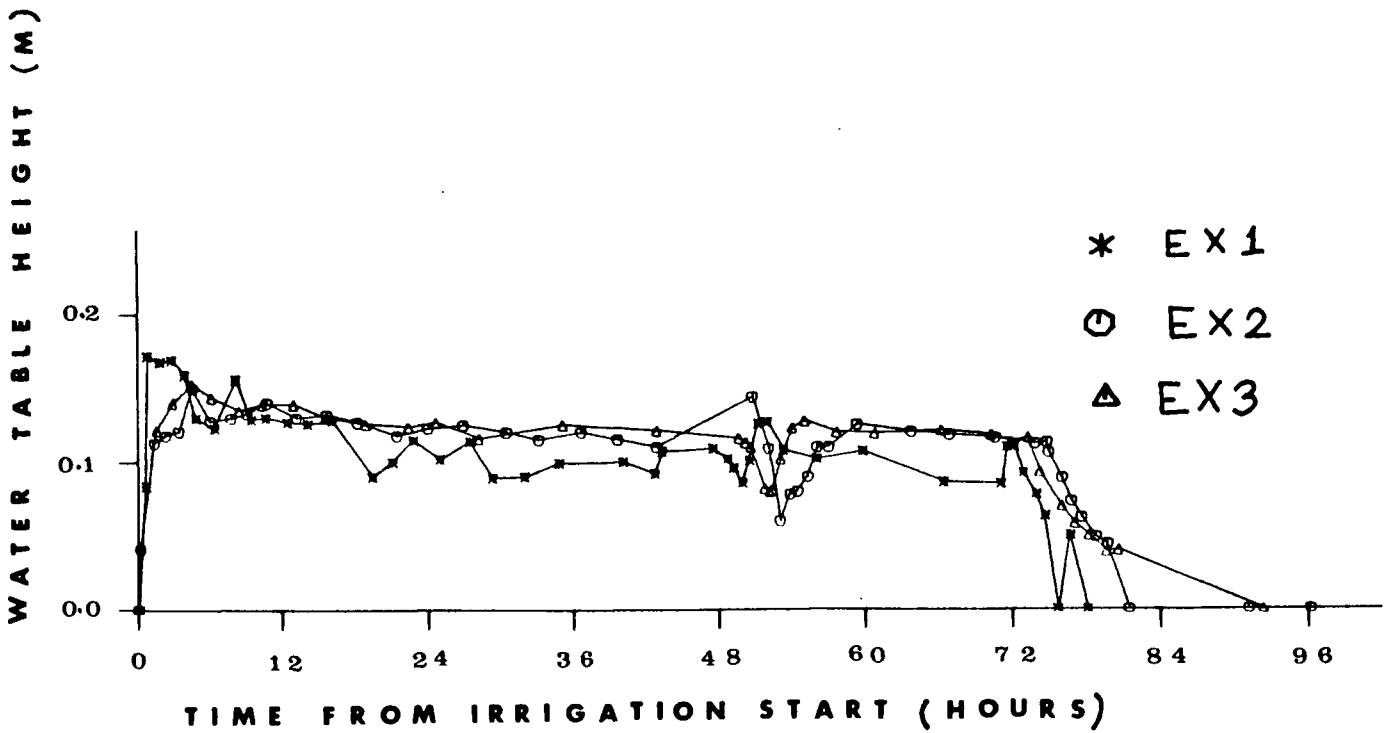

Fig. 1.4.3.1 Water table behavior at pipe 1.

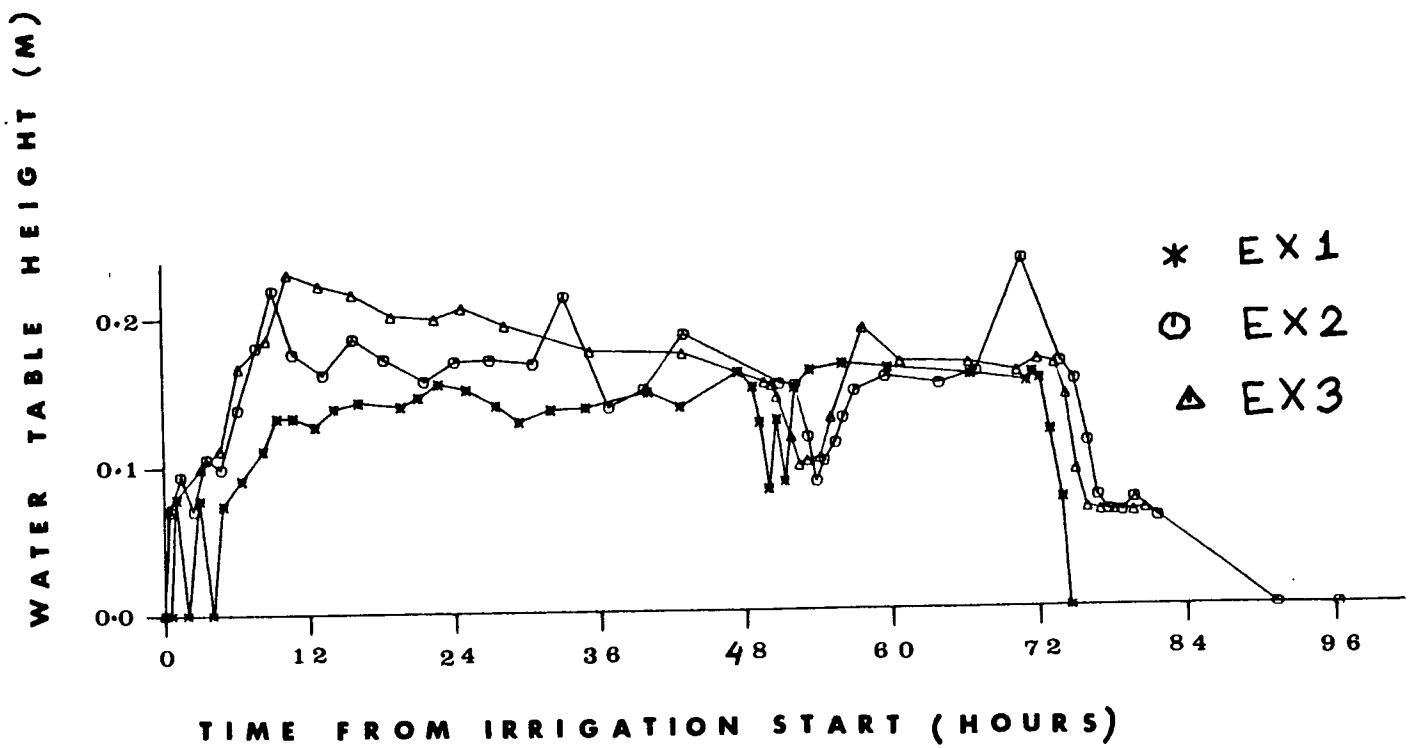

Fig. 1.4.3.2 Water table behavior at pipe 2.

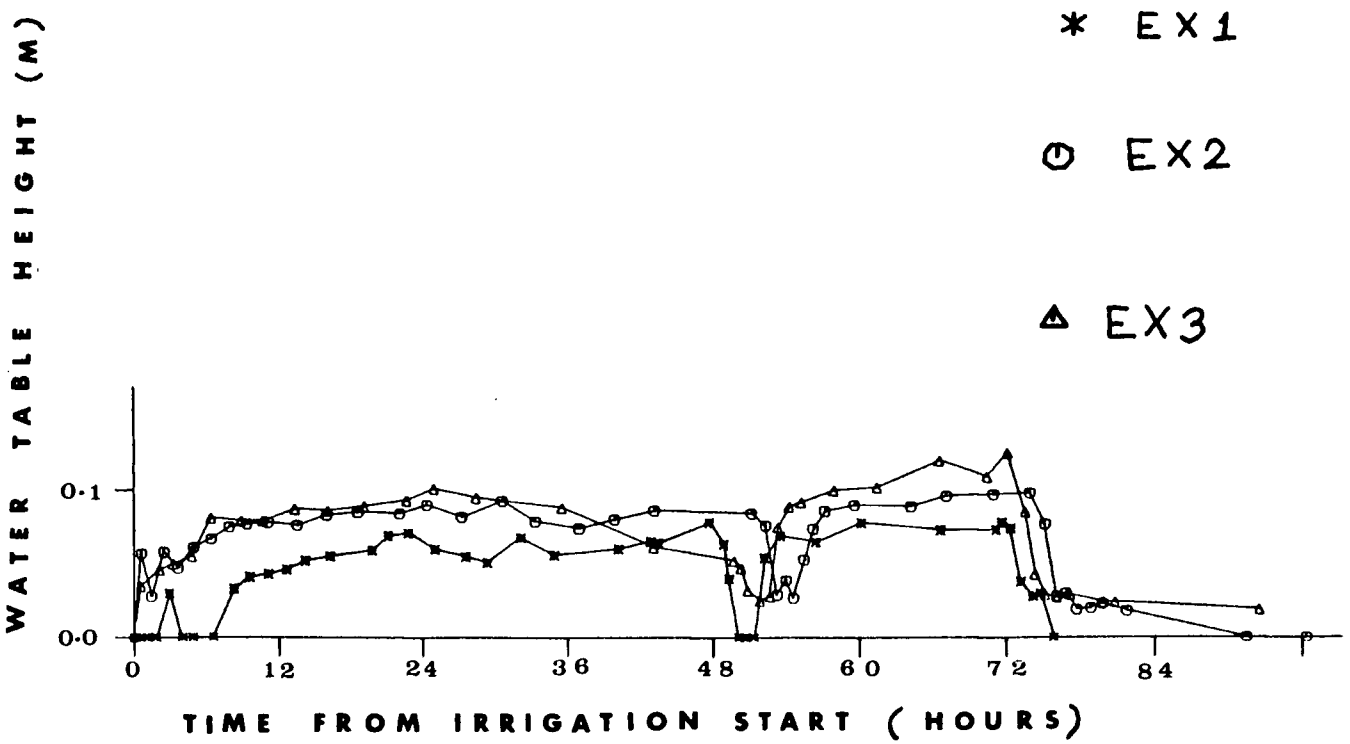

Fig. 1.4.3.3 Water table behavior at pipe 4.

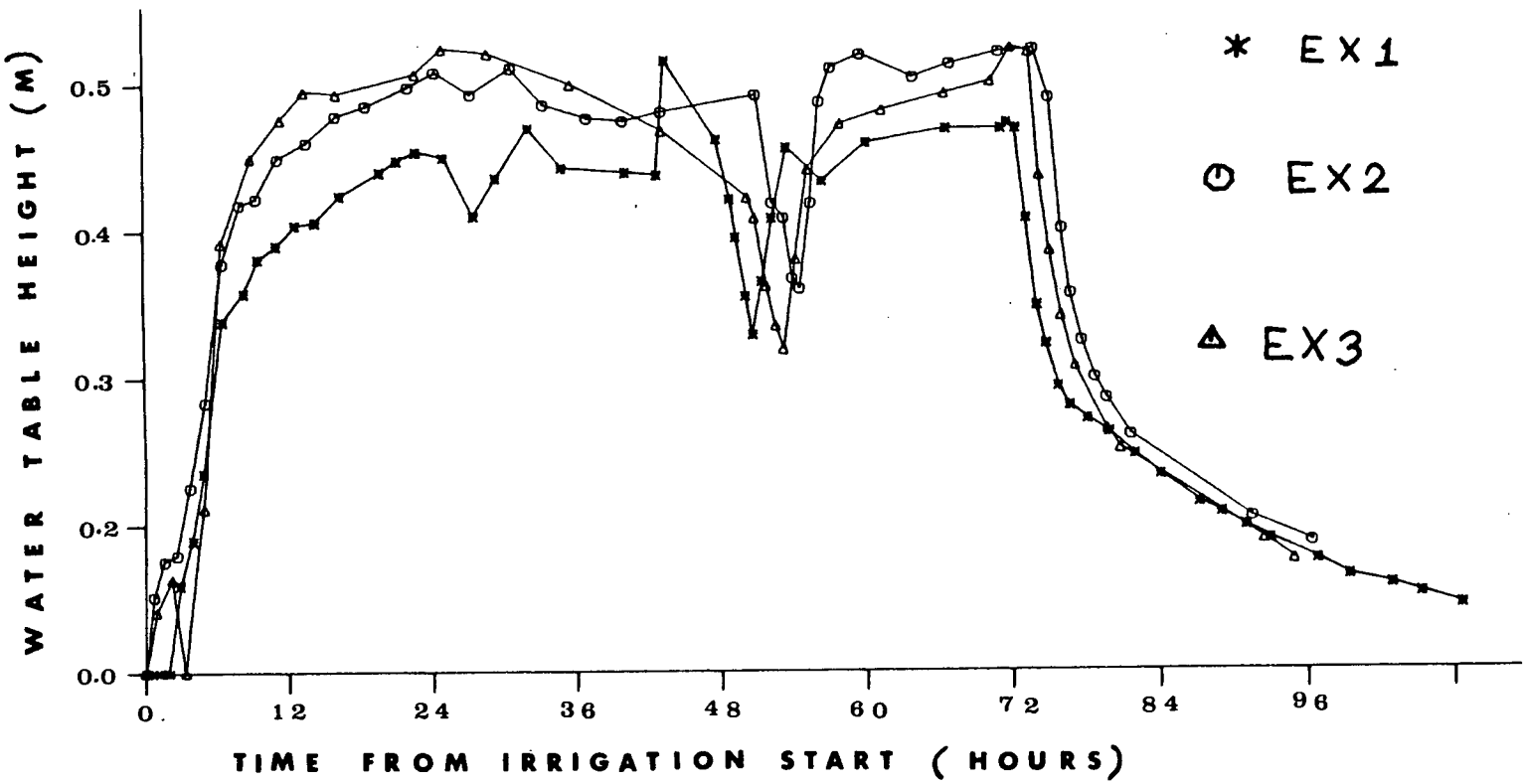

Fig. 1.4.3.4 Water table behavior at pipe 5.

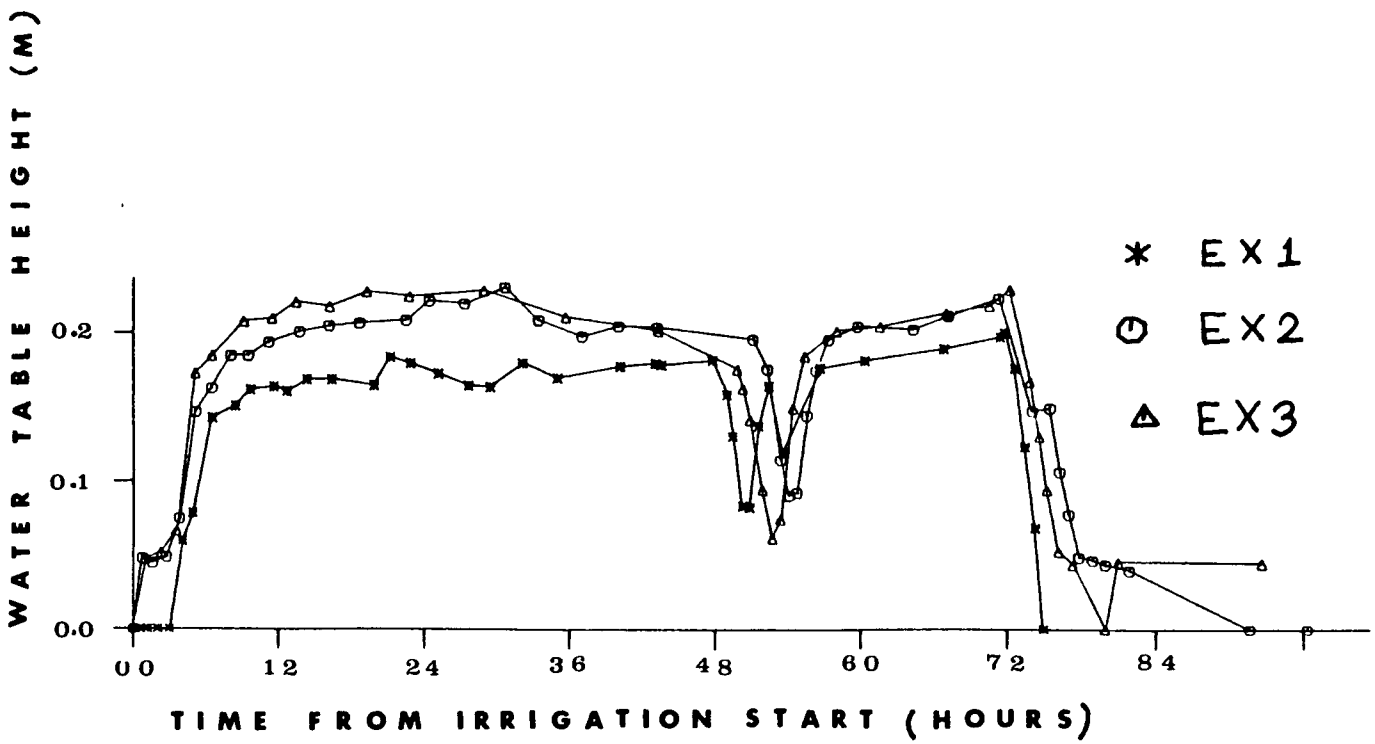

Fig. 1.4.3.5 Water table behavior at pipe 6.

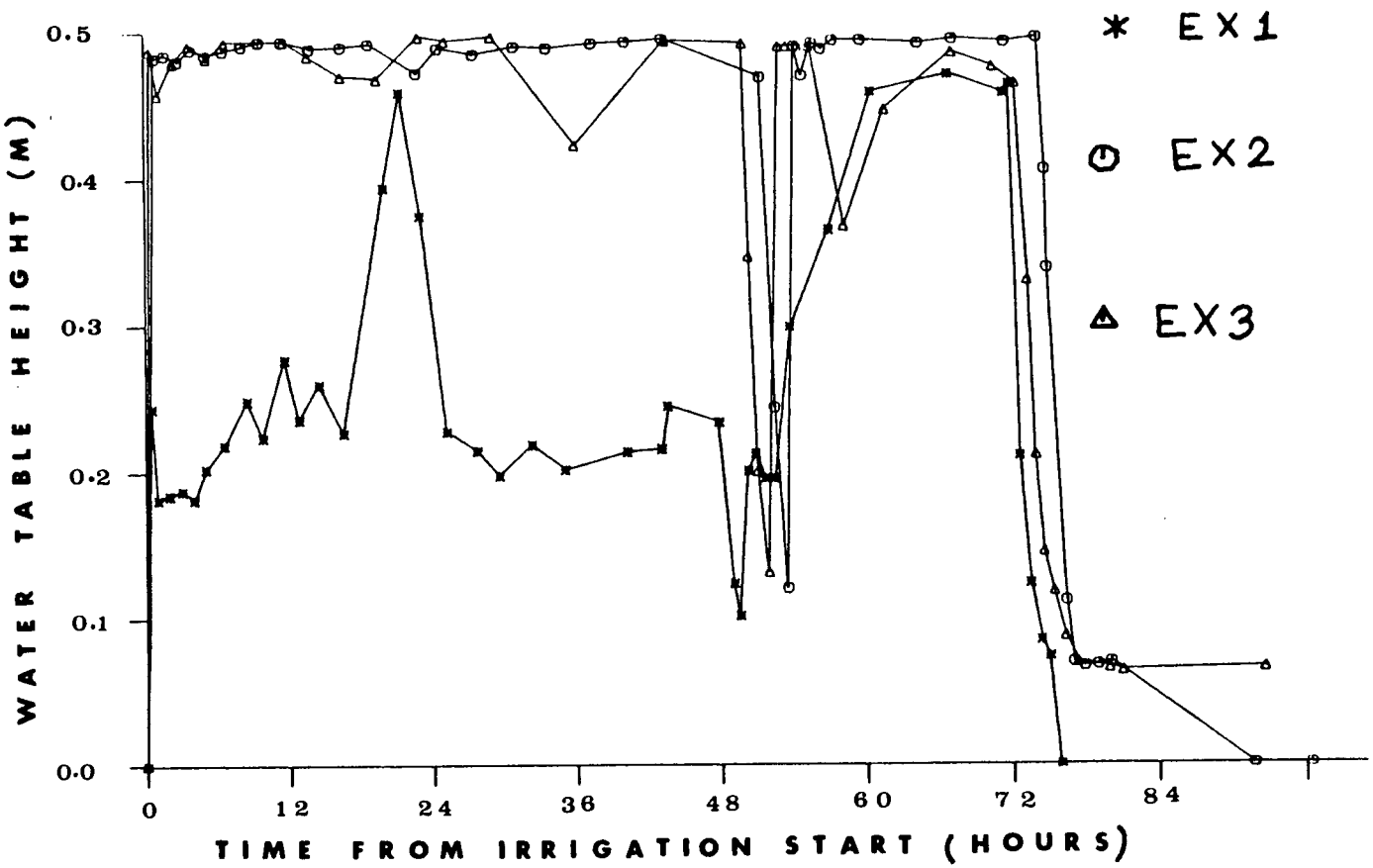

Fig. 1.4.3.6 Water table behavior at pipe 8.

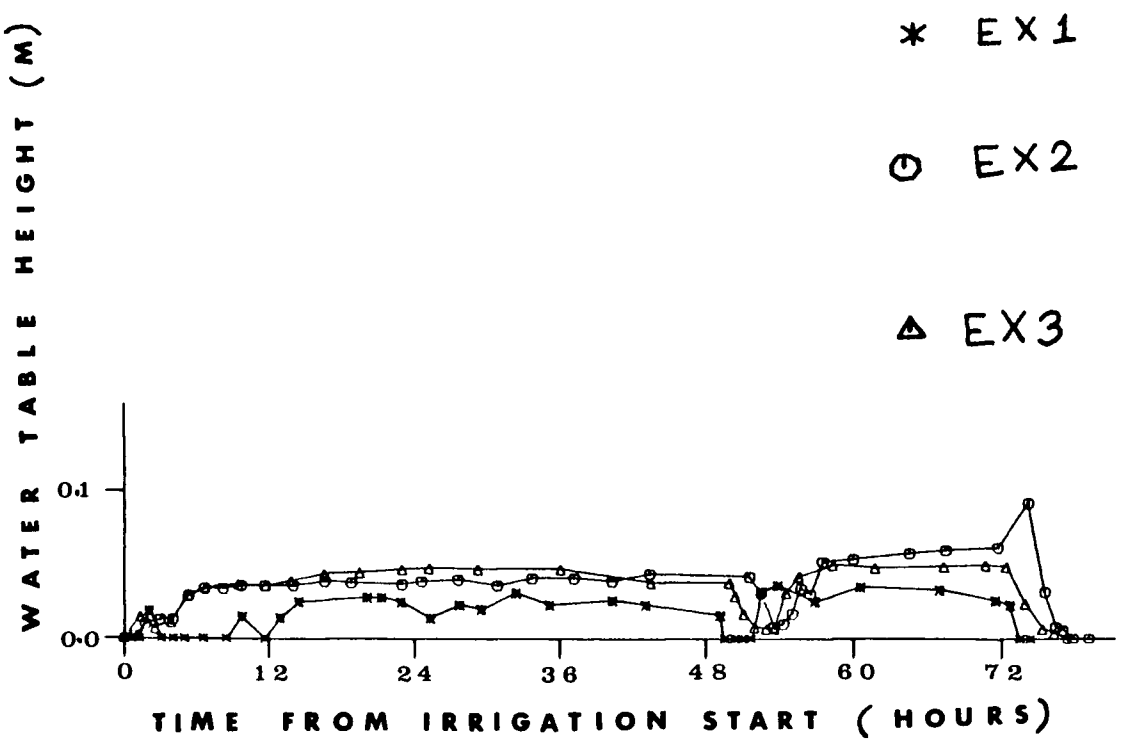

Fig. 1.4.3.7 Water table behavior at pipe 12.

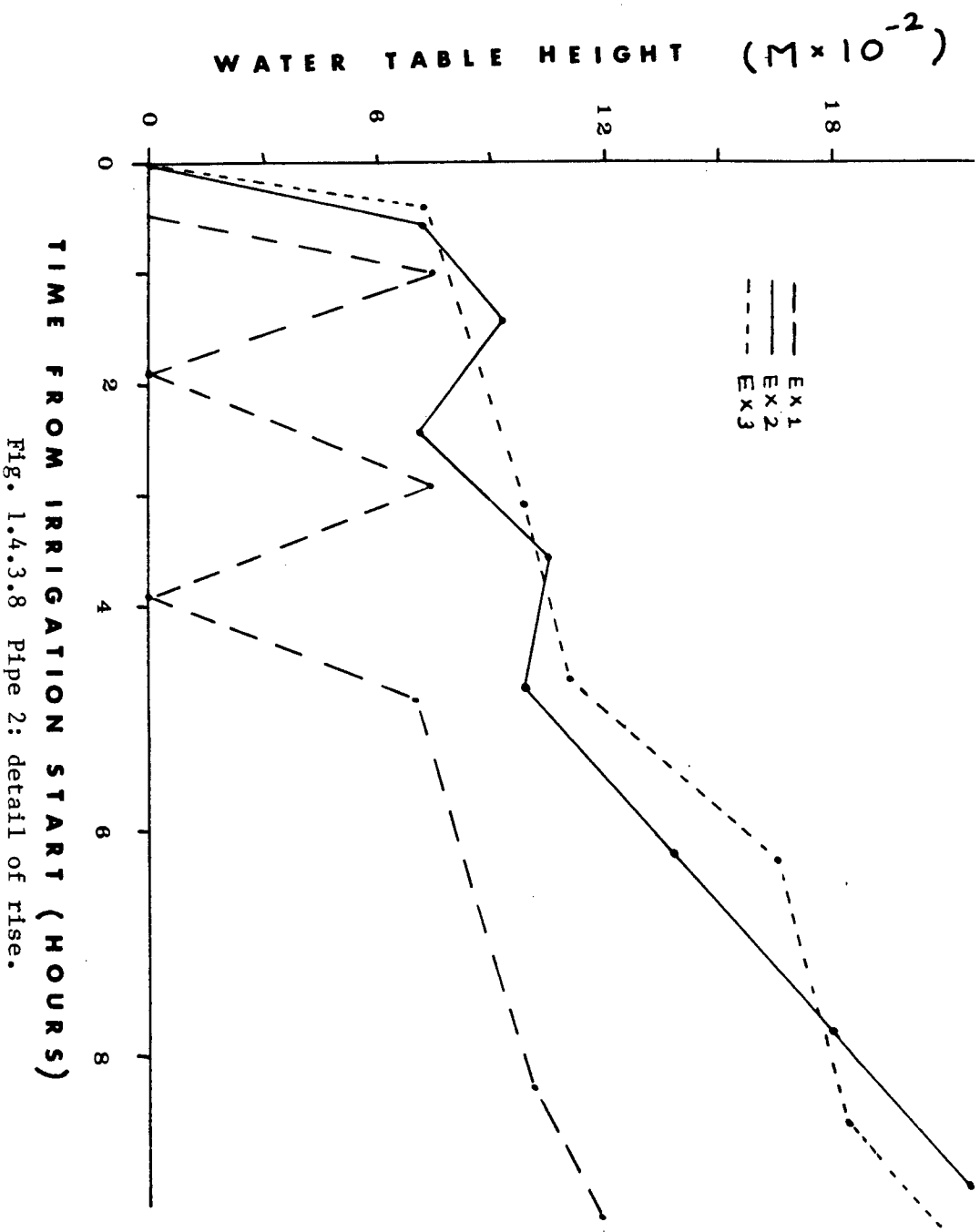

Fig. 1.4.3.8 Pipe 2: detail of rise.

1.4.3.9 show the rise of pipes 2 and 12 drawn at a larger scale for clarity.

Due to the errors linked to the pipes' data, no quantitative comparison can be made of the behavior of the water table from experiment to experiment. Instead, a qualitative comparison based on the graphs will be made. Because the lags between the rises in general either are large, or are negligible, the qualitative comparison between lags is generally not affected by error. It will be assumed that similarity in rates of rise is real and not a "chance outcome" of error. For the purpose of this qualitative comparison, the rise of a pipe will be considered to be the continuous rise to steady state. That is, an initial rise followed by a fall back to zero will be ignored.

Figures 1.4.3.1 to 1.4.3.7 show that for the three experiments, there was no water in the pipes prior to irrigation.

Comparison of the rises for Ex1 and Ex3 using Figs. 1.4.3.1 to 1.4.3.7 shows the following: Pipes 1 and 8 rise as soon and as fast for Ex1 as for Ex3. Pipes 4 and 12 rise later for Ex1.

The rate of rise of pipe 4 is slower for Ex1. For pipe 12, the comparison is difficult to make. Pipes 2 and 6 rise later for Ex1 but at the same rate.

Pipe 5 rises slightly earlier for Ex1 but at the same rate. Thus the water table has some tendency to rise later for Ex1 but in general rises at the same rate. The delay in rise must be due to drier initial conditions.

Comparison of the rises for Ex2 and Ex3 shows that rises occur at the same time for Ex2 as for Ex3, except that pipe 5 starts to rise

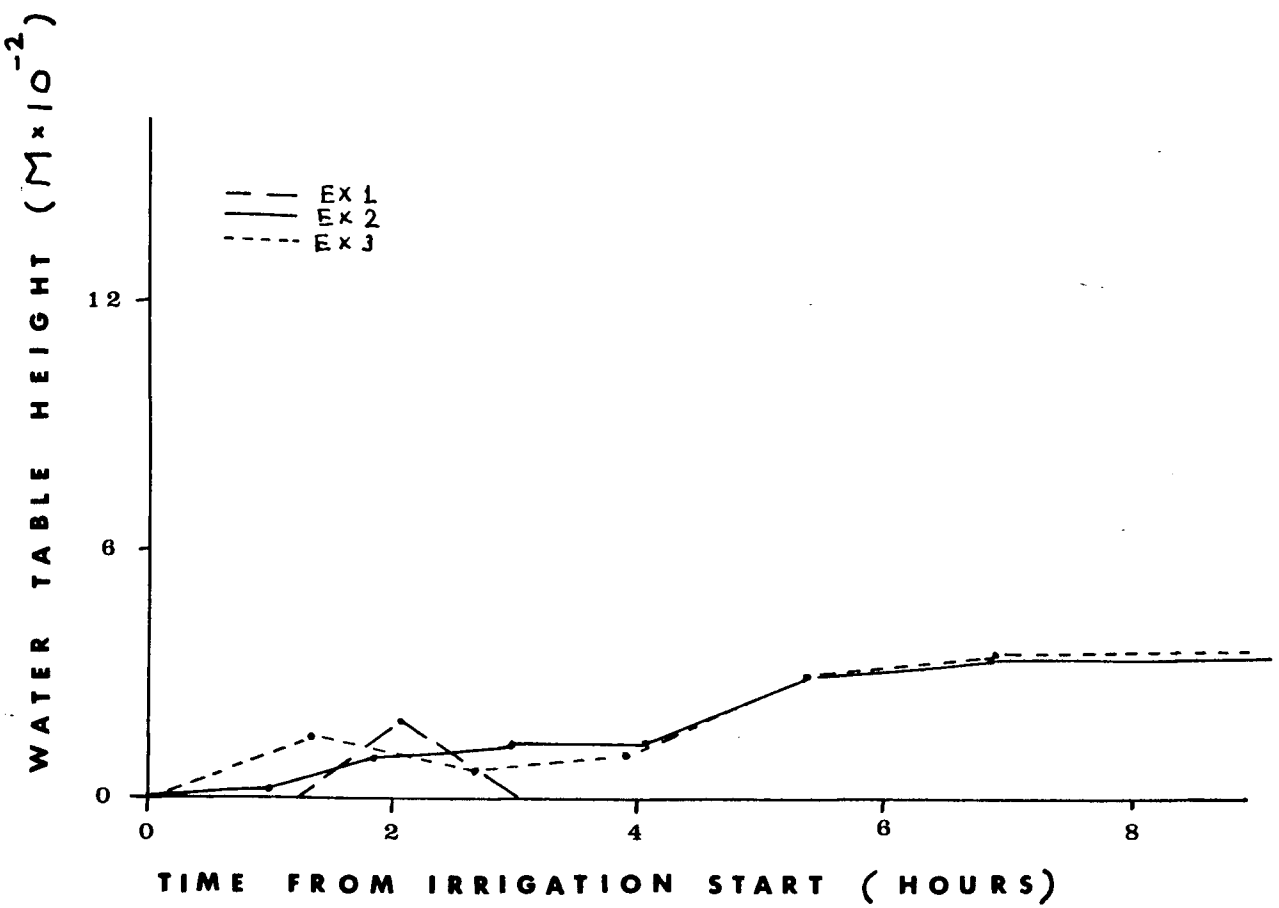

Fig. 1.4.3.9 Pipe 12: detail of rise.

later for Ex3. Rates of rise are similar for the two experiments. Thus concentration of irrigation does not, in general, yield an earlier rise. Neither does it yield a faster rise.

Table 1.4.3.2 gives steady state values obtained from the standpipes for the 3 experiments. These values are averages estimated by eye.

Table 1.4.3.2 shows that differences between steady state values for Ex2 and Ex3 are less than 2 cm. Relative differences were obtained as the ratio of the absolute value of the difference between the value for Ex2 and the value for Ex3 to the average of these values. The largest relative difference found was 0.2 and was obtained for the shallowest pipe, pipe 12.

Thus, concentrating the irrigation has no significant effect on the shape of the water table at steady state.

Figures 1.4.3.10 to 1.4.3.12 show the water table behavior during rise and recession. Pipes are shown on a cross section downslope. That is, horizontal distances between pipes in Figs. 1.4.3.10 to 1.4.3.12 are distances between their projections onto the ordinate of Fig. 1.3.1.1. This ordinate is the horizontal projection of a line taken in the general direction of the slope. The times chosen for steady state are not necessarily the times at which steady state was first reached.

Problems with Figs. 1.4.3.10 to 1.4.3.12 are that the hillslope is not long enough and there are not enough measurement points to make a definite statement about the shape of the water table. Moreover, except at pipes 4 and 6, it is not certain that the shape of the bed is correct because it is not certain the pipes reached the bed.

Table 1.4.3.2 Steady state values for standpipes (m); relative differences between Ex2 and Ex3 (absolute values)

Pipe	Ex1	Ex2	Ex3	Relative Differences Between Ex2 and Ex3*
1	0.114	0.120	0.120	0.0
2	0.150	0.168	0.183	0.08
4	0.066	0.081	0.090	0.10
5	0.354	0.393	0.396	0.008
6	0.174	0.201	0.210	0.04
8	0.300	0.483	0.480	0.006
10	0.318	0.336	0.336	0.0
11	0.126	0.147	0.156	0.06
12	0.030	0.039	0.048	0.20
Average	0.181	0.219	0.224	

* $\frac{|Ex2 - Ex3|}{(Ex2 + Ex3)/2}$

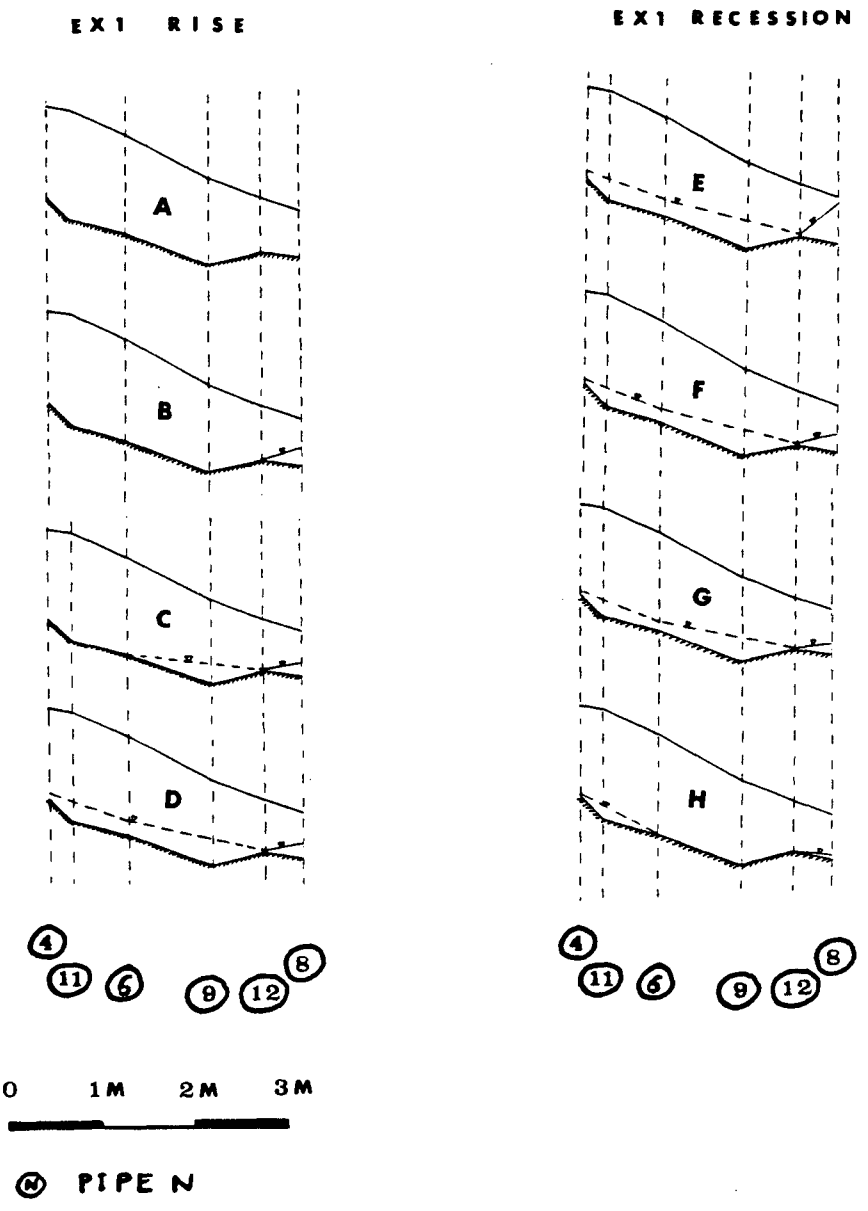

Fig. 1.4.3.10 Water table shape for EX1. See p. 68 for explanation.

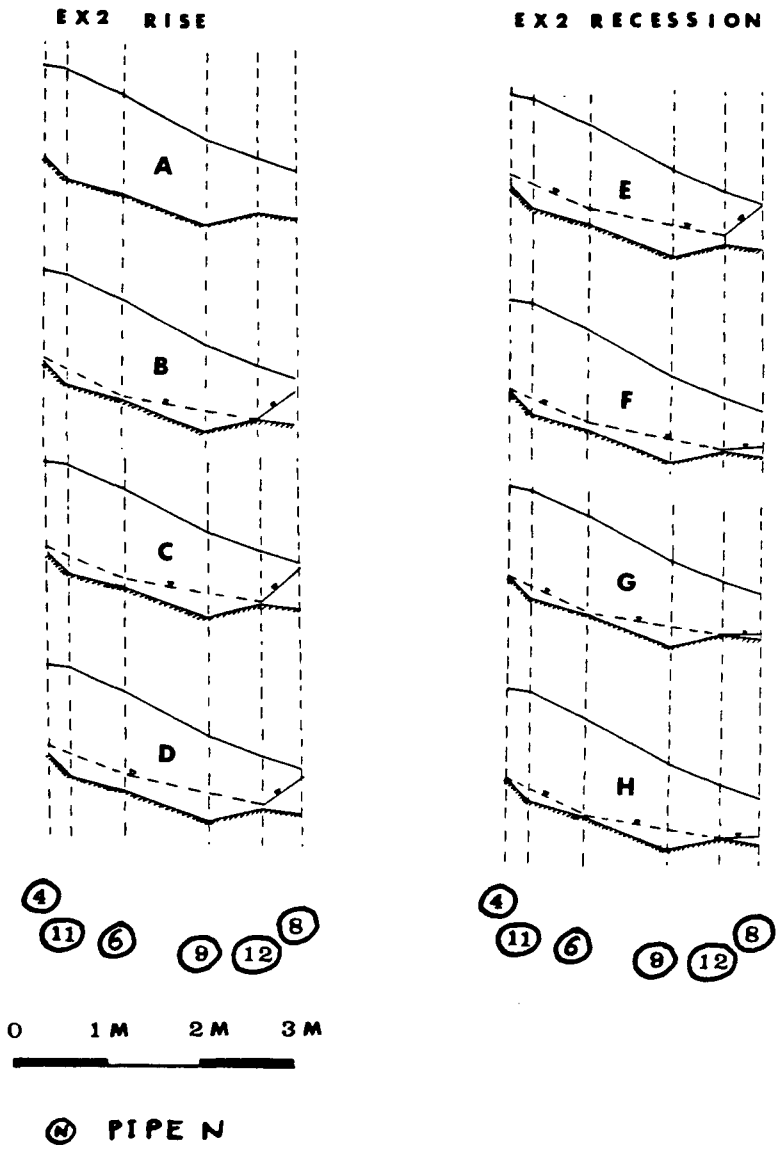

Fig. 1.4.3.11 Water table shape for EX2. See p. 68 for explanation.

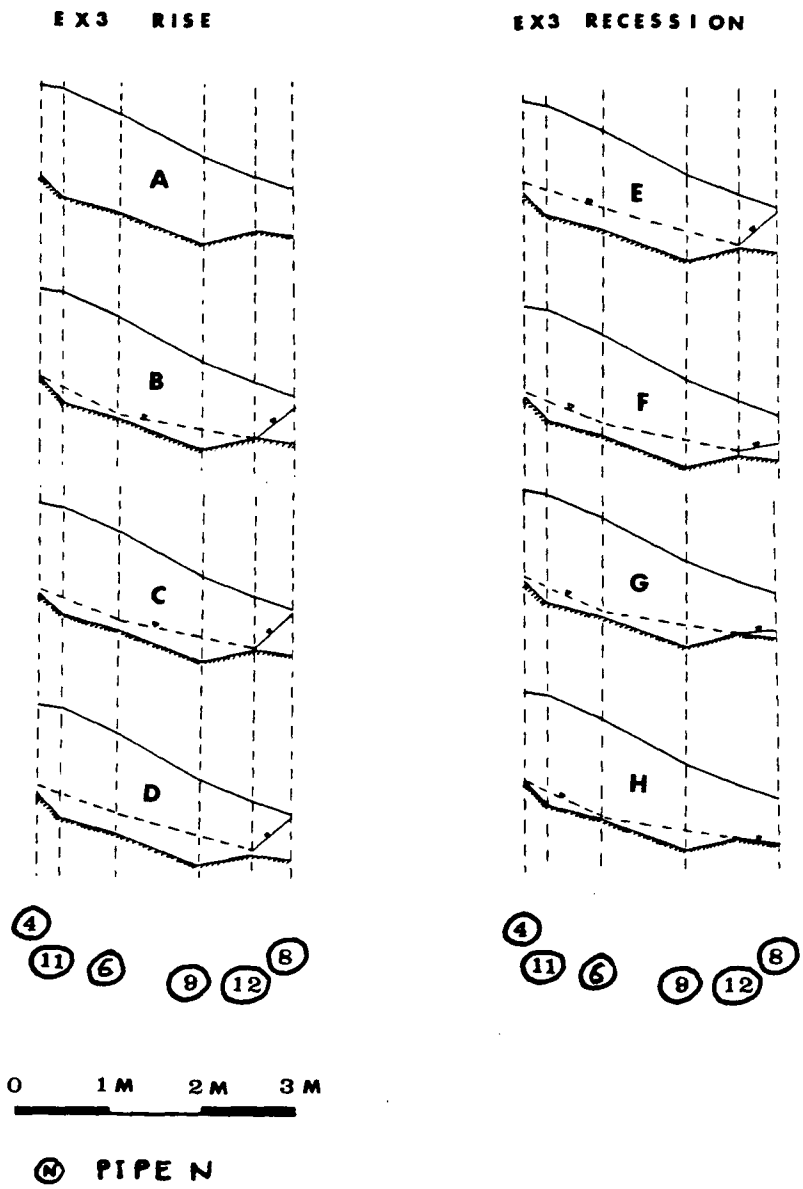

Fig. 1.4.3.12 Water table shape for EX3. See p. 68 for explanation.

Ex1

Rise:
- A: Before start of irrigation
- B: 14:18 July 31, i.e. 37 min after start of irrigation
- C: 15:12 July 31 i.e. 1 h 31 min after start of irrigation
- D: 03:30 August 2nd, steady state (about 38 hours after start of irrigation)

Recession
- E: Before turning irrigation off; (12:00 August 03)
- F: 14:36 August 03 i.e. 56 min after irrigation stop
- G: 15:12 August 03 i.e. 92 min after irrigation stop
- H: 17:00 August 03 i.e. 200 min after irrigation stop

Ex2

Rise:
- A: Before irrigation start
- B: 12:24 August 11 i.e. 39 min after irrigation start
- C: 16:00 August 11 i.e. 4 h 15 min after irrigation start
- D: Steady state, 09:00 August 12 (about 21 hours after start of irrigation)

Recession
- E: Before turning irrigation off; (13:30 August 14)
- F: 16:00 August 14 i.e. 111 min after irrigation stop
- G: 19:00 August 14 i.e. 4 h 51 min after irrigation stop
- H: 21:00 August 14 i.e. 6 h 51 min after irrigation stop

Ex3

Rise:
- A: Before start of irrigation
- B: 12:36 August 20, i.e. 41 min after start of irrigation
- C: 16:12 August 20 i.e. 4 h 17 min after start of irrigation
- D: 14:00 August 21, steady state (about 26 hours after start of irrigation)

Recession
- E: 1 h before irrigation stop
- F: 1 h 20 min after irrigation stop
- G: 3 h 20 min after irrigation stop
- H: 4 h 20 min after irrigation stop

As mentioned in Section 1.3.5, data for pipes 9 and 11 are not reliable. Hence a dotted line has been drawn at these pipes, joining the water levels of pipes 4 to 6, then 6 to 12. If there was no water in both pipes 4 and 6, the dotted line was drawn to follow the bed, except before start of irrigation. The same approach was followed between pipes 6 and 12.

To summarize, under conditions of lower initial water content, the water table has some tendency to rise later but in general rises at the same rate. Concentration of irrigation did not, in general, cause the water table to rise earlier or faster. Neither did it affect the shape of the water table at steady state.

1.4.4 Comparison of the Recession with Hewlett and Hibbert's (1963) Recession

In order to determine how steep the recessions are relative to a recession obtained for a disturbed sandy loam, the recession obtained in the present work was compared to the one reported in the literature by Hewlett and Hibbert (1963). These authors built a sloping trough, filled it with sandy loam, saturated it and observed the recession. The trough was 0.91 m deep, 0.91 m wide and 13.7 m long. At the start of the recession, the saturated zone was 0.9 m deep, as compared to a maximum depth of 0.5 m in the present work. Also, the slope was 14 m long, as compared to a length of 10.5 m in the present work. The slope angle was smaller, 22° versus 32°. The soil's texture was sandy loam, the same as the one of this study. Soil, however, had been excavated

and packed into the trough hence it had lost its original structure.

Appendix C discusses the normalization of the results for comparison purposes, and the limitations of the comparison.

Figure 1.4.4.1 shows the recession for Ex1 and Figure 1.4.4.2 the recession obtained by Hewlett and Hibbert. The outflow rate for Ex1 has been expressed in $m^3 s^{-1}$ per 0.91 m of hillslope width in order to be comparable with Hewlett and Hibbert's work. Outflow rate has been plotted at the middle of the time interval used to calculate this outflow rate.

In Table 1.4.4.1, comparisons of some of Hewlett and Hibbert's data with some of those obtained in the present work for Ex1 are presented. Data have been extracted from Figs 1.4.4.1 and 1.4.4.2. t' is the time from start of recession. Q is the outflow rate or discharge (volume per unit time). Table C-1 in Appendix C gives the normalization summary for the results of the present work given in Table 1.4.4.1. The ratio of the outflow rate at one day to the one at 0.1 day is 0.64 for Hewlett and Hibbert and 0.06 for the present work. These numbers have not been corrected for the effect of a steeper slope for the present work.

The recession rate calculated between an outflow rate of 6.6×10^{-6} $m^3\ s^{-1}$ and 4.2×10^{-6} $m^3\ s^{-1}$ is 16 times larger for the present work. For the calculation of this latter number, the recession rate for the present work has been corrected as indicated in Table 1.4.4.1 so that it gives the rate that would be obtained for a hillslope of slope similar to the one occurring in Hewlett and Hibbert's work.

These results show that within the limitations stated in Appendix

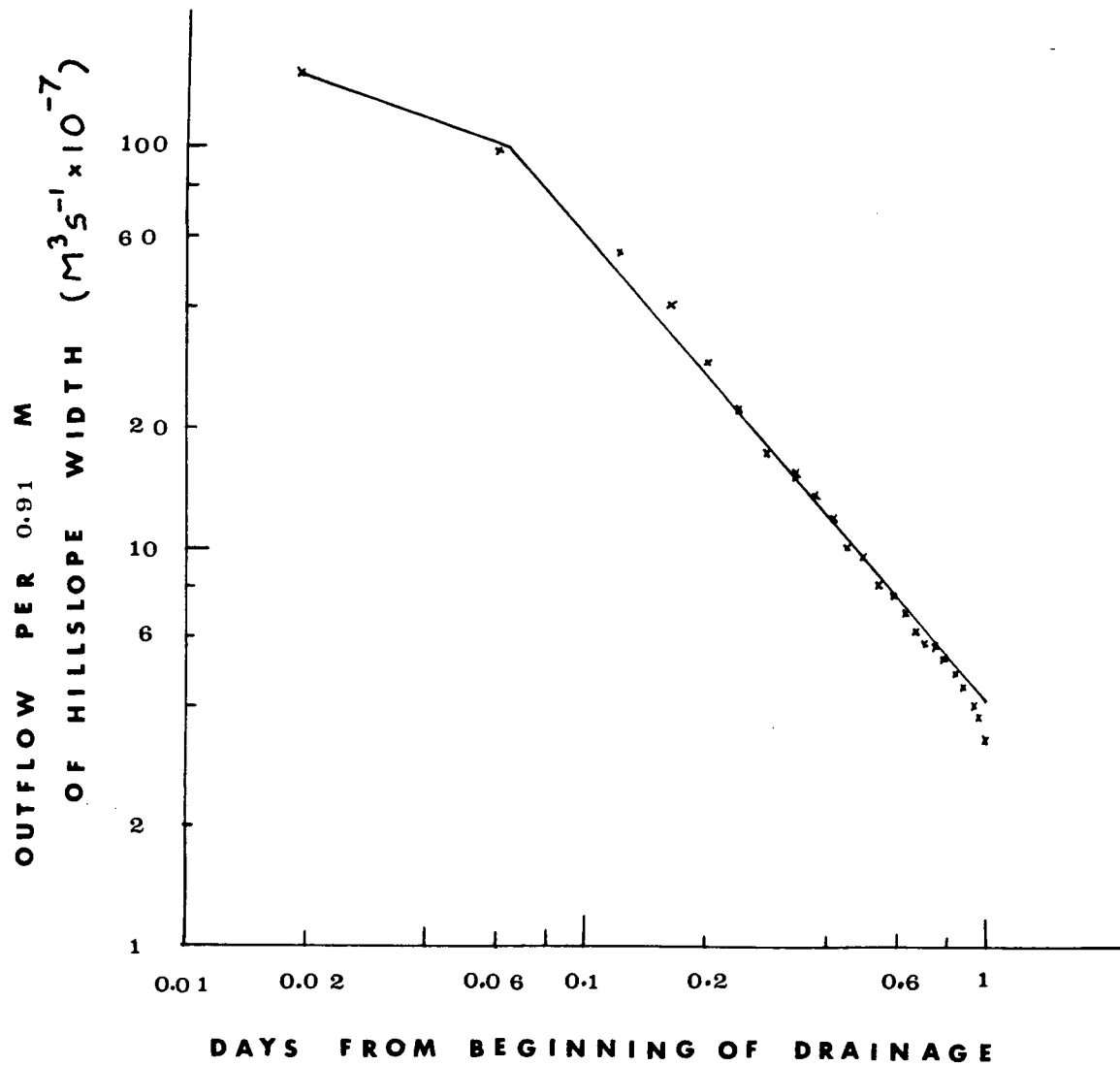

Fig. 1.4.4.1 Outflow recession for EX1.

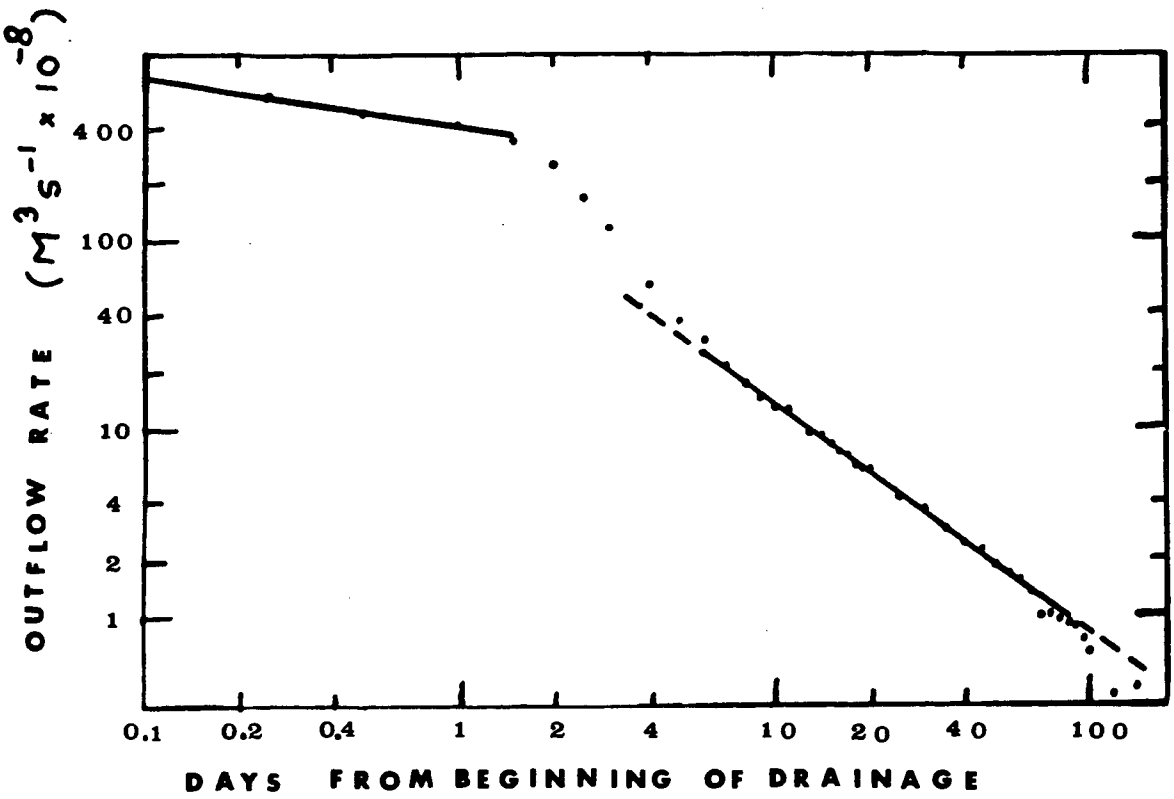

Fig. 1.4.4.2 Recession obtained by Hewlett and Hibbert (1963). Adapted from Hewlett and Hibbert's Fig. 2.

Table 1.4.4.1 Comparison of Hewlett and Hibbert's work with the the present work. Exl was chosen for the present work. Values for the present work are for 0.91 m of hillslope width.

Drainage from .1 to 1 day			
	Q at .1 day $= Q_1$ (m^3s^{-1})	Q at 1 day $= Q_2$ (m^3s^{-1})	Q_2/Q_1
Hewlett and Hibbert (H&H) (1963)	6.6×10^{-6}	4.2×10^{-6}	0.64
Present work (P.W)	6.0×10^{-6}	3.6×10^{-7}	0.06

Drainage from 6.6×10^{-6} m^3s^{-1} to 4.2×10^{-6} m^3s^{-1}				
	Time at 6.6×10^{-6} m^3s^{-1}	Time at 4.2×10^{-6} m^3s^{-1}	$\Delta t'$[1]	$\frac{\Delta t'_{H\&H}}{\Delta t'_{P.W.}} = \frac{\frac{\partial Q}{\partial t'_{P.W.}}}{\frac{\partial Q}{\partial t'_{H\&H}}}$
Hewlett & Hibbert	0.1 day	1 day	0.9 day	
Present work	0.09 day	0.13 day	0.04 day	22.5[2]
Present work corrected for slope*			0.06 day	15.8[3]

*See Appendix C.

[1] $\Delta t'$ = Time at 6.6×10^{-6} m^3s^{-1} - Time at 4.2×10^{-6} m^3s^{-1}.

[2] 0.9/0.04

[3] 0.9/0.06

C, the recession for the present work is much faster than for Hewlett and Hibbert's.

1.4.5 Visual Observation of Low Resistance Paths in the Forest Floor and the B Horizon

This section contains descriptive information about the structure of the forest floor and the B horizon. The information is based on visual examinations carried out in the field. Emphasis is placed on the presence of low resistance paths. The purpose of the section is to understand better the soil hydrologic behavior as determined by soil structural features and as reflected by the shape of the hydrograph.

The first 5 mm or so of forest floor are made up mainly of needles and twigs and are probably sufficiently open for water from individual rain drops to drip down needles. The F layer still contains large voids but a concentrated inflow is required for water to flow through these voids because water from individual rain drops would be sucked in by the humified material. The H layer contains fewer large voids. In the Seymour Watershed of the Greater Vancouver Water District, de Vries and Chow (1978) indeed noticed that the H layer together with the Ae layer formed a lower conductivity layer.

Under a large irrigation rate, larger than the one used for Ex1, Ex2 and Ex3, lateral flow was observed to occur within the forest floor. Part of the forest floor can thus act as a low resistance path.

Also, the forest floor was irrigated from a distance within one meter of a cut, using a watering can. This irrigation took place during

a rainfall occurring after several days of rain. During irrigation water was observed to come out flowing on top of a flat piece of bark of size approximately 10 by 5 cm^2 in the lower part of the forest floor.

As mentioned in Section 1.2, Mosley also observed underground lateral flow. A difference with the observation made in the present work is that he observed flow on top of the mineral layer and in the humified layer whereas in the UBC Forest, flow probably occurred on top of the composite H-Ae layer.

In the B horizon, and at the interface between the bed and the B horizon, the main source of pipelike low resistance paths are live or decaying roots. Four kinds of pipelike low resistance paths due to root material were distinguished:

(i) The decaying bark of a root. While decaying, the bark has become spongy and hence a high conductivity material.

(ii) Roots in which the interior part is decaying or missing. At places, the interior of roots was noticed to have become a fibrous material with insterstices or to have been washed away. Sometimes the bark was hard and brittle and if the interior was washed away, a cylindrical conduit resulted.

(iii) A rootmat on top of the low condutivity layer. As noted by Utting (1978), roots accumulate over the low conductivity layer because it is harder to penetrate. Utting (1978) noted that root accumulation needs a sharp B horizon-till interface to occur.

(iv) "Dark material" consisting mainly of decayed organic matter (Martin, 1983, pers. comm.) was observed in the saturated

zone. It can contain stained mineral matter and recognizable root debris. The decayed organic material is thought to consist of decayed roots (as also observed elsewhere by Martin, 1983, pers. comm.).

Points (ii) and (iv) are probably what is meant by "root channels" in the literature.

The difference between the rootmat and the dark material is not a clearcut one as the latter can be interlaced with roots and can be found in a rootmat.

In the channel dug at the bottom of the plot used for the present work, roots with decaying bark were found at places to occur in clusters and are more common than low resistance paths described under (ii).

At the North tip of the channel, a well defined and 0.5 to 1 cm thick rootmat was found between two layers of till. Interstices between the roots were clearly seen. Some mineral material and some decayed organic material was also seen. Because of the large size of the pores, this rootmat must have had a water entry pressure of zero.

At places along the channel bank, dark material appeared as lenses or around roots. A good sized lens extended 4 cm above the till. Dark material and rootmat usually coincide with concentrated outflow points. After a natural event, outflow was noticed from lenses of dark material and from the rootmat occurring at the bottom of the B horizon. Because of the hydrologic significance of the rootmat and of the dark material in the saturated zone, it would be desirable to determine the lateral extent and the depth of these features on the top of the bed which is

the zone where saturation occurs during a storm event. Unfortunately, this is difficult because the color of dark material grades from dark to almost the same color as the mineral soil.

A number of pipelike low resistance paths have been observed in the vicinity of the plot. On a 60 by 30 cm^2 vertical area of a pit dug uphill from the plot, 6 root channels of type (ii) were found, ranging in size from a few mm to 1 cm. This type of root channels was less frequent in the channel dug for the present work than in this pit. On the cut at the foot of Nagpal and de Vries' site, water was noticed flowing out through a section of decayed root bark.

Pipelike low resistance paths on the top of the bed are hydrologically more important than in the unsaturated zone. The first reason is that they are probably more widespread. The second is that since they occur in the saturated zone, there is no problem about water being able to enter them like there is in the unsaturated zone.

Small underground streams are extreme examples of flow in low resistance paths. At two places near the hillslope where the plot for the present work was chosen, small streams were seen to emerge from the ground. Similar features were already observed by Chamberlin (1972) as described in Section 1.2. It is speculated that the streams form uphill on low conductivity ground surfaces like rock, then go underground.

Some observation of short low resistance paths due to the presence of stones was also made. A few stones were observed to have roots or

rootmat against them. One had rootmat and fungi hyphae between its two split halves. A rootmat will provide a low resistance path. The few observations made indicated that low resistance paths due to stones are few and far between but observation was difficult due to the disturbance it necessitated. More work is required to determine whether free water actually flows around stones and how widespread this mechanism is.

1.4.6 Water Balance

Table 1.4.6.1 gives irrigation rates, outflow rates, average water table height and the ratio of outflow to irrigation for the three experiments.

Steady state values for the outflow have been obtained as follows: for Ex1 it is the eye average of the outflow rate recorded from 22 to 42 hrs after the start of irrigation. For Ex2 it is the plateau occurring 38 hrs after the start of irrigation. For Ex3, the plateau occurring 35 hrs after the start of irrigation has been used. For Ex2 and Ex3, the values used have been dictated by consideration of the tipping bucket behavior.

Steady state irrigation rates are time averages of the pooled irrigation rates estimated by eye as explained in Section 1.3.3 for a period extending from 6 hours before the period of outflow used till the end of this period. The rationale for using 6 hours was that it took less than 6 hours for the outflow rate to reach steady state again after the dry pulse. It can be assumed that the outflow rate is influenced by

Table 1.4.6.1 Irrigation rates, outflow rates, average water table height and ratio of outflow to irrigation for the 3 experiments

		Ex1	Ex2	Ex3	Average
Time average pooled irrigation rate (ms^{-1})	with RG11	3.17×10^{-6}	3.21×10^{-6}	(2.87×10^{-6})	
	without RG11	3.99×10^{-6}	4.04×10^{-6}	3.63×10^{-6}	
Time average steady state outflow rate	(m^3s^{-1})	1.18×10^{-4}	1.29×10^{-4}	1.30×10^{-4}	
	(ms^{-1})(1)	2.38×10^{-6}	2.61×10^{-6}	2.63×10^{-6}	
Average steady state water table height (m)		0.18	0.22	0.22	
Outflow/Irrigation	with RG11	0.75	0.81	(0.92)	0.83
	without RG11			0.72	

(1)Obtained by dividing the above entry by the area of the plot, 49.5 m^2.

the irrigation rate occurring not more than 6 hours earlier, provided the soil water content had already adjusted itself to a similar irrigation rate 6 hours earlier. The period of 6 hours may appear a little short for Ex1 for which outflow was just reaching steady state at the beginning of the outflow period used. However, it turns out that the same averages are obtained if the time average pooled irrigation rates are taken from the start of irrigation.

Values in brackets are calculated by multiplying the value obtained experimentally without RG11 by 0.8 in order to take RG11 into account as explained in Section 1.3.3. The average steady state water table height is the arithmetic mean of the steady state values given in Table 1.4.3.2.

One puzzling result is the fact that the irrigation rate is lower for Ex3 than for Ex1 and Ex2 but the steady state outflow rate and the average steady state water table height are higher for Ex2 and Ex3 than for Ex1.

The way in which the steady state value for the outflow rates have been estimated is perhaps partly responsible for their being inconsistent with the irrigation rate.

Errors in outflow rate mentioned in Appendix E and irrigation rate are also responsible.

Note that multiplying the pooled irrigation rate by 0.8 for Ex3 is possibly ludicrous in view of the errors attached to the irrigation rate. Also, for the time periods chosen for Table 1.4.6.1 the value multiplied by 0.8 is hardly closer to the values obtained for Ex1 and Ex2 than the value obtained without RG11.

However, comparing the irrigation rates for the whole lengths of the experiments (Fig. 1.4.2.2 to 1.4.2.5) shows that the irrigation rate for Ex3 is closer to the one for Ex1 and Ex2 when all three rates are calculated without RG11 than when the rates for Ex1 and Ex2 are calculated with RG11. By the same token, the rate for Ex3 should be closer to the rates for Ex1 and Ex2 when all three rates are calculated with RG11 than when only the rates for Ex1 and Ex2 are calculated with RG11. It is therefore thought that the correction has some value, especially because the ratio of time average of the pooled irrigation rate with to without RG11 is 0.8 for both Ex1 and Ex2. Table 1.4.6.1 shows that about 10% to 25% of the water is lost. The average ratio of outflow to irrigation for the three experiments is 0.83. A value of 0.80 will be used whenever the water balance will have to be taken into account for calculations. In spite of the uncertainties linked to the outflow and the irrigation rates, the average water loss found for the Forest plot corresponds approximately to the loss of about 20% found by Utting (1978) in Nagpal and de Vries' site.

Some water was lost by tree water uptake, and some was lost at the south end of the channel.

Utting states that the loss he observed is due to infiltration into the till and possibly into the fractured bedrock. It is likely that most of the loss observed for the Forest plot is due to the same cause.

1.5 Discussion

The transformation of a rainfall hyetograph into an outflow hydrograph reflects the integrated effect of the hydrologic behavior of

both the saturated and the unsaturated zone (de Vries, pers. comm.). This behavior is related to the soil's texture and structure, and the mechanism of water flow through it. In this section, we shall attempt to infer flow mechanisms in the Forest soil from the outflow hydrograph, the behavior of the water table and the visual observation of low resistance paths.

Because the outflow hydrograph reflects flow in both the unsaturated and saturated zones, the transformation of the rainfall hyetograph into an outflow hydrograph occurs in two steps.

The first step is the transformation of the rainfall hyetograph into a "recharge hyetograph." This transformation results from travel of water through the unsaturated zone from the ground surface to the bed or to the water table.

The second step is the transformation of the recharge hyetograph into an outflow hydrograph as water flows over the bed to the channel.

In the Forest plot, the unsaturated zone generally extends through the forest floor and through all or part of the B horizon. The saturated zone occurs on top of the bed. The low resistance paths present on top of the bed, although they may be considered to be technically structural features of the B horizon, will not be considered to be part of the B horizon. The bed can be considered as a second infiltrating surface since water reaching it either flows laterally on top of it or infiltrates into it, in the same way as rainfall reaching the ground surface.

Definitions of the terms used for various parts of the hydrograph rise were given in Section 1.4.2. Also, the term "steady" is used with

the meaning of constant in time while the term "uniform" means constant in space.

In the following two subsections, soil hydrologic behavior will be inferred from the main hydrograph features presented in Section 1.4.2. Flow of water in the unsaturated zone will be discussed first, followed by a discussion of the saturated flow taking place laterally on top of the bed.

1.5.1 Water Flow in the Unsaturated Zone

Because an important hypothesis of the present work is that short-circuiting alters the shape of the outflow hydrograph, some time will be devoted to the consideration of short-circuiting and of its effect on the outflow hydrograph.

The expected effects of short-circuiting within the unsaturated zone on the hydrograph rise are depicted schematically in Figures 1.5.1.1 (a) to (e). For simplicity, a straight line rise has been chosen for the case when flow through the unsaturated zone is uniform. A straight line rise is consistent with the kinematic wave model that will be used below. It is also consistent with the straight line main limbs of rise obtained for the present work. The reasoning presented below can easily be extended to a more general shape of rise.

In Fig. 1.5.1.1 it is also assumed that outflow is recorded as soon as water reaches the bed at the bank of the channel. It ignores the time to break through into the channel and routing in the channel. Soil properties in the saturated zone are assumed to be uniform.

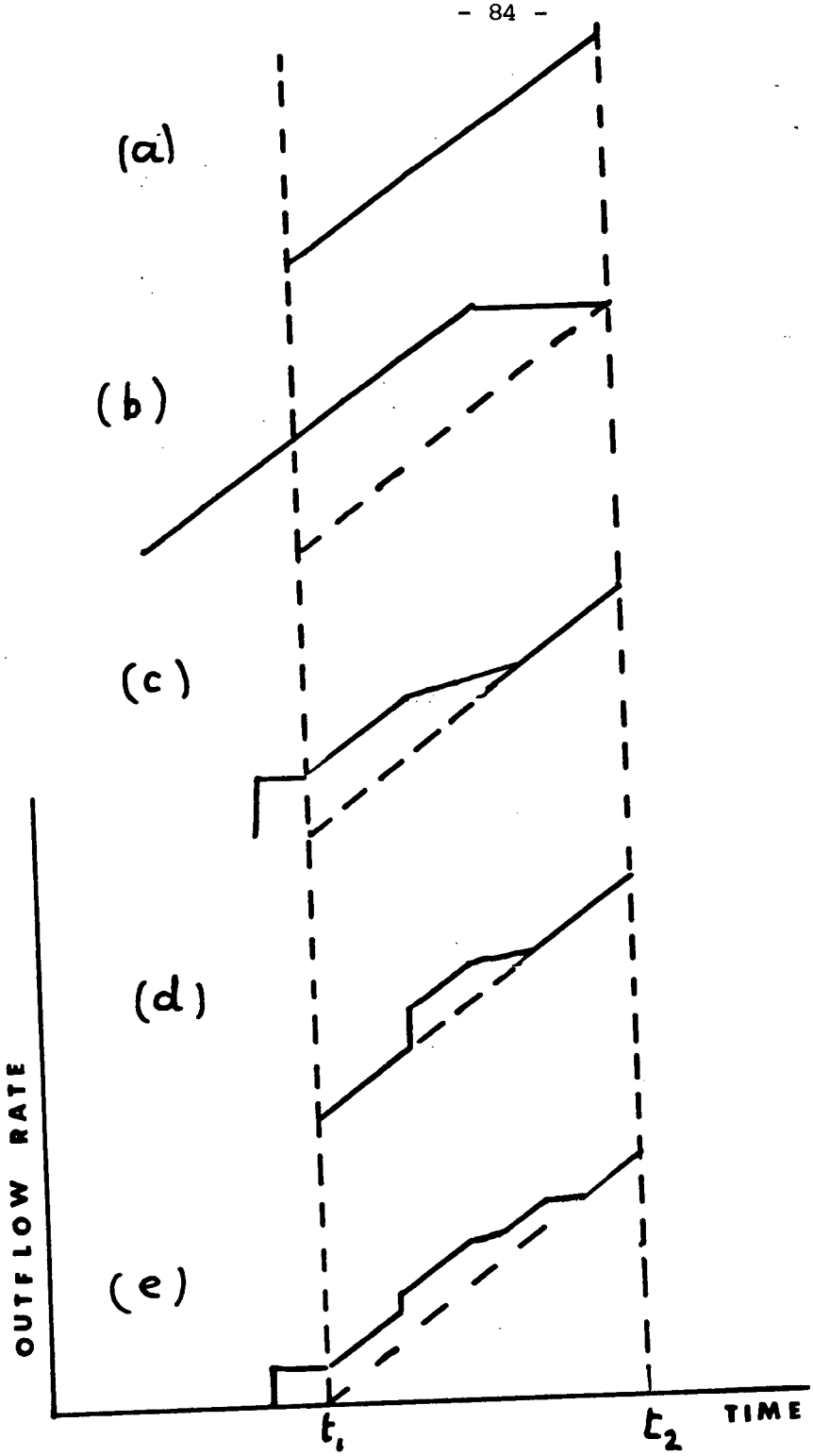

Fig. 1.5.1.1 Schematic hydrograph rises showing the effect of short-circuiting in the unsaturated zone.

Figure 1.5.1.1 (a) shows the rise expected from uniform flow reaching the bed everywhere at the same time. The main limb of rise consists of the whole rise, from t_1 to t_2.

In Figs. 1.5.1.1 (b) to (e), dashed lines indicate the shape the hydrograph rise would have if flow down to the bed occurred uniformly.

Figure 1.5.1.1 (b) shows the rise expected if all the water short-circuits the soil matrix and reaches the bed at the same time. The shape of the rise is the same as for the uniform case because as in the uniform case, it is governed solely by flow on top of the bed but the rise is shifted to the left. In this case as well, the main limb of rise consists of the whole rise. This case is extreme and in general unrealistic.

In Figs. 1.5.1.1 (c) to (e), some short-circuiting occurs but a significant proportion of flow still occurs through the matrix. Therefore, for these cases, the main limb of rise still starts when the water having travelled uniformly in the unsaturated zone reaches the bed. The time at which the main limb of rise starts is thus independent from short-circuiting and is equal to t_1 like for the uniform case.

Also, it is likely that for both the uniform and the nonuniform cases, the water being last to reach the channel will be water having travelled uniformly down the unsaturated zone in the remotest parts of the watershed or plot. Therefore, it is likely that steady state will be reached at the same time t_2 whether flow in low resistance paths and as fingers occurred or not. In Figs. 1.5.1.1 (a) to (e), because a straight line rise has been assumed for uniform flow through the

unsaturated zone, the main limb of rise ends when steady state is reached.

In Fig. 1.5.1.1 (c), it is assumed that all the water short-circuiting the soil matrix in the unsaturated zone reaches the channel before the water having travelled uniformly. An initial step occurs, followed by a main limb of rise broken into two by a less steep rise. This less steep rise occurs when the water that has short-circuited the soil matrix and has already reached the channel would reach the channel had it travelled uniformly in the unsaturated zone. It is possible that in practice this less steep rise will not be discernable. The overall slope of the whole rise and of the main limb of rise will be less steep than for the uniform case.

Figure 1.5.1.1 (d) depicts the rise expected for the case where water that has short-circuited the soil matrix reaches the channel only after water that has travelled uniformly. A sharp increase in flow occurs due to the arrival at the channel of the water that has short-circuited the matrix. This increase is followed by the continuation of the rise due to uniform flow, then by a less steep rise caused by the same mechanism as in Figure 1.5.1.1 (c). It is possible that these irregularities in the rise would not be significant enough to be noticed in practice. The overall slope of the rise and of the main limb of rise will be the same as for the uniform case.

Figure 1.5.1.1 (e) is a combination of (c) and (d) and the most likely to occur in reality for all but very short hillslopes. The overall slope of the rise and of the main limb of rise will be less steep than for the uniform case.

In order for flow in low resistance paths to occur, two things are necessary: the presence of low resistance paths within the unsaturated zone and a supply of free water. If it occurs, flow in pipelike low resistance paths due to root material within the unsaturated zone may have a significant lateral component as roots grow laterally as well as downward.

In order for flow as fingers to occur, a supply of free water is necessary.

In the Forest, free water necessary for flow in low resistance paths and as fingers is supplied by concentration of water by concentrating elements. These elements include the tree canopy, logs, litter on top of the forest floor as suggested for other forest soils by Whipkey (1968), and de Vries and Chow (1978), pieces of wood within the forest floor, stones and water repellent spots. Fungi observed in the Forest may be responsible for water repellency and corresponding concentration since, according to Bond (1964), Bond and Harris (1964) noted that water repellency may be due to fungi.

The presence of both low resistance paths and concentrating elements suggests that some short-circuiting may take place.

Now that a theoretical basis has been set the observed outflow hydrographs will be used to shed some light on flow mechanism in the unsaturated zone.

The mechanism of flow in the unsaturated zone should be inferred from the "recharge hyetographs." However, since these hyetographs are unknown, the outflow hydrographs must be used. The main features of the

hydrographs presented in Figs. 1.4.2.2 to 1.4.2.5 will be discussed in turn.

(i) Little Preliminary Outflow Before the Main Limb of Rise

The outflow hydrographs pictured in Figs. 1.4.2.2 to 1.4.2.5 show little preliminary outflow before the main limb of rise. This is confirmed by the detailed rises in Fig. 1.4.2.6 which show an initial step with only a very low outflow rate for Ex1 and Ex3.

For Ex2, the steep small rise before the main limb of rise has been called technically an early rise. Practically, being steeper than the main limb of rise, it could be considered that it is part of it and that there is thus no preliminary outflow for Ex2.

The only error listed in Appendix E that may decrease significantly the recorded initial outflow and shed some doubt as to whether the initial outflows before the main limbs of rise are indeed small is the fact that some water escaped collection by the channel. However, hydrographs obtained by Utting (1978) and by Nagpal and de Vries (1976) on the latter authors' site also display very little initial outflow. Therefore it is likely that there is little initial outflow from the Forest plot.

An error that limits the comparison of the hydrographs of the 3 experiments is that they were not normalized with respect to irrigation rate.

An initial step is due to water reaching the channel before the main limb of rise starts. This water could have reached the bed via low

resistance paths or by finger flow, thus "short-circuiting" the soil matrix.

The fact that the outflow rate during the initial step of Ex1 and Ex3 shown in Fig. 1.4.2.6 is so small suggests that only very little short-circuiting took place.

One result that perhaps appears to confirm the occurrence of some short-circuiting is the fact that pipes 1, 5 and 8 displayed a rise as early and as fast for Ex1 as for Ex3. Indeed, if flow were to occur all the way through a low resistance path, initial conditions would have no effect.

Appendix B shows that for Ex2 the plastic sheets concentrated water at least 100 times. Plastic sheets covered 20% of the Forest plot. It was expected that such a large concentration of irrigation water and hence increase in free water supply would trigger or enhance short-circuiting, possibly causing an initial step to occur, or causing an initial step already occurring under uniform irrigation to occur earlier or be larger. Contrary to this expectation, the hydrograph for Ex2 does not display an initial step although the ones for Ex1 and Ex3 do display a small one.

Note that it is possible that no enhanced early step was observed for Ex2 because the plastic sheets were not close enough to the channel. Consequently, a rise of the type depicted in Fig. 1.5.1.1 (d) might be expected for Ex2, rather than of the type of Fig. 1.5.1.1 (c). Due to the fact that irregularities in the main limb of rise may not be observable in practice, it could be argued that a rise similar to the

one depicted in Fig. 1.5.1.1 (d) may have occurred. However, the possibility of a rise of type 1.5.1.1 (d) will be rejected in favor of what is actually observed. Also, the plastic sheets were close to the pipes and no effect of concentration was noted on the pipes, although some effect might have been noticed had the resolution been better. Hence the result that the plastic sheets did not enhance short-circuiting will be accepted as an apparent result.

Further experiments, better controlled and monitored should be performed in order to confirm that concentration has no effect. In particular, plastic sheets should be placed uniformly.

The presence of an area of shallow soil could be another cause of preliminary outflow. Whatever the reason for the preliminary outflow, the hydrographs of Figs. 1.4.2.2 to 1.4.2.6 show that the amount of water involved is very small. Thus it can be concluded that the system behaves as if the front were uniform.

To summarize, it appears that the soil and water system in the integrated unsaturated and saturated zones domain behaves as if very little short-circuiting, if any, occurred at the beginning of the outflow, and as if, within the limitations of the experimental design, short-circuiting at the beginning of the outflow was not enhanced by concentration of irrigation.

(ii) Linearity of the Main Limb of Rise

A striking feature displayed by the hydrographs of Figs. 1.4.2.2 to 1.4.2.5 is the linearity of the main limb of rise. Outflow hydrographs

obtained by Nagpal and de Vries (1976) and by Utting (1978) on Nagpal and de Vries' site also display linear rises. One way to infer a flow mechanism from an outflow hydrograph is to consider a physically based model of flow yielding a similar outflow hydrograph and to speculate that the real flow occurs according to the same mechanism as the one described by the model. There is, however, no guarantee that the speculation will be correct. Even so, the similarity of the theoretical and the experimental results is interesting in that it indicates the real system behaves as if the assumptions of the model were met.

A very simple model of saturated flow in a porous medium over a sloping bed is offerred by Beven (1981). This model, hereafter referred to as "the kinematic wave model," will be described in more detail below and in Chapter II. For the moment it will be mentioned that it assumes among other things a recharge rate constant in time and uniform over the bed. It also assumes the validity of Darcy's law which means that flow must be linear. The kinematic wave model yields a straight line rise, that is, a constant $\frac{\partial Q}{\partial t}$ during the rise. The validity of Darcy's law for the Forest plot is discussed in Chapter III. It is not certain whether flow in the saturated zone of the Forest plot is linear. In order to apply the kinematic wave model to the Forest plot, it is necessary to assume flow is linear, or that nonlinearity is negligible.

Since both the observed hydrograph and the hydrograph obtained by the kinematic wave model yield a straight line main limb of rise, it can

be speculated (de Vries, pers. comm.) that the assumptions of steady and uniform recharge rate are valid for the hillslope plot. A steady and uniform recharge rate means that the recharge hyetograph is a step function and is the same step function everywhere on the bed. This would mean that apart from the small amount of water involved in the initial step for Ex1 and Ex3, all the water reaches the bed at the same time and that the recharge rate is uniform over the bed.

A number of conclusions about the hydrologic behavior of the unsaturated zone will now be drawn from a uniform and steady recharge rate during the main limb of rise.

First, uniform and steady recharge rate during the main limb of rise is consistent with no short-circuiting taking place during this period of time. In particular, this appears to indicate that flow of the type depicted by Fig. 1.5.1.1 (d) does not occur. That is, no water from short-circuiting flow reaches the channel after the arrival of water originating from uniform flow. One reason for the absence of short-circuiting could be that there are not enough pipelike low resistance paths for their entrances to receive concentrated inflow from either natural concentrating elements or from the plastic sheets. Possibly water spreads into the forest floor or the B horizon before reaching a pipelike low resistance path. Another reason may be that the walls of pipelike low resistance paths are sufficiently permeable for water to flow quickly into the matrix. This reasoning of course applies to flow in low resistance paths at all times, not only during the main limb of rise. Note that it is possible that short-circuiting does occur

but that a straight main limb of rise is due to an averaging process (de Vries, pers. comm.).

Second, a uniform and steady recharge rate is consistent with flow within the unsaturated zone being approximately vertical downward. Vertical flow in the unsaturated zone is theoretically sound since Childs (1969) notes that in the unsaturated zone, flow of water due to precipitation is mainly vertical. He explains that it is so because unsaturated soils have such low hydraulic conductivities that pressure potential gradients larger than those "commonly observed in the horizontal direction, are required to produce appreciable movements of water." Note however that Hewlett and Troendle (1975) mention the occurrence of lateral flow in the unsaturated zone of a sloping soil model. Whether lateral flow occurred in the unsaturated zone of the Forest plot should be determined experimentally.

Third, a uniform and steady recharge rate is consistent with a uniform soil thickness. The soil within the plot, however, is not uniformly thick since at the pipes its thickness varies from 0.50 m at pipe 8 to 1.66 m at pipe 10.

There can be two ways of explaining the fact that nonuniformities in soil thickness do not affect the main limb of rise.

One possibility is that nonuniformity and unsteadiness in the recharge rate due to nonuniformities in soil thickness occur only for a short period of time at the beginning of the recharge and do not influence the main limb of rise.

Another possibility is that a straight line main limb of rise is due to an averaging process. Continuous monitoring of the water table

height during the early part of irrigation would help determine whether the recharge actually started everywhere at the same time.

To summarize, a linear main limb of rise indicates that the system apparently behaves as if the recharge hyetograph were a uniform step function. That is, the system behaves as if recharge were steady and uniform from the moment it begins.

(iii) Steep and Approximately Parallel Main Limbs of Rise

The main limbs of rise in Figs. 1.4.2.2 to 1.4.2.5 have steep slopes and are approximately parallel. Moreover, the main limbs of rise of Ex2 and Ex3 are more or less on top of each other while the main limb of rise of Ex1 occurs later. A slope can appear to be steep due to the scale chosen. In order to be able to say that the slope of the rise is steep, one should be able to compare it with the rise obtained for flow within less open soils such as agricultural soils.

It was not possible to find in the literature outflow hydrographs together with rainfall hyetographs adequate for comparison purposes, or with the indication as to whether or not overland flow took place. Later on, it will be shown that due to low resistance paths on top of the bed and to a relatively high recharge rate, the slopes of the main limbs of rise can be expected to be steep.

It is important to note that for the case where water travels vertically down through the unsaturated zone, a steep main limb of rise is not a proof that short-circuiting occurred in the unsaturated part of

the B horizon, as can be seen from Fig. 1.5.1.1. Figure 1.5.1.1 (b) for instance shows that if all the water travelled down to the low conductivity layer through low resistance paths, and reached it at the same time, the slope of the outflow hydrograph rise would not be steeper than for the corresponding case where all the water would travel down through the soil matrix. Therefore, an open soil in the unsaturated zone does not mean a steeper rise.

In the remainder of this discussion, it should be kept in mind that the hydrographs have not been normalized with respect to irrigation rate, and errors mentioned in Appendix E may affect the time of occurrence of the main limbs of rise and their slopes.

The average steady state outflow rates for Ex2 and Ex3 are the same (1.25×10^{-4} and 1.24×10^{-4} m^3 s^{-1} respectively. See Appendix F). There is no physical reason why the ratio of outflow to irrigation should not be the same at steady state for the three experiments. Therefore, on the average, the irrigation rate for Ex2 must be the same as for Ex3, although Fig. 1.4.2.2 shows it is not the case, probably due to error. Since the irrigation rate is not constant with time, normalization of the outflow rate using a time dependent irrigation rate should still have been performed in order to compare specific parts of the hydrograph such as the rises but it has not been performed. The lag of the main limb of rise of Ex1 with respect to the main limb of rise of Ex3 is at least one hour. Moreover, the fact that the main limb of rise of Ex1 lags the main limb of rise of Ex3 is verified to some extent by

the fact that 4 pipes out of 7 rise later for Ex1 than for Ex3. Therefore the lag of the main limb of rise of Ex1 with respect to the one of Ex3 is real, although its numerical value may have been different, had the outflow rate been normalized with respect to rainfall and were there no errors. The exact position of the main limb of rise of Ex2 with respect to Ex3 is unknown due to the same limitations.

The effect of initial conditions on the timing and slopes of the main limbs of rise are as follows: The main limb of rise of Ex1 is delayed with respect to the one of Ex3 due to drier initial conditions. This delay must be due to storage in the unsaturated zone. The main limb of rise of Ex1 is parallel to the one of Ex3, showing that a different initial water content did not affect the slope of the main limb of rise.

In order to determine if concentration has any effect on the shape and timing of the main limbs of rise, let us first review what effects are expected from short-circuiting.

As shown in Fig. 1.5.1.1, the only modifications of the hydrograph rise that are expected from short-circuiting are an initial step, irregularities in the main limb of rise, and less steep overall rises and main limbs of rise. If a more general hydrograph shape, including a late part of rise, is used, irregularities may appear in the late part of the rise. The extreme case of Fig. 1.5.1.1.b where the overall rise gets shifted to the left is considered to be unrealistic.

Within the limitations mentioned above and the resolution of the graph, the hydrograph for Ex2, as can be observed in Fig. 1.4.2.2, does

not display any of the features expected from short-circuiting. Indeed, the initial step is suppressed rather than enhanced, as can be observed also from Fig. 1.4.2.6. Moreover, no irregularities are noticed in the main limb of rise and the ones occurring later can be due to other causes than short-circuiting. Finally, the slope of the main limb of rise of Ex2 is approximately equal to the one of Ex3.

It can also be noticed from Fig. 1.4.2.2 that the main limb of rise of Ex2 does not occur earlier than the one of Ex3. It would, however, be desirable to observe what would happen when the initial conditions are exactly the same for the concentrated and the uniform irrigations. Initial conditions for Ex2 were slightly drier than for Ex3, perhaps masking the effect of concentration. However, except for Fig. 1.5.1.1.b which represents an unrealistic case, short-circuiting is not expected to shift the main limb of rise.

From Fig. 1.4.2.2, it can also be observed that Ex2 does not reach steady state earlier than Ex3, but short-circuiting is not expected to decrease the time to steady state. The fact that concentration has apparently no effect on flow in the unsaturated zone is in agreement with the standpipes data given in Section 1.4.3

In summary, within the limits of experimental design and of errors, the hydrograph rise due to concentrated irrigation obtained for Ex2 does not display the features expected from short-circuiting. Moreover, it is not steeper, nor shifted earlier than the hydrograph for Ex3, obtained from uniform irrigation and slightly wetter initial conditions.

(iv) Steep and Parallel Recessions

Recessions as shown in Figure 1.4.2.2 are remarkably parallel. Errors likely to influence the recessions are drift in the tipping bucket calibration, and for Ex2 and Ex3, natural rainfall. However, given the parallel nature of the recessions, it is likely that these errors were negligible during the recessions for the graphs at the scale used for Fig. 1.4.2.2.

It is likely that flow in low resistance paths and as fingers down to the low conductivity layer will precipitate and steepen the beginning of the recession. Thus, in contrast with the rises, recessions may be steeper due to the structure of the unsaturated zone.

From Fig. 1.4.2.2, one can note that recessions occur soon after irrigation is stopped and are fast. It might thus be concluded that a significant flow in low resistance paths occurs.

However, reaching a conclusion is difficult in view of the fact that there is no means of determining the shape a recession should have if short-circuiting exists.

It should also be noted that, as in the case of the rises,the fact the recessions are fast must be proved by the presence of low resistance paths on top of the bed. Because of water drainage in the unsaturated zone, it is not clear if a relatively high recharge rate is also responsible for fast recessions.

Figure 1.4.2.2 shows that the recessions for Ex2 and Ex3 are similar. There is thus no indication that concentration precipitates the beginning of the recession.

Concentration of irrigation had thus no noticeable influence on the recessions, indicating that concentration did not affect the proportion of water short-circuiting the soil matrix to a point where the effect was observable. This is in agreement with the observations made for the rises.

No effect from initial conditions should be expected since initial conditions are not expected to have any effect on recessions occurring after steady state has been reached.

To summarize, although the recessions occur soon after the end of irrigation, and are fast, they cannot be used as a proof of short-circuiting. Moreover, concentration has no detectable effect on the shape of the recession of Ex2, as can be observed from the parallel nature of the recession limbs for Ex2 and Ex3. It apparently has no effect either on the timing of the recession.

After having inferred the apparent hydrologic behavior of the unsaturated zone from the major features of the outflow hydrograph in points (i) to (iv) above, one must note the following. Although it was concluded that the soil behaves almost as if the wetting front were uniform, the actual mechanism of flow in the unsaturated zone has not been uncovered.

One observation concerning this mechanism is that the effect of initial conditions is important. This suggests that a significant proportion of the flow must occur within the soil matrix.

As a summary, from the outflow hydrograph, it is inferred that the soil and water system in the integrated unsaturated and saturated zones

domain apparently behaves as if little or no short-circuiting occurred. More generally, it behaves as if the wetting front, except for a little initial flow, were uniform and sharp.

The actual flow mechanism within the unsaturated soil however remains unknown. For instance, the lack of effect of initial conditions on pipes 1, 5 and 8 is puzzling.

1.5.2 Lateral Saturated Flow in Low Resistance Paths

In this section, the hydrologic behavior of the material on top of the bed and in which saturated flow takes place will be inferred from the shape of the outflow hydrograph. The kinematic wave model will again play a central role in the discussion.

The conditions that must be met for the kinematic wave model to be applicable are a low, steady, and uniform recharge rate, a steep and uniform bed slope, a high, uniform and steady hydraulic conductivity, a steady and uniform effective porosity, and the validity of Darcy's law. Also, flow must be unidirectional. A steep bed slope and a high hydraulic conductivity yield fast flow over the bed. Together with a low recharge rate they yield a thin saturated zone, hence a water table approximately parallel to the bed.

The model yields a hydrograph rise which is a straight line, and a water table parallel to the bed while it is rising. From the straight line rise observed in Figs. 1.4.2.2 to 1.4.2.5, it appears that the soil of the Forest plot behaved as if the assumptions necessary for the kinematic wave model were satisfied. Section 1.5.1 already treated

steadiness and uniformity of the recharge rate. The recharge rate was fairly large. However, a low recharge rate is required for the saturated zone to be thin, and hence for the water table to be approximately parallel to the bed. Consequently, a high recharge rate can be compensated by a large hydraulic conductivity and a steep bed slope. The bed slope of 30° is indeed steep. Whether a high hydraulic conductivity exists within the saturated zone will now be established.

The kinematic wave model allows the calculation of an effective hydraulic conductivity for the saturated zone, using the slope of the outflow hydrograph rise. Values of 1.6×10^{-4} to 3.2×10^{-4} ms^{-1} are obtained in Chapter II for this conductivity.

As shown in Section 2.4, these values correspond to the hydraulic conductivities of fine or fine to medium sand. Proofs that this can be considered to be a high hydraulic conductivity are offered by a recession rate about 16 times the one obtained by Hewlett and Hibbert for disturbed sandy loam, by visual observations and hydraulic conductivities measured at outflow points.

In Section 1.4.4, a comparison of the outflow hydrograph recession obtained for the present work with the one obtained for a soil of similar texture by Hewlett and Hibbert was presented. It was concluded that, within the limitations linked to the comparison, the recession for the present work is much faster than the one obtained by Hewlett and Hibbert. Since the soil used by Hewlett and Hibbert had been excavated and had lost its original structure, it can be concluded that the higher conductivity of the soil in the saturated zone of the Forest plot is due to the low resistance paths.

The rootmat and dark material found on top of the bed are obviously materials responsible for high conductivities. Within the saturated zone, flow in low resistance paths is not restricted by lack of free water like in the unsaturated zone, therefore the effect of low resistance paths occurring in this zone can be large. Flow on top of the bed takes place according to topography and the various low resistance paths water can find. It does not take place uniformly downhill but as a network of concentrated flow and thus violates the assumptions of uniform hydraulic conductivity and unidirectional flow made in the kinematic wave model. Yet the system behaves as if the hydraulic conductivity were uniform and flow unidirectional.

Points of concentrated outflow observed at the bottom of the channel bank are proof of a network of pipelike low resistance paths. Since outflow was not observed to start from all outflow points at the same time, not all the low resistance paths on top of the low conductivity layer contribute to flow at the beginning. As explained earlier, hydraulic conductivities at two outflow points at the bottom of the channel may be bracketed by 5×10^{-4} and 5×10^{-3} ms^{-1}. The lower of these conductivities is of the same order of magnitude as the one of medium sand (0.25 - 0.5 mm).

Quick, saturated flow over the bed must be a general mechanism in places similar to the plot. This flow, and on a larger scale, streams flowing alternatively over the surface or underground, must be the main causes of creek flashiness. It may also be a major cause of nonlinear flow, as discussed in Chapter III.

The slope of the main limb of rise and of the recession is influenced by saturated flow over the bed. Due to fast saturated flow over the bed, it can be expected that rise and recession slopes are steep. If it can be assumed that the water velocity in the saturated zone is not influenced by the thickness of the saturated zone, the time from the start of the main limb of rise to steady state will be independent of the irrigation rate. Since a higher irrigation rate means a higher outflow rate, it will also mean a steeper hydrograph rise. Thus a relatively high recharge rate is also responsible for a steep rise. The effect of the recharge rate on the recession is more difficult to determine due to the drainage of the unsaturated zone.

The presence of low resistance paths on top of a steep bed and hence fast flow should be expected to yield a thin saturated zone and therefore a water table approximately parallel to the bed if the recharge rate is steady and uniform. Technically, a water table parallel to the bed while it rises is yielded by the kinematic wave model. It is not possible to conclude from Figs. 1.4.3.10 to 1.4.3.12 that the water table rose parallel to the bed because of the small size of the hillslope plot and the small number of measurement points. The system however behaves as if the water table were rising parallel to the bed. A water table rising parallel to the bed would be the outcome of approximately uniform and vertical downward flow in the unsaturated zone, a large hydraulic conductivity in the saturated zone, and a steep bed slope.

To summarize, two of the assumptions necessary for the kinematic wave model are readily verified: a steep bed slope and a high hydraulic

conductivity. One difference with the kinematic wave model, however, is the presence of discrete paths of low resistance rather than of a uniform layer of high conductivity.

1.5.3 Discussion of Beven's 1982 Model in Relation to the Present Work

In Section 1.2, it was mentioned that Beven (1982) compared the hydrograph obtained experimentally by Weyman (1970, 1973) for a slope segment with the hydrograph obtained using a model based on the kinematic wave model described in Chapter II. Beven's work will now be discussed in more detail.

First, the difference between Beven's work and the use of the kinematic wave model in the present work should be noted. Beven used Weyman's field data in order to obtain the parameters necessary for the simulation of a hydrograph by his model. He also compared this hydrograph with a hydrograph obtained experimentally by Weyman. In the present work, the similarities between the general shape of the hydrographs obtained experimentally and the shape of the hydrograph yielded by the kinematic wave model are used to infer flow mechanisms in the saturated and the unsaturated zones and to calculate an effective hydraulic conductivity.

Second, it is likely that the soil in Weyman's plot is less suited for the kinematic wave model or the extension thereof used by Beven (1982) than the one of the Forest plot. Although it is possible to obtain a hydraulic conductivity distribution from Weyman's data, it was not possible to obtain a distribution that agreed with the one Beven

obtained. Therefore it was considered preferable not to attempt to use either distribution. This means that the hydraulic conductivity of Weyman's plot cannot be compared quantitatively with the one of the Forest plot. From the soil description given by Weyman (1970, 1973), it can however be inferred that the soil in Weyman's plot has a lower hydraulic conductivity. Especially, it does not have the special feature of an accumulation of pipelike low resistance paths over the bed, like the one found in the Forest plot. One expected effect of a lower hydraulic conductivity is that, in order to have the water table parallel to the bed, the recharge rate has to be smaller.

1.5.4 Comparison with Other Fast Flow Situations

It is interesting to determine whether the presence of low resistance paths on top of the bed, which contributes to a high hydraulic conductivity for the saturated zone, has been observed by other authors.

As mentioned in Section 1.2, Utting, in a site close to the Forest plot, noted the presence of a rootmat on top of the till.

A situation possibly close to the one observed in the Forest plot has been observed by Mosley (1979). He noticed "points of concentrated seepage, usually at the base of the B horizon, at which high rates of outflow were observed during storms." Although he does mention the existence of flow in root channels higher up in the profile, he does not say if the seeps are due to root material. He also notes that "it seems probable that eluviation has increased hydraulic conductivities [in the

seepage zone at the interface between the B horizon and the bed]" and that in some locations of this interface pipes exist. It is not clear, however, if the hydraulic conductivity at the base of the B horizon is larger than higher up in the profile.

Seeps were also observed by Harr (1977) and by Weyman (1970). The seeps observed by Harr apparently were on top of the bed.

Downslope flow in pipes (e.g., Atkinson, 1978) also resembles the fast flow above the bed occurring in the Forest, although in a more remote way.

1.5.5 The Flow Model

As a conclusion, based on the outflow hydrograph and visual observations, the following model of flow is presented for the Forest plot.

A little water reaches the channel before the main limb of rise starts. This water may have reached the bed early because it flowed through low resistance paths or as fingers. Another possibility is that it came from an area where the soil was shallow. Because the amount of water involved in this initial flow is small and because the main limb of rise is a straight line, one can conclude that the system behaves as if the recharge rate were a step function and the same step function at every location of the bed.

Water having reached the bed flows rapidly towards the channel in a network of low resistance paths offered by the rootmat and by dark material present on top of the steep bed. In spite of this nonuniform

flow, the system behaves as if the hydraulic conductivity of the saturated zone were uniform.

The fast flow on top of the low conductivity layer is a major cause of flashiness and may even be nonlinear.

1.5.6 Validity of the Kinematic Wave Model

One may wonder whether other models rather than the kinematic wave model could yield the straight line rise of the hydrographs obtained for the Forest plot and if another model would be more satisfactory than the kinematic wave model. While answering this question fully is beyond the scope of the present work, some attention will now be devoted to it.

First, the saturated zone will be examined.

The kinematic wave model assumes a water table approximately parallel to the bed. Because of a high hydraulic conductivity and a steep bed slope, one can expect a thin saturated zone, and hence a water table approximately parallel to the bed for the Forest plot.
The kinematic wave model thus appears a reasonable model for the Forest plot in this respect. Not all the assumptions necessary for the kinematic wave model are met by the saturated zone, though.

In particular, the hydraulic conductivity and the effective porosity as defined in Appendix G are not uniform and the flow is not unidirectional. As said earlier, a straight line rise could be due to an averaging process.

The unsaturated zone will now be examined.

The recharge rate is nonuniform and unsteady, at least at the very

beginning of the recharge. Here too an averaging process can be invoked unless nonuniformity and unsteadiness occur only for a short period of time at the beginning of the recharge and not during the main limb of rise.

The possibility of a significant proportion of flow taking place in low resistance paths within the unsaturated zone is not totally rejected, especially due to the lack of response of pipes 1, 5 and 8 to change in initial conditions. A straight line rise would be due to averaging. More attempts should be made in order to check the occurrence of short-circuiting experimentally.

The only value of the kinematic wave model for understanding the flow mechanism in the unsaturated zone is that the integrated flow in the unsaturated and saturated zones occurs as if it were valid.

As a summary, the kinematic wave model applies to the Forest plot only to the extent that the observed hydrograph rise is a straight line and that the saturated zone exhibits a high hydraulic conductivity and rests on a steep bed. Other assumptions for the saturated zone are not met and it can only be said that the system behaves as if they were. In Chapter III, it is shown that it is not certain whether flow can be nonlinear and what the implications of nonlinearity would be. In order to apply the kinematic wave model, it is necessary to assume that nonlinearity, if existant, is negligible.

The assumptions of a uniform and steady recharge rate are probably not met, and therefore all that can be said is that the unsaturated zone and the saturated zone together behave as if the kinematic wave model

were valid. Formulation of a model that represents reality more closely would require more experimental work.

1.6 Conclusions

Visual observations showed that the soil has a very stable structure. It is open due to the presence of low resistance paths. Pipelike low resistance paths are due mainly to root material.

Uniform and concentrated irrigation of the small forested hillslope plot chosen for the present work yielded the following results:

(i) Drier initial conditions increased the time lag to the main limb of rise. They also delayed the water table rise. They did not alter the slope of the main limb of rise.

(ii) Concentration of irrigation did not change the general shape of the outflow hydrograph nor did it decrease the time lag to the main limb of rise. It did not cause the water table to rise earlier, neither did it affect the shape of the water table at steady state.

It did not enhance the initial step of the outflow hydrograph observed for uniform irrigation. Rather, it suppressed it.

(iii) Outflow hydrographs are characterized by little or no preliminary outflow, by steep and straight main limbs of rise and by steep recessions. These observations led to the conclusion that the soil system behaves as if the kinematic wave model were valid. It should be remembered that the term "kinematic wave model" denotes exclusively the model described in the second chapter.

Transformation of the outflow hydrograph into a recharge hyetograph using the kinematic wave model indicates that the soil and water system

in the integrated unsaturated and saturated zones domain apparently behaves as if the recharge hyetograph were a uniform step function. In other words it behaves as if little or no short-circuiting occurred and as if recharge started everywhere at the same time and reached steady state instantaneously. The lack of effect of initial conditions on pipes 1, 5 and 8 may however suggest short-circuiting.

Comparison between Ex2 and Ex3 of the outflow hydrograph and of the water table indicates that the system behaves as if short-circuiting were not enhanced by concentration.

The fact that the system behaves as if the kinematic wave model were valid also suggests a steep bed and a high hydraulic conductivity in the saturated zone. Both these features are readily verified, a high hydraulic conductivity on top of the bed being due to a network of low resistance paths.

It is possible that a large hydraulic conductivity over the bed has also been noticed by Mosley (1979).

About the value of the kinematic wave model for the Forest plot, it can be said that it is reasonable for the saturated zone to the extent that two major assumptions are satisfied. For the unsaturated zone, however, it is probable that its only value is the fact that the system behaves as if it were valid. More experimental work is necessary to determine flow conditions there. For instance, the lack of effect of initial conditions on pipes 1, 5 and 8 is puzzling and suggests short-circuiting.

1.7 References

Anderson, M.G. and T.P. Burt. 1980. Interpretation of recession flow. Jour. of hydrology, Vol. 46: 89-101.

Atkinson, T.C. 1978. Techniques for measuring subsurface flow on hillsopes. In Kirkby, M.J. (ed.) Hillslope hydrology. John Wiley. 389 pp.

Aubertin, G.M. 1971. Nature and extent of macropores in forest soils and their influence on subsurface water movement. U.S. Forest Exp. Sta. Res. Paper, NE-192.

Baker, F.G. and J. Bouma. 1976. Variability of hydraulic conductivity in two subsurface horizons of two silt loam soils. Soil Sci. Soc. Amer. Jour. Vol. 40: 219-222.

Barnes, B.S. 1939. The structure of discharge-recession curves. Amer. Geophys. Union Trans., Vol. 20: 721-725. Cited by Anderson and Burt.

Beasley, R.S. 1976. Contribution of subsurface flow from the upper slopes of forested watersheds to channel flow. Soil Sci. Soc. Amer. Jour., Vol. 40: 955-957.

Betson, R.P., J.B. Marius and R.T. Joyce. 1968. Detection of saturated interlow in soils with piezometers. Soil Sci. Soc. Amer. Proc., Vol. 32: 602-604.

Beven, K. 1981. Kinematic subsurface stormflow. Water resources research, Vol. 17, No. 5: 1419-1424.

Beven, K. 1982. On subsurface stormflow: predictions with simple kinematic theory for saturated and unsaturated flows. Water resources research, Vol. 18, No. 6: 1627-1633.

Beven, K. and P. Germann. 1980. The role of macropores in the hydrology of field soils. Institute of hydrology report 69, Wallingford, England.

Bouma, J. and L.W. Dekker. 1978. A case study on infiltration into dry clay soil. 1. Morphological observations. Geoderma, Vol. 20: 27-40.

Bond, R.D. 1964. The influence of the microflora on the physical properties of soils. II. Australian Jour. Soil Res., Vol. 2: 123-131.

Bond, R.D. and J.R. Harris. 1964. The influence of the microflora on the physical properties of soils. I. Effects associated with filamentous algae and fungi. Australian Jour. Soil Res., Vol. 2: 111-122. Cited by Bond (1964).

Chamberlin, T.W. 1972. Interflow in the mountainous forest soils of coastal British Columbia. In Mountain Geomorphology: Geomorphological processes in the Canadian Cordillera. B.C. geographical series, number 14, Tantalus Research Ltd., Vancouver, B.C., Canada.

Childs, E.C. 1969. An introduction to the physical basis of soil water phenomena. Wiley. 493 pp.

Chow, T.L. 1976. A low-cost tipping bucket flow meter for overland flow and subsurface stormflow studies. Canadian Journal of Soil Science, Vol. 56: 197-202.

de Vries, J. 1979. Prediction of non-Darcy flow in porous media. American Society of Civil Engineers, Journal of the irrigation and drainage division, Vol. 105, No. IR2, Proc. Paper 14610: 147-162.

de Vries, J. and T.L. Chow. 1978. Hydrologic behavior of a forested mountain soil in coastal British Columbia. Water Resources Research, Vol. 14, No. 5: 935-942.

Dunne, T. and R.D. Black. 1970. Partial area contributions to storm runoff in a small New England watershed. Water resources research, Vol. 6, No. 5: 1296-1311.

Gray, D.M. (editor). 1970. Handbook on the principles of hydrology.

Harr, R.D. 1977. Water flux in soil and subsoil on a steep forested slope. Jour. of hydrology, Vol. 33: 37-58.

Hewlett, J.D. and A.R. Hibbert. 1963. Moisture and energy conditions within a sloping soil mass during drainage. Jour. of geophysical research, Vol. 68, No. 4: 1081-1087.

Hewlett, J.D. and C.A. Troendle. 1975. Non-point and diffused water sources: a variable source area problem. American Society of Civil Engineers, Committee on watershed management. Watershed Management, Utah State University (Symposium): 21-46.

Hill, D.E. and J.Y. Parlange. 1972. Wetting front instability in layered soils. Soil Sci. Soc. Amer., Vol. 36, No. 5: 697-702.

Hillel, D. 1971. Soil and water: physical principles and processes. Academic Press. 288 pp.

Ineson, J. and R.A. Downing. 1964. The groundwater component of river discharge and its relationship to hydrogeology. Institution of water engineers journal. 18: 519-541. Cited by Anderson and Burt.

Mehra, O.P. and M.L. Jackson. 1960. Iron oxide removal from soils and clays by a dithionite-citrate system buffered with sodium bicarbonate, Clays and clay minerals. Vol. 5: 317-325. International series of monographs on earth science, Pergamon Press.

Miller, R.D. and E. Bresler. 1977. A quick method for estimating soil water diffusivity functions. Soil Sci. Soc. Amer. Jour., Vol. 41: 1020-1022.

Mosley, M.P. 1979. Streamflow generation in a forested watershed, New Zealand. Water resources research, Vol. 15, No. 4: 795-806.

Nagpal, N.K. and J. de Vries. 1976. On the mechanism of water flow through a forested mountain slope soil in coastal western Canada. Unpublished material.

Pond, S.F. 1971. Qualitative investigation into the nature and distribution of flow processes in Nant Gerig. Subsurface hydrology, Rept. No. 28, Institute of hydrology, Wallingford, England. Cited by Atkinson.

Schumacher, W. 1864. Die Physik des Bodens. Berlin. (cited by Beven and Germann).

Smith, W.O. 1967. Infiltration in sands and its relation to groundwater recharge. Water resources research, Vol. 3, No. 2: 539-555.

Sowers, G.B. and G.F. Sowers. 1970. Introductory soil mechanics and foundations. Macmillan. 556 pp.

Utting, M.G. 1978. The generation of stormflow on a glaciated hillsope in coastal British Columbia. M.Sc. thesis. University of British Columbia, Vancouver.

Weyman, D.R. 1970. Throughflow on hillslopes and its relation to the stream hydrograph. International association of scientific hydrology. Bulletin, XV^{e} Année, No. 3: 25-33.

Weyman, D.R. 1973. Measurements of the downslope flow of water in a soil. Jour. of hydrology, Vol. 20: 267-288.

Whipkey, R.Z. 1968. Storm runoff from forested catchments by subsurface routes. Int. Assoc. Sci. Hydrology, publ. 85: 773-779.

CHAPTER II

DETERMINATION OF AN EFFECTIVE HYDRAULIC CONDUCTIVITY USING THE KINEMATIC WAVE MODEL

2.1 Introduction

One of the pillars of the discussion of the experimental results presented in Chapter I is the kinematic wave model. The term "kinematic wave model" denotes exclusively the model described in the present chapter. This model allowed us to make inferences with respect to soil hydrologic behavior. It is a very simple model of saturated flow over a sloping bed, described by an equation that can be solved analytically. It has been developed by Henderson and Wooding (1964) and Beven (1981). A major underlying assumption of the kinematic wave model is that the water table is approximately parallel to the bed. Using a reasoning similar to the one made by Henderson and Wooding (1964) for the case of overland flow, the water table is approximately parallel to the bed if the water depth is small. Moreover, a thin saturated zone occurs when the recharge rate is low, the bed slope steep and the hydraulic conductivity high.

In this chapter, the kinematic wave equation for saturated flow in a porous medium over a sloping bed will be derived and solved following mainly Beven (1981) whose work is based on Henderson and Wooding's. This will include a presentation of the behavior of the water table and of the outflow hydrograph yielded by the solution. The equation describing the hydrograph rise will then be used to obtain an effective satiated hydraulic conductivity for the Forest plot.

2.2 Literature Review

A number of approximate equations have been proposed to describe flow in a porous medium over a sloping bed.

For flow taking place between an approximately horizontal free water surface and an approximately horizontal impermeable bed, it can be assumed that flow lines are horizontal. Hence the hydraulic gradient is equal to the slope of the water table. This is the Dupuit-Forchheimer theory (Childs, 1969).

On steep slopes, one should rather assume that the flow lines are parallel to the bed. This was done by Henderson and Wooding (1964), Childs (1971) and Beven (1981).

Henderson and Wooding derived the equation of flow for this case, equation that Beven calls "extended Dupuit-Forchheimer equation." From this equation they obtained analytically the profile of the water table at steady state. Using a numerical method they obtained the profile during rise and recession. Beven obtained the rising limb of the hydrograph for the "extended Dupuit-Forchheimer equation" by the finite differences method.

Henderson and Wooding, then Beven (1981), simplified the equation of flow further by assuming the water table is approximately parallel to the bed. The equation thus obtained will be called the kinematic wave equation and describes kinematic wave motion.

2.3 The Kinematic Wave Equation for Flow in a Porous Medium

In this section, the assumptions linked to the kinematic wave model will be presented. The kinematic wave equation describing the model

will be derived and the solution of this equation presented. For doing so, the work of Henderson and Wooding (1964), Beven (1981) and Eagleson (1970) will be followed.

(i) Assumptions

The kinematic wave model is based on the following assumptions found explicitly or implicitly in Beven's work. The fact that a thin saturated zone is a necessary assumption has been stated by Henderson and Wooding.

(a) The saturated zone is thin, leading to a water table approximately parallel to the bed (Henderson and Wooding). A thin saturated zone is yielded by a steep bed slope, a high hydraulic conductivity and a low recharge rate. Flow lines are parallel to the bed.

(b) Recharge occurs as a uniform step function. It is equal to i_o during rise and steady state, and zero during recession. The recharge rate is thus both steady and uniform. Note that, as said in Chapter I, a uniform recharge rate is consistent with flow occurring vertically in the unsaturated zone.

(c) The effective porosity and the hydraulic conductivity are steady and uniform. Flow is unidirectional and the bed slope uniform. The medium is isotropic.

(d) Flow is linear hence Darcy's law can be used.

(ii) Derivation

The kinematic wave equation used by the kinematic wave model can be derived from Darcy's law and a continuity equation.

For saturated flow over steep beds Henderson and Wooding assumed flow lines to be parallel to the bed, which enabled them to write Darcy's law as

$$qT = -KT \left(\frac{\partial T}{\partial x} \cos \omega - \sin\omega\right) \qquad 2.3.1$$

where

q = discharge per unit area or macroscopic flow velocity, often called Darcy's velocity. In the present work, q is in the main flow direction.

T = thickness of the saturated zone measured perpendicular to the bed. Thus

qT = discharge per unit width of hillslope ($m^3\ s^{-1}\ m^{-1}$)

K = satiated hydraulic conductivity.

x = downslope distance from the highest point on the bed where recharge occurs.

ω = angle of the bed with respect to the horizontal.

Flow over a steep slope is depicted in Fig. 2.3.1.

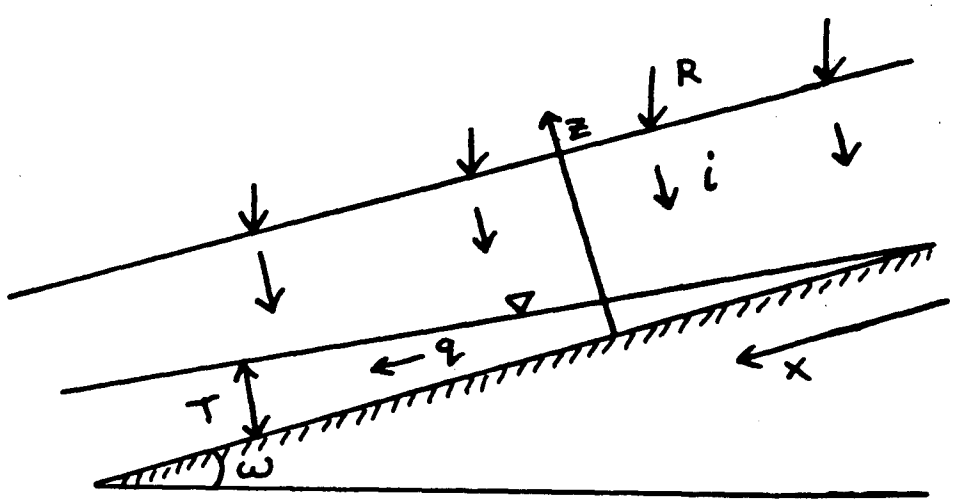

Figure 2.3.1 Saturated flow in a porous medium resting on a sloping bed. ω is the bed slope angle with the horizontal.

R is the irrigation rate.

Note that by assuming qT is discharge per unit width of hillsope, it is assumed that K is uniform with respect to z, where, as shown in Fig. 2.3.1, z is upward and perpendicular to the bed. K will be assumed uniform in the kinematic wave model. Also, the medium is assumed to be isotropic.

If the water table is approximately parallel to the bed,

$$\frac{\partial T}{\partial x} \cos\omega << \sin\omega$$

and Eq. 2.3.1 becomes (Beven, 1981)

$$qT = TK \sin\omega \qquad 2.3.2$$

Note that Eq. 2.3.2 is equivalent to Darcy's law with the hydraulic gradient taken to be $\sin\omega$.

The equation of continuity for flow in the x direction is (Beven, 1981)

$$\frac{\partial(nT)}{\partial t} = - \frac{\partial}{\partial x} (Tq) + i \qquad 2.3.3$$

where

n = effective porosity; see Appendix G for definition.

t = time

i = recharge rate per unit area parallel to the bed. i can vary with time and be zero.

Let y be a direction perpendicular to both x and z, and along the hillslope width. Assuming n steady and uniform with respect to z and

y, assuming also K and ω uniform with respect to x and y, and combining Eqs. 2.3.2 and 2.3.3. yields the kinematic wave equation (Beven, 1981)

$$n\frac{\partial T}{\partial t} = -K\sin\omega \frac{\partial T}{\partial x} + i \qquad 2.3.4$$

Adapting for the flow in a porous medium treated here the derivation offered by Henderson and Wooding for overland flow, the wave velocity c is

$$c = \frac{dx}{dt} = \frac{K \sin\omega}{n} \qquad 2.3.5$$

Using Eq. 2.3.5 and assuming n uniform with respect to x, Eq. 2.3.4 can be rewritten as

$$\frac{\partial(nT)}{\partial t} + c \frac{\partial(nT)}{\partial x} = i \qquad 2.3.6$$

(iii) Solution

Eq. 2.3.6 is solved in Note 1, Appendix H. Fig. 2.3.2, adapted from Eagleson (1970) depicts the behavior of the water table during rise and steady state. Initial conditions are T = 0 for all x's before the start of recharge. Boundary conditions are T = 0 at x = 0 for all times.

Recharge occurs from x = 0 to x = L. In other words, L is the length of the saturated zone. Recharge rate is a constant for the kinematic wave model.

At time t_1, the water table shape is given by the curve OAE; at time t_2 it is given by the curve OBF. Finally, when steady state is

reached by the entire saturated zone, the water table is the straight line OD.

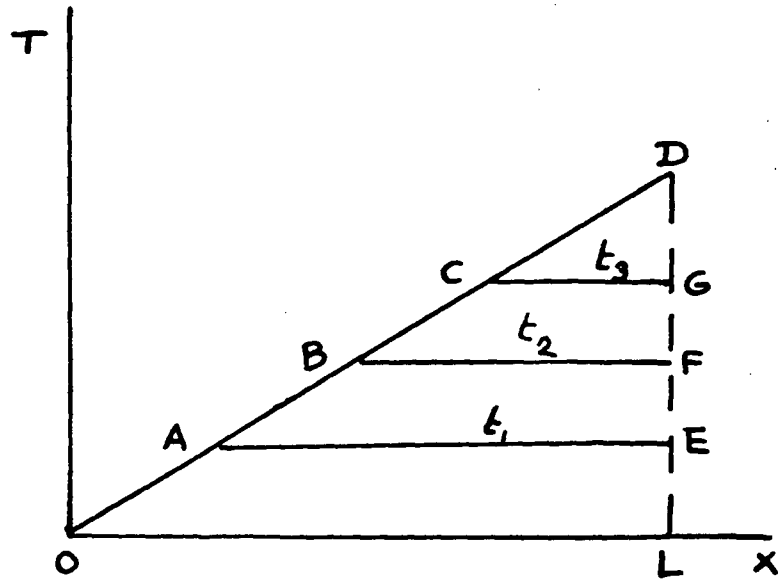

Figure 2.3.2 Adapted from Eagleson, 1970, Fig. 15-5. Shape of the water table during rise and steady state.

It is shown in Appendix H that at a time t* after the start of the recharge, the thickness of the saturated zone for the part of the saturated zone having reached steady state is given by (Beven, 1981)

$$T = \frac{i_o}{n}\frac{x}{c} \qquad 2.3.7$$

where i_o is the recharge rate per unit area parallel to the bed during rise and steady state. For the part still rising (Beven, 1981)

$$T = \frac{i_o}{n} t^* \qquad 2.3.8$$

where t* = time from the start of recharge.

Figure 2.3.3 depicts the shape of the water table during recession.

It is interesting to note that the assumption that the water table is approximately parallel to the bed yields a water table parallel to the bed during the rise but not at steady state and neither during the recession.

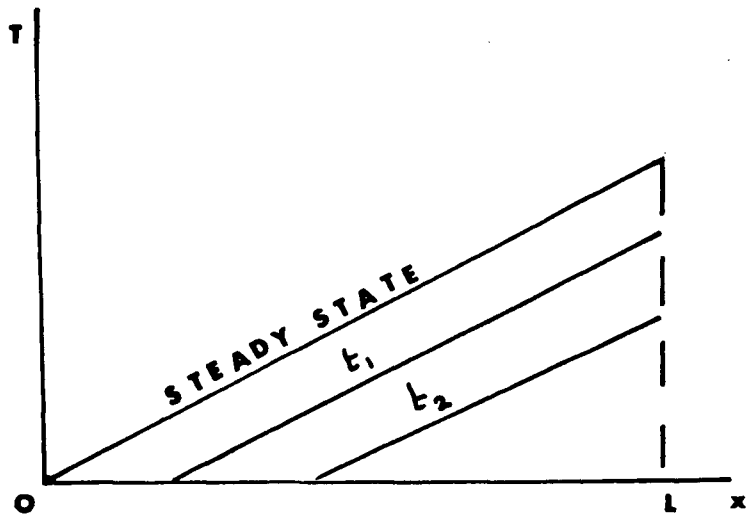

Figure 2.3.3 Shape of the water table during the recession

Figure 2.3.4 pictures the outflow hydrograph. It is very simple, with straight line rise and recession. As shown in Appendix H, Note 1, the discharge at the bottom of the hillslope is

$$Q = K\sin\omega \, D\frac{i_o}{n} \, t^* \qquad \text{during the rise} \qquad 2.3.9$$

$$Q = D \, i_o \, L \qquad \text{at steady state} \qquad 2.3.10$$

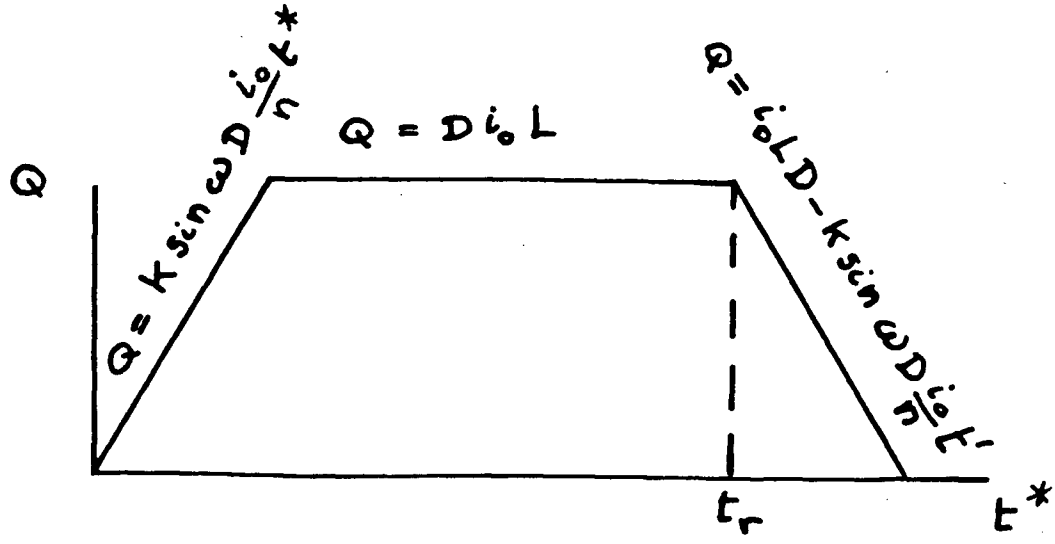

Figure 2.3.4 Hydrograph given by the kinematic wave model

$$Q = i_o L D - K \sin \omega D \frac{i_o}{n} t' \quad \text{during the recession} \qquad 2.3.11$$

where

Q = discharge $(\frac{\text{volume}}{\text{time}})$

D = width of the hillslope

$t^* - t_r = t'$

t_r = time at which recharge stopped

The effective porosity n has been assumed to be the same for the rise and the recession. In Appendix H, Note 4, it is shown that if the effective porosity during the recession is n_{re}, then n in Eq. 2.3.11 should be replaced by n_{re}.

It is of interest to note that Eqs. 2.3.9 and 2.3.11 indicate that the rise and recession rates are larger for a larger recharge rate.

Finally, note that although Beven (1981) does not give Eqs. 2.3.6, 2.3.9, 2.3.10 and 2.3.11, he gives equations used in the derivation of Eqs. 2.3.2, and 2.3.4 and plots the hydrograph rise and steady state.

2.4 Use of the Kinematic Wave Model to Calculate an Effective K

It was shown in Chapter I that the soil and water system in the Forest plot behaved as if the kinematic wave model assumptions were satisfied. In particular, two of these assumptions are readily verified: a steep bed slope and a high hydraulic conductivity.

In Section 3.4 it is shown that it is not certain if the kinematic wave model can be applied to the Forest plot as far as nonlinear flow is concerned. It must be assumed that nonlinearity, if present, is negligible. Note that use of the kinematic wave model will always present the problem of the need for flow to be sufficiently fast, yet not too fast.

A number of the assumptions necessary for the kinematic wave model have not been considered in Chapter I. They are a uniform bed slope, steady hydraulic conductivity and effective porosity and a uniform effective porosity. These will now be briefly examined.

The bed slope is not uniform. However, it will be assumed that, as a result of an averaging process, nonuniformity effects can be neglected. The hydraulic conductivity and the effective porosity are probably steady since the soil structure is very stable. The effective porosity is not uniform. However, it can be argued, like in the case of

nonuniformities in the hydraulic conductivity, that the system behaves as if it were uniform.

The water table behavior is an important criterion for the use of the kinematic wave model. The shape of the water table was given in Figs. 1.4.3.10 to 1.4.3.12. As mentioned in Section 1.4.3, the shape of the bed is uncertain and the data insufficient to make a definite statement as regard to the shape of the water table. However, since the system behaves as if the kinematic wave model were valid, it behaves as if the water table were approximately parallel to the bed.

Differentiating Eq. 2.3.9 with respect to t* and solving the equation thus obtained for K yields an effective K

$$K_{eff} = \frac{\frac{\partial Q}{\partial t^*} n}{Di_o \sin\omega} \qquad 2.4.1$$

K_{eff} can thus be calculated from measured data.

Since Eq. 2.4.1 is derived from the hydrograph rise equation, n in Eq. 2.4.1 should be the effective porosity of the soil the water table is rising in.

The water content of the soil just before the water table rises in it will be called $\theta_{in\ s.z.}$, s.z. standing for "saturated zone."

This will allow us to distinguish it from the initial water content found before irrigation start and denoted by θ_{in}.

A maximum value of n has been obtained by using for $\theta_{in\ s.z}$ the minimum θ_{in}. A minimum value has been similarly obtained by using for $\theta_{in\ s.z}$ the maximum $\theta_{st.st.}$ The minimum and the maximum values of n

lead to a minimum and a maximum value for an effective K.

Since the recharge rate is not known, it has to be obtained from the irrigation rate, taking the water balance into account. This is done in Note 3, Appendix H.

D is the length of the channel measured perpendicular to the slope. The angle of the bed with the horizontal has been taken to be equal to the angle of the ground surface with the horizontal. Table 2.4.1 shows the calculation of K_{eff}. For Ex1, K_{eff} is found to be between 1.6×10^{-4} and 3.1×10^{-4} ms^{-1}. For Ex2 it is between 1.8×10^{-4} and 3×10^{-4} ms^{-1} and for Ex3 it is between 2.1×10^{-4} and 3.2×10^{-4} ms^{-1}.

A number of errors are attached to the estimate of K_{eff}. They are errors due to possible nonlinearity and to inaccuracies in the values used for calculation. The magnitude of these errors is unknown. Also, it should be remembered that K_{eff} is calculated using simplifying assumptions.

An effective satiated hydraulic conductivity should be found to be the same for any rainfall event. It is not clear why the minimum K_{eff} is larger for Ex2 than for Ex1 and is larger for Ex3 than for Ex2.

In Table 2.4.2, the effective K obtained by the kinematic wave model is compared with the K's obtained at two outflow points, with an effective K obtained by Utting (1978) on Nagpal and de Vries' site, with the K's obtained by the in situ cores, and with the K's of medium and fine sand.

The effective K obtained by Utting (1978) was mentioned by this author to be probably a lower estimate. In order to obtain an effective

Table 2.4.1 Calculations of effective hydraulic conductivities using the kinematic wave approximation

	Ex1	Ex2	Ex3
Max θ steady state	0.40 (at 0.63 m depth, lower neutron probe access tube)	0.38 (at 0.63 m depth, lower neutron probe access tube)	0.38 (at 0.63 m depth, lower neutron probe access tube)
Smallest n (a)	0.23	0.25	0.25
Minimum θ_{in}	0.18 (at 0.15 m depth, lower neutron probe access tube)	0.23 (at 0.15 m depth, lower neutron probe access tube)	0.24 (at 0.15 m depth, lower neutron probe access tube)
Largest n (b)	0.45	0.40	0.39
$R_{ap}(ms^{-1})$ from start of irrigation to end of main limb of rise (c)	3.19×10^{-6}	2.8×10^{-6}	2.9×10^{-6} (f)
Slope of the main limb of rise ($m^3 s^{-2}$) (d)	5.5×10^{-9}	5.1×10^{-9}	5.8×10^{-9}
Minimum K_{eff} using the main limb of rise (ms^{-1}) (e)	1.6×10^{-4}	1.8×10^{-4}	2.1×10^{-4}
Maximum K_{eff} using the main limb of rise (ms^{-1})	3.1×10^{-4}	3.0×10^{-4}	3.2×10^{-4}

a. Smallest n = n_a - Max θ steady state; n_a = 0.63 = porosity

b. Largest n = n_a - Minimum θ_{in}

c. R_{ap} = Time averaged pooled irrigation rate

d. Slope of the main limb of rise = $\frac{\partial Q}{\partial t^*}$ read off the outflow hydrograph

e. $$K_{eff} = \frac{n \quad \frac{\partial Q}{\partial t^*}}{\sin\omega \; D \; i_o}$$

D = Length of channel measured perpendicular to the slope = 7 m

i_o = recharge rate per unit area parallel to the bed.

$i_o = 0.80 \; R_{ap} \cos\omega$

$R_{ap}\cos\omega$ is multiplied by 0.80 in order to take into account the loss found by the water balance

ω = Angle of the ground surface with the horizontal, assumed to be equal to the angle of the bed with the horizontal. $\omega = 30°$

Thus: $i_o = (0.85)(0.80)R_{ap}$

R_{ap} = time averaged pooled irrigation rate

f. Corrected to the value that would have been observed, had RG11 been present.

Table 2.4.2 Comparison of the K_{eff} obtained by the kinematic wave model with other values.

K_{eff} by kin wave	K at 2 outflow points	Effective K obtained by Utting on Nagpal and de Vries' site
1.6×10^{-4} ms^{-1} to 3.2×10^{-4} ms^{-1}	Between 5×10^{-4} ms^{-1} and 5×10^{-3} ms^{-1}	8×10^{-5} ms^{-1}

K by in situ cores	K medium sand	K fine sand
8×10^{-4} ms^{-1}	5×10^{-4} ms^{-1}	10^{-4} ms^{-1}

K, Utting used Eq. 2.3.2 and values of Q and T at steady state. His solution is thus only partly independent of the solution obtained by the kinematic wave model. The solutions differ in that both Q and T used for the estimate of K were observed values for Utting, whereas when the kinematic wave model is used, the observed $\frac{\partial Q}{\partial t^*}$ is used, but T is obtained theoretically. They are alike in that for both estimates, Eq. 2.3.2 is used.

Table 2.4.2 shows that K_{eff} is 2.5 to 5 times smaller than the K's obtained by in situ cores. This is perhaps a little too small, considering the concentration of low resistance paths at the bottom of the saturated zone. It would indicate that, on the average, the conductivity of the top of the soil profile, where the in situ core measurements have been made, is still larger than the conductivity of the saturated zone.

Table 2.4.2 also shows that the value of K_{eff} corresponds to the one obtained for fine or fine to medium sand.

Finally, Table 2.4.2 shows that the values obtained by the kinematic wave model are up to four times the effective K found by Utting and are one order of magnitude smaller than the larger of the two K values obtained from outflow points. It is thus likely that its order of magnitude of 10^{-4} ms^{-1} is reasonable.

Also, the variation of the calculated value of K_{eff} from 1.6×10^{-4} to 3.2×10^{-4} ms^{-1} is acceptable. Most of the variation is due to the fact that, as explained earlier, for one experiment, a minimum or a maximum value of K_{eff} is obtained depending on what value

is used for θ_{in} s.z..

To conclude, use of the kinematic wave equation in order to calculate an effective hydraulic conductivity for the Forest plot indicates that K_{eff} may be bracketed by 1.6×10^{-4} and 3.2×10^{-4} ms^{-1}. Comparison of the value obtained by the kinematic wave model with other values indicates that the order of magnitude obtained can be considered to be a reasonable estimate.

One important note must be made concerning nonlinearity and the kinematic wave model. If the water table is parallel to the bed, the hydraulic gradient is constant since it is equal to $\sin\omega$. Hence there is no physical reason why q should vary at one given place since the driving force is constant. It is possible, however, that flow is fast enough for Darcy's law to fail. Instead of Darcy's law,

$$q = K_{gen} \sin\omega$$

would apply. K_{gen} is defined in Section 3.1. As shown for instance by de Vries' (1979) experimental results, K_{gen} in the nonlinear range is smaller than K. It would however be constant since q and $\sin\omega$ are constant.

Theoretical research is needed in order to investigate further the effects of nonlinearity on the kinematic wave model. In particular, it is not clear whether the equations used for the kinematic wave model, and hence the kinematic wave model, would still be valid. It is not clear either, whether theoretically K_{eff} would vary due to nonlinearity. One reason why $\frac{dh}{ds}$, q, and hence K_{eff} might vary is that the kinematic wave model does not assume the water table is exactly

parallel to the bed, as seen in Eq. 2.3.4.

2.5 Conclusions

In this chapter, the kinematic wave equation for flow in a porous medium over a steep bed and subject to a number of simplifying assumptions was derived and solved using the literature. The term kinematic wave model denotes exclusively the model described in this chapter. The main features of the solution are straight line rises and recessions for the outflow hydrograph and a water table rising parallel to the bed.

Similarity of the hydrograph rise given by the kinematic wave model with the hydrograph rises obtained experimentally was the basis for determining an effective hydraulic conductivity for the saturated zone of the Forest plot.

As mentioned in Chapter I, there are several reasons for this similarity. Two important ones are the steepness of the hillslope's bed and the high hydraulic conductivity of the saturated zone, due to the presence of pipelike low resistance paths on top of the bed.

It is not certain flow in the Forest plot is linear, and the kinematic wave model requires linear flow. In order to apply the kinematic wave model to the Forest plot, it was necessary to assume that nonlinearity, if present, is negligible. Further research is needed to determine the effects of nonlinearity on the kinematic wave model.

Calculations show that the effective K obtained using the kinematic wave model is bracketed by 1.6×10^{-4} and 3.2×10^{-4} ms^{-1}.

The order of magnitude of the K_{eff} thus obtained is within the range of other values measured in the Forest plot or nearby and hence appears reasonable.

2.6 References

Beven, K. 1981. Kinematic subsurface stormflow. Water resources research, Vol. 17, No. 5: 1419-1424.

Childs, E.C. 1969. An introduction to the physical basis of soil water phenomena. Wiley. 493 pp.

Childs, E.C. 1971. Drainage of groundwater resting on a sloping bed. Water resources research, Vol. 7, No. 5: 1256-1263.

Eagleson, P.S. 1970. Dynamic hydrology. McGraw-Hill, New York.

Henderson, F.M. and R.A. Wooding. 1964. Overland flow and groundwater flow from a steady rainfall of finite duration. Journal of geophysical research, Vol. 69, No. 8: 1531-1540.

Utting, M.G. 1978. The generation of stormflow on a glaciated hillslope in coastal British Columbia. M.Sc. Thesis, University of British Columbia, Vancouver.

CHAPTER III

NONLINEAR FLOW

3.1 Introduction

Flow in porous media is generally linear. This means it can be described by a linear relationship between the driving force which is the macroscopic hydraulic gradient $\frac{dh}{ds}$ and the macroscopic flow velocity q. This linear relationship is represented by Darcy's law.

Many authors, however, have noticed that Darcy's law ceases to be valid for either very small flow velocities (e.g., Dudgeon, 1966) or large flow velocities (e.g. de Vries, 1979). Only the loss of linearity at large flow velocities will be discussed here. Flow must be satiated in order for velocities to be large enough for this kind of nonlinearity to be noticeable.

One practical implication of nonlinear flow is that the hydraulic conductivity cannot be obtained from Darcy's law. Using Darcy's law would yield a "general" conductivity $K_{gen} = q(\frac{dh}{ds})^{-1}$ depending on q. Moreover, the validity of mathematical models using Darcy's law would be questionable since they use constant hydraulic conductivities.

In this chapter, it will be assumed that K and K_{gen} are uniform and that the medium is isotropic. When the uniformity of K and K_{gen} is in question they can be thought of as overall values. The assumption of isotropy is not a good one for the forest plot but has been considered to be a necessary simplification.

High hydraulic conductivities are found in the forest soil used for the present work (see Chapters I and II). Also, in their site (see Chapter I), Nagpal and de Vries (1976) calculated the Reynolds number for flow occurring in a root channel, assuming flow was similar to flow in a pipe. They obtained a Reynolds number of 2000, large enough for turbulent flow to occur. A study of nonlinear flow therefore appears relevant to the present work.

In this chapter, a literature review will first be presented. One technical problem, namely the effect of plotting the data as a friction factor versus Reynolds number relationship will then be addressed. Finally, the possibility of occurrence of nonlinear flow in the Forest plot will be examined.

A number of terms used in the following sections need to be defined. These definitions will now be given. The friction factor is treated in detail in Section 3.3, therefore its definition will not be given below.

(i) Reynolds Number

The Reynolds number can be defined in several ways. One group of definitions uses

$$Re = \frac{v_{ch} L_{ch}}{\nu}$$

where

L_{ch}: a characteristic (or representative) length

v_{ch}: a characteristic flow velocity, generally taken to be q

ν : kinematic viscosity of the fluid = $\frac{\mu}{\rho}$

μ : dynamic viscosity of the fluid

ρ : fluid density

This definition of Re will be used in the present work. When a number is given for the Re characterizing flow in a porous medium, the diameter of the particles forming the porous medium will be used for L_{ch} and the macroscopic flow velocity will be used for v_{ch}.

(ii) Flow Velocity

The macroscopic flow velocity, or discharge per unit area q (volume per unit area per unit time) is often called Darcy's velocity. Because this term is confusing when Darcy's law is not valid, it will not be used in this chapter. Also, as mentioned earlier, in the present work, q is taken in the main direction of flow.

(iii) Hydraulic Conductivity and General Hydraulic Conductivity

The general hydraulic conductivity or for short general conductivity K_{gen} is calculated from

$$K_{gen} = \frac{q}{\frac{dh}{ds}} \qquad 3.1.1$$

where $\frac{dh}{ds}$ is the hydraulic gradient.

It is called "general" because although it is equal to the true hydraulic conductivity in the linear range, it is not equal to it anymore in the nonlinear range. As shown for instance by de Vries' (1979) experimental results, K_{gen} in the nonlinear range is smaller than the hydraulic conductivity.

(iv) Permeability

Whereas the hydraulic conductivity K is a function of both the properties of the porous medium and the fluid, the permeability k is only a function of the properties of the porous medium. The two are related by

$$K = \frac{k \rho g}{\mu} \qquad 3.1.2$$

where g = gravitational acceleration

(v) Linear and Nonlinear Range

Some authors consider that there is no strictly linear range but admit the existence of an approximately linear range at small q. Whether authors consider this range to be strictly or only approximately linear, it will be called linear. When judged necessary, linear will be put in quotations marks to mean "so-called linear." The term nonlinear range will be used for the decidedly nonlinear range following the "linear" range. Because it will be suggested turbulence is possibly not necessary for nonlinearity, nonlinear means "laminar nonlinear."

Note also that since the nonlinearity specific to very small q is not considered, the type of nonlinearity mentioned in the "linear" range will be the same as the one at large q.

The flow velocity and the Reynolds number at which flow becomes nonlinear are called "critical." Careful note should be taken of this since authors often use the term "critical" for the apparition of turbulence (e.g., Chauveteau and Thirriot, 1967).

3.2 Literature Review

Loss of linearity was probably first observed by Forchheimer (1901a,b) (Bear, 1972) using data obtained by Masoni (1896) (de Vries, 1979). According to Engelund (1953), nonlinearity for porous media has been noticed to start at a Reynolds number Re varying from 1 to 10. Lindquist (1933) using leadshot 1 to 5 mm in diameter found that nonlinearity started at a Re of 4. de Vries (1979) using sand and glass beads of diameter 0.4 - 0.6 mm and 0.8 - 1.4 mm observed nonlinearity starting at a Re varying from 1.6 to 5.4. Schneebeli (1955) noticed that nonlinearity occurred at a Reynolds number of about 5 in 27 mm diameter glass beads.

Since Forchheimer's work, a fair amount of research has been done in order to determine the causes of nonlinearity, and the equations governing flow both in the linear and the nonlinear range. The rest of this Section will be devoted to a brief review of this research.

(i) Causes of Nonlinearity

Although Ward (1964) attributes nonlinearity to turbulence, there may be a possibility that turbulence is not necessary for nonlinearity. This possibility is offered by both experimental (Schneebeli, 1955; Chauveteau and Thirriot, 1967; Dudgeon, 1966; Wright, 1968) and theoretical work (Hubbert, 1956; Ahmed and Sunada, 1969; Stark, 1969; Lindquist, 1933; Irmay, 1964).

Experimental evidence that turbulence is not necessary for nonlinearity is based on the fact that nonlinearity has been observed at flow velocities smaller than the ones at which turbulence has been observed. It is not entirely convincing, however, since it is restricted, or even contradicted.

First, experimental evidence is restricted by the fact that turbulence has been detected either on a large scale (Schneebeli, 1955) or at one or several points (Dudgeon, 1966; Wright, 1968). In both these cases, the first occurrence of turbulence in the porous medium may have been at a flow velocity smaller than the one at which turbulence was first detected since the flow domain was not monitored at every point. The experiments of Wright offer more evidence that turbulence is not necessary for nonlinearity than those of the other two authors, since he monitored flow at 9 points. Yet even from his work, the observation that nonlinearity started at a flow velocity smaller than the one at which turbulence started may be debated. One reason is that the entire flow domain was not monitored. Another reason is that he did not monitor the flow for turbulence and for nonlinearity appearance

using the same materials but assumed he could combine the results invoking similarity.

Apparently Chauveteau and Thirriot were able to observe the onset of turbulence in individual pores. However, they observed flow in a two-dimensional model built to reproduce a porous medium.

Second, and more importantly, for some of Dudgeon's runs, turbulence was detected at the point where flow was monitored when the overall flow was still linear. (Contrary to the other three authors, Dudgeon does not claim nonlinearity starts at flow velocities smaller than the ones at which turbulence starts but some of his results show it is the case.) It is interesting that Dudgeon found turbulence starting at a Reynolds number as low as 1 whereas Schneebeli observed turbulence start at a Re of 60 and Chauveteau and Thirriot at a Re of 80. It appears that more experimental work is needed.

A theoretical approach used by several authors (Irmay, 1964; Ahmed and Sunada, 1969; Stark, 1969) to prove that laminar flow can be nonlinear is to derive Forchheimer's equation from Navier-Stokes equation. The most common cause of nonlinearity proposed by authors for nonturbulent flow is micro-acceleration, the acceleration of water particles within the pores.

It was not possible to determine whether the theoretical evidence that nonlinearity is not necessarily due to turbulence is entirely satisfactory.

If it is accepted that turbulence is not necessary for nonlinearity, the turbulent range occurs at flow velocities larger than

the ones at which nonlinearity starts (e.g. Schneebeli, 1955) and follows the nonlinear range as q increases.

(ii) Mathematical Description of Linear and Nonlinear Flow

The following equation, suggested by Forchheimer is probably the most commonly used to describe nonlinear flow:

$$\frac{dh}{ds} = \nu aq + bq^2 \qquad (3.2.1)$$

where a,b are constants determined by the properties of the fluid and the porous medium (or possibly of the porous medium only. This was not fully investigated in the present work.)

This equation is generally called Forchheimer's equation.

Two other types of equation, a power law also called Missbach equation (Dudgeon 1966; Trollope et al. 1971) and an infinite series equation (Rummer and Drinker 1966) have been proposed.

Authors using Forchheimer's equation have done so in various ways. Ward, Schneebeli, and Ahmed and Sunada consider that the same quadratic equation is valid for both the linear and the nonlinear ranges, the Darcy's law followed by the data in the "linear" range being an approximation of the quadratic equation at small q.

Other authors (Engelund 1953; de Vries 1979) consider that data follow two distinct equations. These latter two authors consider that the data points follow Darcy's law in the linear range and Forchheimer's equation in the nonlinear range. What makes the two equations distinct

is that the equation describing the linear range is not an approximation of the equation describing the nonlinear range. This point will now be examined in more detail using de Vries' work.

de Vries (1979), following Lindquist (1933) and Engelund, plots his data as impermeability r versus q where r is defined by

$$r \equiv \frac{\rho g}{\mu} \frac{\frac{dh}{ds}}{q} \qquad (3.2.2)$$

(The r's used by Lindquist and Engelund differ slightly from de Vries'). de Vries' data, schematically shown in Figure 3.2.1, first follow approximately Darcy's law

$$\frac{dh}{ds} = \frac{1}{K} q \qquad (3.2.3)$$

recast as

$$\frac{1}{k} = r \qquad (3.2.4)$$

then Forchheimer's equation recast as

$$r = a' + b'q \qquad (3.2.5)$$

where $a' = ga$

$$b' = \frac{\rho g}{\mu} b$$

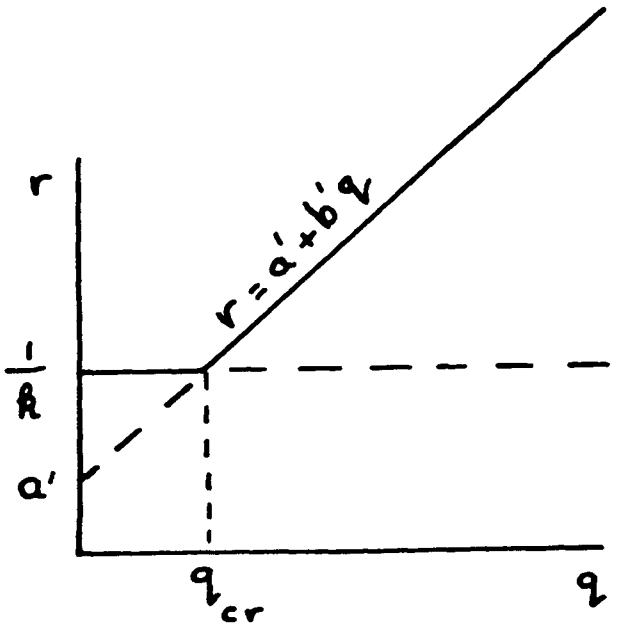

Fig. 3.2.1 Schematic representation of the plot of r versus q obtained by de Vries (1979). Data follow approximately the solid line.

A similar behavior was observed earlier by Lindquist plotting data from Zunker (1920).

de Vries stresses that, as can be seen from Fig. 3.2.1, for small q, r is equal to 1/k and not to a', which would be the case were Eq. 3.2.4 an approximation of Eq. 3.2.5 for small q. It is interesting that both Engelund and de Vries find from experimental data that

$$\frac{1}{k} = 1.07\ ga \qquad (3.2.6)$$

Incidently, Fig. 3.2.1 shows particularly well what is meant by "linear" range, the range during which r is approximately constant, and by nonlinear range, the range where r obeys approximately Forchheimer's equation. The nonlinear range starts at the critical flow velocity q_{cr}.

The third way in which Forchheimer's equation has been used consists of extending it to an equation similar in form, but with variable coefficients. This equation can be written as

$$\frac{dh}{ds} = \varepsilon_1 q + \varepsilon_2 q^2 \qquad (3.2.7)$$

where ε_1 and ε_2 vary with q.

Stark (1969) and Trollope et al. (1971) consider that, strictly speaking, such an equation applies as soon as q is non-zero. As they point out, a consequence of this is that the hydraulic conductivity in Darcy's law is only approximately constant.

Eq. 3.2.7 is interesting from a theoretical point of view. However, it does not say much about the actual behavior of the data points since, due to the fact that ε_1 and ε_2 are allowed to vary with q, it can fit any data points.

Using Darcy's law in the "linear" range and Forchheimer's equation in the non-linear range appears in reasonable agreement with the data. In addition, it shows that at a certain q, some mechanism, possibly microacceleration, modifies the $\frac{dh}{ds}$ versus q relationship.

Whether Forchheimer's equation can be used in both the linear and the nonlinear ranges depends on how accurate a representation of the data is needed.

3.3 Discussion on the Use of Friction Factor Versus Reynolds Number Relationships

As mentioned in the preceding section, some authors (Lindquist, plotting data from Zunker, and de Vries), obtained two distinct $\frac{dh}{ds}$ versus q relationships, one for the "linear" range, and one for the nonlinear range. The two relationships were distinct in that the Darcy's law obtained for the linear range was not an approximation of Forchheimer's equation at small q.

On the other hand, Schneebeli apparently obtained a unique friction factor versus Reynolds number relationship for both ranges. This finding is equivalent to finding that the Darcy's law followed by the data in the linear range is an approximation of the Forchheimer's equation they follow in the nonlinear range.

Since Lindquist and de Vries plot data as a r versus q relationship whereas Schneebeli plots them as a friction factor versus Reynolds number relationship, it is interesting to determine whether the difference in the results is due to differences in the data, or may be due to the different methods used to plot the data. In order to do so, we shall express Darcy's law and Forchheimer's equation as friction factor relationships. Then, using data from de Vries, we shall determine whether it is possible for authors using a friction factor versus Reynolds number representation to notice that the equation describing the data's behavior in the linear range is not an approximation of the equation describing behavior in the nonlinear range.

(i) Expressing Darcy's Law and Forchheimer's Equation as Friction Factor Versus Reynolds Number Relationships

In order to facilitate the following discussion, Darcy's law Eq. 3.2.3 and Forchheimer's Equation Eq. 3.2.1 will be rewritten as

$$\frac{dh}{ds} = \nu\alpha_{lin}\, q \tag{3.3.1}$$

and

$$\frac{dh}{ds} = \nu\alpha_{nonlin}\, q + \beta_o q^2 \tag{3.3.2}$$

Comparison of Eqs. 3.3.1 and 3.3.2 with Eqs. 3.2.3 and 3.2.1 shows that

$$\nu\alpha_{lin} = \frac{1}{K} \tag{3.3.3}$$

$$\alpha_{nonlin} = a \tag{3.3.4}$$

$$\beta_o = b \tag{3.3.5}$$

Authors using a friction factor f and a Reynolds number Re define them as

$$f \equiv C \frac{\frac{dh}{ds}\, d}{q^2} \tag{3.3.6}$$

$$Re \equiv \frac{qd}{\nu} \tag{3.3.7}$$

where d is some measurement related to the size of the pores and C is a constant.

In the present work, a nondimensional friction factor will be defined as either

$$f \equiv \frac{\frac{dh}{ds}}{\alpha_{lin}\, q^2\, d} \tag{3.3.8}$$

or

$$f \equiv \frac{\frac{dh}{ds}}{\alpha_{nonlin}\, q^2\, d} \tag{3.3.9}$$

When used in conjunction with the friction factor, the Reynolds number will be defined by Eq. 3.3.7.

Eqs. 3.3.8 and 3.3.9 are seemingly different from Eq. 3.3.6 in that d occurs explicitly in the denominator rather than in the numerator.

However, by Eqs. 3.1.2 and 3.3.3

$$\alpha_{lin} \propto \frac{1}{k}$$

The permeability k carries the units of length^2 and $\sqrt{k}$ has indeed been used by Ward as d. Hence, it is reasonable to assume that

$$\alpha_{lin} \propto \frac{1}{d^2}$$

and thus, although occurring explicitly in the denominator of f as given by Eq. 3.3.8, d is really implicitly in the numerator.

Because $\nu\alpha_{nonlin}$ is not equal to $\frac{1}{K}$, it is not certain a similar reasoning can be made for Eq. 3.3.9.

Eqs. 3.3.1 and 3.3.2 can now be rewritten as f versus Re relationships using Eq. 3.3.7 and either Eq. 3.3.8 or Eq. 3.3.9. Eq. 3.3.9 will not be used here. Dividing Eq. 3.3.1 by $\alpha_{lin}\, q^2\, d$, using Eqs. 3.3.7 and 3.3.8 and taking logarithms yields the relationship valid in the linear range as

$$\log f = \log \frac{1}{Re} \tag{3.3.10}$$

(Natural logarithms will be used. However, the discussion remains the same if common logarithms are used).

Similarly, Eq. 3.3.2 can be written to yield the relationship in the nonlinear range as

$$\log f = \log\left(\frac{\alpha_{nonlin}}{\alpha_{lin}} \frac{1}{Re} + \frac{\beta_o}{\alpha_{lin}\, d}\right) \tag{3.3.11}$$

(ii) Discussion of the Behavior of the f Versus Re Relationships

Eqs. 3.3.10 and 3.3.11 are schematically represented in Fig. 3.3.1, as well as the asymptote of Eq. 3.3.11 for small Re. This asymptote is

$$\log f = \log \left(\frac{\alpha_{nonlin}}{\alpha_{lin}} \frac{1}{Re}\right) \tag{3.3.12}$$

and is below the line

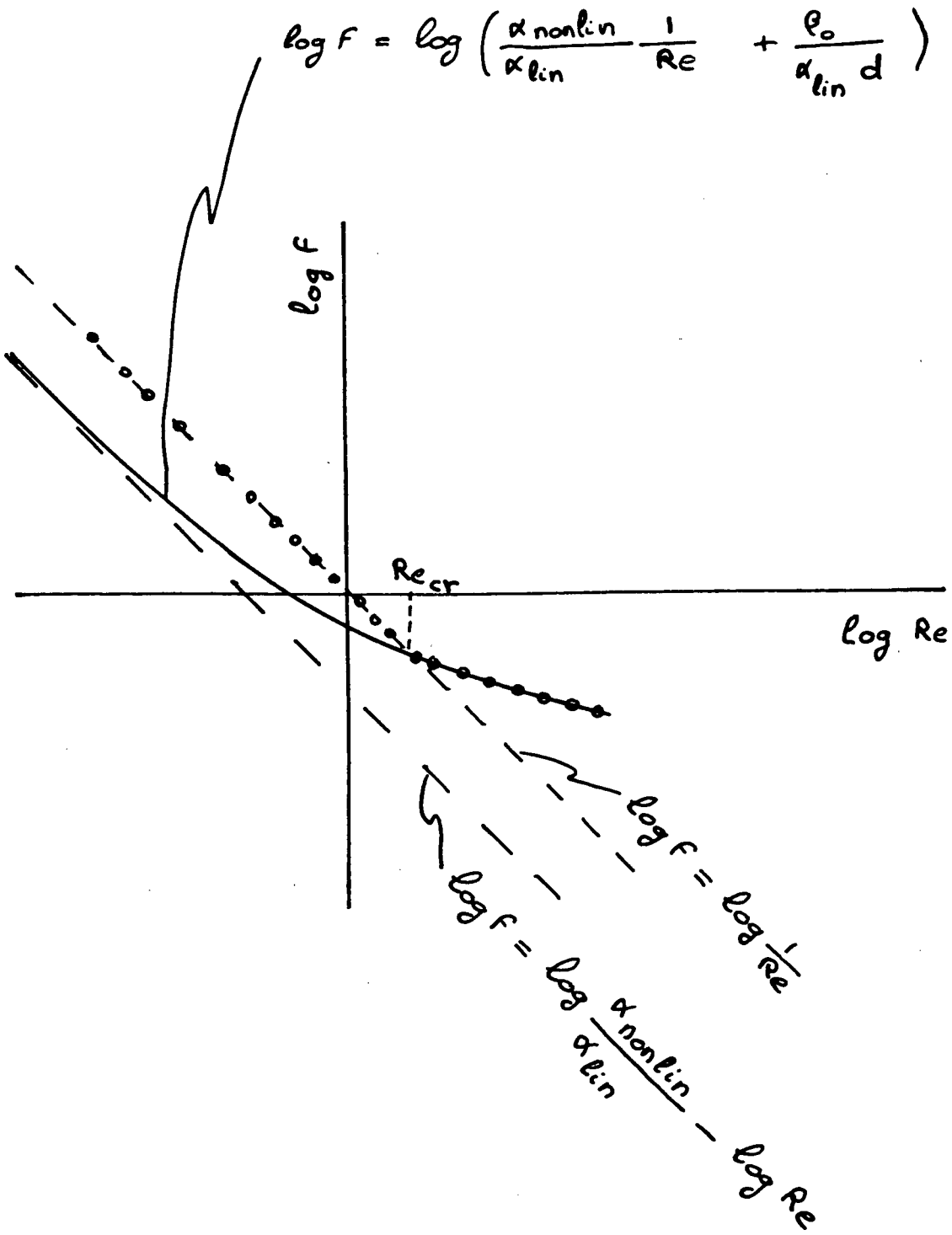

Fig. 3.3.1 f versus Re relationship according to Eqs. 3.3.10 and 3.3.11. o o o hypothetical data points assuming these 2 equations to hold.

$$\log f = \log \frac{1}{Re}$$

because $\log \frac{\alpha_{nonlin}}{\alpha_{lin}}$ is negative as will now be shown.

Using Eqs. 3.3.3, 3.3.4, 3.1.2 and 3.2.6

$$\frac{\alpha_{lin}}{\alpha_{nonlin}} = 1.07$$

Hence $$\frac{\alpha_{nonlin}}{\alpha_{lin}} < 1.$$

This result can also be observed more generally from Fig. 3.2.1, using Eqs. 3.3.3, 3.3.4, 3.1.2 and the fact that a' = ga.

The hypothetical data points obtained assuming Eq. 3.3.10 to be valid in the linear range and Eq. 3.3.11 to be valid in the nonlinear range are also shown. These data points stop following Eq. 3.3.10 to follow Eq. 3.3.11 at the critical Reynolds number Re_{cr} defined by

$$Re_{cr} = \frac{q_{cr} d}{\nu}$$

where q_{cr} is the critical flow velocity, that is, the flow velocity at which flow becomes nonlinear. A graph similar to the one depicted in Fig. 3.3.1 would be obtained were f defined by Eq. 3.3.9.

The behavior of the f versus Re curve followed by the hypothetical data will now be examined.

Since r, as depicted by Fig. 3.2.1 is continuous, the $\frac{\frac{dh}{ds}}{q}$ at q_{cr} obtained from Eq. 3.3.1 can be equated to the $\frac{\frac{dh}{ds}}{q}$ obtained at q_{cr} from Eq. 3.3.2.

This yields

$$\alpha_{lin}\ \nu = \alpha_{nonlin}\ \nu + \beta_o\ q_{cr} \tag{3.3.13}$$

Dividing by $q_{cr}\ \alpha_{lin}\ d$:

$$\frac{1}{Re_{cr}} = \frac{\alpha_{nonlin}}{\alpha_{lin}} \frac{1}{Re_{cr}} + \frac{\beta_o}{\alpha_{lin}\ d} \tag{3.3.14}$$

It follows that the straight line given by Eq. 3.3.10 and the curve given by Eq. 3.3.11 cross each other at Re_{cr}. Thus, if r is continuous, the f versus Re relationship followed by the data is continuous. The slope of the log f versus log Re curve followed by the data, however, is discontinuous at q_{cr}, as will now be shown.

Using the chain rule of differentiation, $\frac{d\log f}{d\log Re}$ can be found to be -1 for Eq. 3.3.10. For Eq. 3.3.11:

$$\frac{d\log f}{d\log Re} = \frac{-1}{1 + \frac{\beta_o}{\alpha_{lin}\ d} \frac{\alpha_{lin}\ Re}{\alpha_{nonlin}}} = \frac{-1}{1 + \frac{\beta_o}{\alpha_{nonlin}} \frac{q}{\nu}} \tag{3.3.15}$$

Experimental values obtained by de Vries (1975, 1979) for 0.4 - 0.6 mm sand and 0.8 - 1.4 mm sand can be used to obtain $\frac{d\log f}{d\log Re}$ at q_{cr} from Eq. 3.3.15. The detail of the calculations is given in Appendix I, Note 1. The results are shown in Table 3.3.1.

Table 3.3.1. $\frac{d\log f}{d\log Re}$ at q_{cr} calculated from Eq. 3.3.15 using data from de Vries (1975, 1979).

Material	$\frac{d\log f}{d\log Re}\Big\|_{q_{cr}}$
0.4 - 0.6 mm sand	- 0.97
0.8 - 1.4 mm sand	- 0.93

It can be seen from Table 3.3.1 that there is indeed a break at q_{cr}, since there the slope changes from -1 to -0.97 for the 0.4 - 0.6 mm sand and from -1 to -0.93 for the 0.8 - 1.4 mm sand. The change in slope for the materials used for Table 3.3.1 is so small that it is likely that authors will not notice it, especially when there is some scatter due to experimental error. Also, authors will not be able to see that the data follow two distinct equations and that therefore the asymptote of the curve the data follow in the nonlinear range is not the straight line they follow in the linear range. They will deduce that the data follow the same quadratic equation in both the linear and the nonlinear ranges.

Note that one may wish to check whether the friction factor as it is defined in the present work is close enough to the friction factors used by other authors for the reasoning presented above to be valid. Such a check might be done by considering the works of other authors individually.

As a summary, if data following two distinct equations, a linear one in the linear range and a quadratic one in the nonlinear range, are plotted as a friction factor versus Reynolds number relationship, the following problem is likely to result: It will not be possible to observe on the f versus Re plot that the straight line followed by the data in the linear range is not the asymptote of the curve followed in the nonlinear range. Rather, data will apparently follow a unique quadratic relationship. As a result, authors will erroneously conclude that Darcy's law is an approximation of Forchheimer's equation at small q.

3.4 Occurrence of Nonlinear Flow in the Forest

In this section, the possibility of occurrence of nonlinear flow in the Forest plot and its vicinity will be examined. Implications of nonlinear flow will be briefly examined and suggestions for further research presented.

(i) Investigation of the Possibility of Occurrence of Nonlinear Flow In and Near the Site

For the purpose of investigating the occurrence of nonlinear flow in and near the site, observed flow velocities will be compared with the critical flow velocity obtained by de Vries for 0.4 to 0.6 mm sand. The reason for using this sand fraction is that, among the materials used by de Vries, it is the one considered to be the closest to the Forest plot soil. In order to compare the various flow velocities observed in the

field with the critical flow velocity obtained for 0.4 to 0.6 mm sand, it is necessary to assume the Forest soil behaves like the sand. Comparisons are shown in Table 3.4.1.

Because the temperature and hence the viscosity of the water used by de Vries was different from the temperature of the water in the Forest, it was determined whether it was necessary to correct the critical velocity for temperature. In order to do so, it has been assumed that nonlinear flow will start at the same Re in the sand and in the Forest material and that this is true irrespective of differences in temperatures. Also, it was assumed that the representative length L_{ch} appearing in the Reynolds number is the same for the sand and for the Forest material. This assumption is not likely to be verified, but is necessary for calculation purposes. Using the above assumptions, a q_{cr} of 5×10^{-3} ms^{-1} for flow in the Forest has been calculated for a temperature of 5°C, taken to be a lower estimate for the temperature of the water during the measurements made in the Forest. This calculation, shown in Note 2, Appendix I, uses the q_{cr} of 3×10^{-3} ms^{-1} and the μ given by de Vries (1979 and 1975).

Because the q_{cr} at 5°C is close to the one at 22°C, it will be considered that the difference between the two values is within experimental error and a q_{cr} of 3×10^{-3} ms^{-1} will be used as a conservative estimate.

In order to determine if the conditions for nonlinear flow are fulfilled, it is necessary to separate the flow path in two parts: first, flow down to the bed and second, lateral saturated flow over the

Table 3.4.1 Comparison of measured flow velocities with de Vries' critical flow velocity

Vertical Infiltration		q at 2 outflow points along the channel's bank	q critical at 22°C	q critical at 5°C
concentrated inflow rate from two logs	K for the upper part of the soil profile by in situ cores			
8×10^{-5} to 4×10^{-3} ms^{-1}	8×10^{-4} ms^{-1}	Between 2.7×10^{-4} and 1.1×10^{-3} ms^{-1} Between 8.7×10^{-4} and 2.6×10^{-3} ms^{-1}	3×10^{-3} ms^{-1}	5×10^{-3} ms^{-1}

bed. Although the first part of the flow path is in the generally unsaturated zone, local saturation is necessary for nonlinear flow to occur.

For nonlinear flow during the first part, sufficiently high hydraulic conductivities and sufficiently large inflow rates from concentrating elements are required. For nonlinear flow during the second part, a sufficiently large driving force and a sufficiently large hydraulic conductivity are required.

Measurements of inflow rates from natural concentrating elements were made in the vicinity of the Forest plot during and after rainfall. These measurements are limited by difficulties in measuring the infiltrating area. Also, it is not known how representative they are for an average rainfall event. As mentioned in Chapter I, logs in various states of decay are present on the ground. They are considered to be the major sources of concentrated inflow as they act as more or less impermeable elements. A large inflow rate was found from a rock but rocks are sparse. From two logs, inflow rates at various points were 8.1×10^{-5}, 1.6×10^{-4}, and 4.5×10^{-3} ms^{-1}. The last estimate is possibly too large. It is puzzling that it is one order of magnitude larger than the minimum concentrated inflow rate due to the plastic sheets (see Appendix B). If it is correct, however, it shows the inflow rate may at places be large enough for nonlinear flow to occur.

For flow in the unsaturated zone, the K of 8×10^{-4} ms^{-1} obtained by the *in situ* cores method for the top part of the profile has been used. Apparently, if gravity driven vertical flow takes place, this K

is not large enough to allow nonlinear flow at steady state, since at steady state K = q for gravity driven vertical flow and thus a K of 3 x 10^{-3} ms^{-1} or larger is required.

Since the K obtained by in situ cores is an average value, it is still possible that water can find pathways with conductivities large enough for flow to be nonlinear. Hence nonlinear flow may occur in the unsaturated zone. Because spots where large inflow rates occur are not widespread, it can however be concluded that under natural conditions nonlinear flow down the profile is not common. Also, it probably occurs, if at all, only for short distances since it is likely that in many cases water travelling in a low resistance path would soon get sucked into the soil matrix.

As for lateral flow over the bed, flow velocity was directly measured at 2 outflow points along the channel's bank in the Forest plot (see Section 1.3.1). Outflow was from a natural storm event. As mentioned in Section 1.3.1, there are inaccuracies in the measurements, the true flow velocities being possibly bracketed by 2.7 x 10^{-4} and 2.6 x 10^{-3} ms^{-1}. The largest value is equal to q_{cr}, indicating that flow is close to being non-linear.

The flow velocities calculated at the two outflow points chosen may not be the highest velocities occurring in the Forest plot. In particular, they may not be the highest velocities having occurred during the artificial events Ex1, Ex2 and Ex3. Indeed, during irrigation, the saturated zone thickness is larger and more low resistance paths are used. This increases the chance of finding low

resistance paths in which nonlinear flow occurs. Thus flow in the Forest plot may be nonlinear.

As for flow in the vicinity of the Forest plot, one should remember that in a rootchannel in Nagpal and de Vries' site, "assuming the nature of flow...to be similar to that in a pipe, a Reynolds number larger than 2,000 was calculated [presumably as $\frac{qd}{p}$ with d the diameter of the root channel], indicating the existence of turbulent flow conditions within the rootchannel" (Nagpal and de Vries, 1976). The Reynolds number at which turbulence is expected to start is not definite but for a pipe, the lower limit is 2000 (Ginzburg, 1963). Since it is expected that any small disturbance of flow renders flow turbulent at a Reynolds number of 2000 and that the root channels are not smooth, it is indeed expected that flow will become turbulent at a Reynolds number of 2000.

Note that in this case, pipe flow theory rather than experimental results on sand was used to determine the nature of the flow.

To conclude, it is suggested that both in the Forest plot and in its vicinity, only a small proportion of flow, if any, can be nonlinear in the unsaturated zone under natural conditions.

It is not certain whether nonlinear flow can occur in the saturated zone of the Forest plot.

(ii) implications of nonlinear flow in the Saturated Zone

One implication of nonlinear flow over the low conductivity layer is that hydraulic conductivities determined using outflow to a trench may be "general" hydraulic conductivities (see Sections 2.4, and 3.1),

in fact smaller in the nonlinear range than the true hydraulic conductivities. When used in a model using Darcy's law, general hydraulic conductivities obtained from nonlinear flow would really be valid for only one value of q except if the hydraulic gradient can be taken to be equal to the bed slope, that is, if $q = K_{gen} \sin\omega$ (see section 2.4). In an effort to determine how significant the effect of nonlinearity is on K_{gen}, experiments by de Vries (1975) have been used. These experiments showed the variation of K_{gen} with q, for 0.4 to 0.6 mm sand to be as given by Table 3.4.2.

Table 3.4.2. q and $\rho g \frac{dh}{ds}$ from experiments in 0.4 to 0.6 mm sand by de Vries (1975). K_{gen} calculated from these values.

q ms^{-1}	$\rho g \frac{dh}{ds}$ $kgs^{-2}\ m^{-2}$	$K_{gen} = q\rho g \frac{1}{\rho g \frac{dh}{ds}}$ ($\rho = 10^3$ kg m^{-3}; $g_1 = 9.8$ ms^{-2}) ms^{-1}
3.0×10^{-3}	2.7×10^{4}	0.11×10^{-2}
9.2×10^{-3}	8.9×10^{4}	0.10×10^{-2}
2.0×10^{-2}	2.2×10^{5}	0.089×10^{-2}

Table 3.4.2 shows that as q changes from 3×10^{-3} (q critical) to 9.2×10^{-3} ms^{-1}, K_{gen} changes by 10%. It changes by another 10% as q changes from 9.2×10^{-3} to 2.0×10^{-2} ms^{-1}.

The value of K_{gen} at q_{cr}, 1.1×10^{-3} ms^{-1} can be taken as K since K_{gen} is constant in the linear range.

For the purposes of discussion, it will be assumed that K, a and b are the same for the material in the pipelike low resistance paths over the bed as in the 0.4 to 0.6 mm sand. Although such an assumption cannot be entirely correct, it is not unreasonable since the K for the sand is in between the K's measured at the outflow points.

Table 3.4.2 shows that if q in the pipelike low resistance paths over the bed is about 10 times the highest flow rate observed for the 2 outflow points used (2.6×10^{-3} ms^{-1}, Table 1.3.1.1), K_{gen} is about 20% less than K. Table 3.4.2 will not be used to infer effects of nonlinearity on the K_{eff}'s determined for the forest plot because there are too many uncertainties.

Note that use of the kinematic wave model will always present the problem of the need for flow to be sufficiently fast, yet not too fast. It should be remembered that the term "kinematic wave model" denotes exclusively the model described in Chapter II.

As far as the Forest plot is concerned, it is concluded that it is not certain what the implications of nonlinear flow in the Forest plot saturated zone are on K_{gen}, and hence on Darcy's law and on the kinematic wave model. The reasons are the following:

(i) It is not certain what proportion of the flow, if any, can be nonlinear.

(ii) It is not certain how severely nonlinear the flow can be.

(iii) It is not certain what the effect of the nonlinearity will

be on K_{gen}, on Darcy's law and on the use of the kinematic wave model. One reason is that the calculations of Table 3.4.2 were based on 0.4 to 0.6 mm sand and not on the Forest plot soil. Another reason is the note made on the effect of nonlinearity on the kinematic wave model made at the end of Section 2.4.

(iii) Suggestions for Further Research

There is a need for further research on nonlinearity in the field. First, a way of determining whether flow is nonlinear in the field should be found. Second, it is suspected that flow in underground "streams" may be nonlinear. This should be checked, and more generally, the proportion of nonlinear flow in the saturated zone and the severity of this nonlinearity should be determined. Finally, the implications of nonlinear flow on satiated general conductivities determined in the field and on physically based mathematical models should be determined.

As a summary, it is not certain whether nonlinear flow occurs in the Forest plot saturated zone. The implications of nonlinear flow on use of the kinematic wave model for the Forest plot are also uncertain. It is also suggested that only a small proportion of flow, if any, can be nonlinear in the unsaturated zone under natural conditions.

3.5 Conclusions

A literature review showed that there is a possibility that turbulence is not necessary for nonlinearity. However, more

investigations are needed since some results are contradictory. Microacceleration is often recognized as a cause of nonlinearity for laminar flow.

Forchheimer's equation has been widely used to describe nonlinear flow. Its use, however, varies from author to author. Three different theories have been proposed in the literature:

1. Data obey Darcy's law in the "linear" range and Forchheimer's equation in the nonlinear range.
2. Data obey Forchheimer's equation in both the "linear" and the nonlinear ranges.
3. Data obey an equation similar to Forcheimer's, but in which the coefficients of q and q^2 vary with q as soon as q is nonzero.

Theory (1) appears to be the one to be preferred from a practical point of view as being simple and yet in reasonable agreement with experimental data.

In this chapter, it has been shown that it is likely that authors using a friction factor versus Reynolds number representation of their data will assume theory (2) to be valid even if data follow the graph given by theory (1).

The possibility of occurrence of nonlinear flow in the Forest plot and its vicinity was investigated. It was suggested that, either in the Forest plot or its vicinity, only a small proportion of flow, if any, can be nonlinear in the unsaturated zone under natural conditions.

It was shown that it is not certain whether nonlinear flow can occur in the saturated zone of the Forest plot.

It was also concluded that it is not certain what the implications of nonlinear flow in the saturated zone of the Forest plot would be on Darcy's law and hence on the use of the kinematic wave model.

3.6 References

Ahmed, N. and D.K. Sunada. 1969. Nonlinear flow in porous media. American Society of Civil Engineers, Journal of the hydraulics division, Vol. 95, No. HY6: 1847-1857.

Bear, J. 1972. Dynamics of fluids in porous media. American elsevier. 764 pp.

Chauveteau, G. and Cl. Thirriot. 1967. Régimes d'écoulement en milieu poreux et limite de la loi de Darcy. La houille blanche, No. 2: 141-148.

de Vries, J. 1975. Unpublished data.

de Vries, J. 1979. Prediction of non-Darcy flow in porous media. American Society of Civil Engineers, Journal of the irrigation and drainage division, Vol. 105, No. IR2, Proc. Paper 14610: 147-162.

Dudgeon, C.R. 1966. An experimental study of the flow of water through coarse granular media. La Houille blanche, No. 7: 785-800.

Engelund, F. 1953. On the laminar and turbulent flows of ground water through homogenous sand. Transactions of the Danish Academy of Technical Sciences, No. 3, Contribution from the Hydraulic Laboratories Technical University of Denmark, Copenhagen, Denmark, Bulletin, No. 4.

Forchheimer, P. 1901a. Wasserbewegung durch Boden. Z. ver. Deutsch. Ing. 45: 1782-1788. Cited by Bear.

Forchheimer, P. 1901b. Wasserbewegung durch Boden. Zeitschrift des vereines Deutscher Ingenieure, No. 49: 1736-1749; No. 50: 1781-1788. Cited by de Vries (1979).

Ginzburg, I.P. 1963. Applied fluid dynamics. Translated from Russian. Israel Program for Scientific Translations, Jerusalem.

Hubbert, M.K. 1956. Darcy's law and the field equations of the flow of underground fluids. Transactions of the American institute of mining, metallurgical, and petroleum engineers, Vol. 207: 222-239.

Irmay, S. 1964. Modèles Théoriques d'écoulement dans les corps poreux. Rilem symposium, Paris.

Lindquist, E. 1933. On the flow of water through porous media, 1er congrès des grands barrages, Stockholm, Sweden, Vol. 5: 81-101.

Masoni. 1896. Di alcune determinazioni sperimentali sui coefficienti di filtrazione. Naples, Italy. Cited by de Vries (1979).

Nagpal, N.K., and J. de Vries. 1976. On the mechanism of water flow through a forested mountain slope soil in coastal western Canada. Unpublished material.

Rumer, R.R., Jr., and P.A. Drinker. 1966. Resistance to laminar flow through porous media. American Society of Civil Engineers, Journal of the hydraulics division, Vol. 92, No. HY5: 155-163.

Schneebeli, G. 1955. Expériences sur la limite de validité de la loi de Darcy et l'apparition de la turbulence dans un écoulement de filtration. La Houille blanche, No. 2: 141-149.

Stark, K.P. 1969. A numerical study of the nonlinear laminar regime of flow in an idealized porous medium. International association for hydraulic research. International symposium on the fundamentals of transport phenomena in porous media, Haifa: 86-102.

Trollope, D.H., K.P. Stark and R.E. Volker. 1971. Complex flow through porous media. The Australian Geomechanics journal: 1-10.

Ward, J.C. 1964. Turbulent flow in porous media. American Society of Civil Engineers, Journal of the hydraulics division, Vol. 90, No. HY5, Proc. Paper 4019: 1-12.

Wright, D.E. 1968. Nonlinear flow through granular media. American Society of Civil Engineers, Journal of the hydraulics division, Vol. 94, No. HY4, Proc. Paper 6018.

Zunker, F. 1920. Das allgemeine Grundwasserfliessgesetz, Gasbeleuchtung und Wasserversorgung. Cited by de Vries (1979).

CHAPTER IV

DISCUSSION AND CONCLUSIONS

The observation of low resistance paths due mainly to root material in the Forest plot prompted the investigation of flow mechanisms in both the unsaturated and the saturated zones.

One tool used for investigation of flow mechanism in the unsaturated zone was the kinematic wave model for saturated flow over a steep bed. The term "kinematic wave model" denotes exclusively the model described in the second chapter. The kinematic wave model requires a steep bed slope, a high hydraulic conductivity and a low recharge rate. It also assumes steady and uniform recharge rate, effective porosity and hydraulic conductivity, unidirectional flow and a uniform bed slope. Flow must be linear. The porous medium must be isotropic. The kinematic wave model yields straight line rising limb and recession.

The field observation that the main limb of hydrograph rise for the Forest plot is a straight line indicates that there is some justification for applying the kinematic wave model to the Forest plot.

Soil thickness is not uniform. Hence it might be expected that the recharge rate could be somewhat nonuniform and unsteady. It is not clear for how long nonuniformity and unsteadiness would last, but if they last for longer than for a short period of time at the beginning of the recharge, the main limb of rise would not be a straight line. Yet the main limb of rise is a straight line, indicating that the soil and water system in the unsaturated and the saturated zones behaves as if

the kinematic wave model were valid, and hence as if recharge were uniform and steady.

In particular, a straight line main limb of rise together with the fact that there was little preliminary outflow before the main limb of rise shows that the system behaves as if little or no short-circuiting occurred. A straight line main limb of rise is perhaps due to an averaging process.

Another means used to investigate flow in the unsaturated zone was to compare results obtained from concentrated irrigation with results obtained from uniform irrigation. It was found that concentration of irrigation did not change the general shape of the outflow hydrograph and did not decrease the time lag to the main limb of rise. Also, rather than enhancing the initial step of the outflow hydrograph obtained for uniform irrigation, it suppressed it. It was also observed that concentration did not cause the water table to rise earlier, and did not affect the shape of the water table at steady state. From these observations, it was concluded that the soil and water system in the unsaturated and saturated zones of the Forest plot behaves as if short-circuiting were not enhanced by concentration.

Thus, the outflow hydrograph indicates that within the limits of experimental design the system behaves as if little or no short-circuiting occurred and as if short-circuiting were not enhanced by concentration.

Some aspects of the water table behavior may suggest that short-circuiting occurred. Indeed, pipes 1, 5 and 8 were not affected

by initial conditions. Further experimental work is needed to learn more about flow mechanisms in the unsaturated zone.

The saturated zone in the Forest plot is characterized by low resistance paths which together with a steep bed slope and a high recharge rate are responsible for steep rises and recessions of the outflow hydrograph. Thus two of the assumptions necessary for the kinematic wave model, a high hydraulic conductivity and a steep bed slope are readily verified.

A number of the assumptions necessary for the saturated zone are not satisfied, however. In particular, the hydraulic conductivity and the effective porosity are not uniform and the flow is not unidirectional. Yet the system behaves as if these assumptions were satisfied. Here also an averaging mechanism could be invoked.

On the basis that the system behaves as if the kinematic wave model were valid, effective hydraulic conductivities were calculated for the saturated zone, using the kinematic wave model and the rising limb of the outflow hydrographs. Calculations showed that the effective hydraulic conductivity is bracketed by 1.6×10^{-4} and 3.2×10^{-4} ms^{-1}.

In order for the kinematic wave model to be valid, flow in the saturated zone must be reasonably fast. If it is too fast, it becomes nonlinear and Darcy's law and hence the kinematic wave model fails. Because it is suggested that possibly turbulence is not necessary for flow to be nonlinear, nonlinear means "laminar nonlinear".

The possibility of occurrence of nonlinear flow in the Forest plot and its vicinity was investigated. It was suggested that, either in the

Forest or its vicinity, only a small proportion of flow, if any, can be nonlinear in the unsaturated zone under natural conditions.

It was shown that it is not certain whether nonlinear flow can occur in the saturated zone of the Forest plot.

It was also concluded that it is not certain what the implications of nonlinear flow in the saturated zone of the Forest plot would be on Darcy's law and on the use of the kinematic wave model.

As a summary, the main conclusions about flow mechanisms are as follows: the field observation that the main limb of rise is a straight line indicates that the soil and water system in the unsaturated and the saturated zones behaves as if the kinematic wave model were valid. In particular, it indicates that the system behaves as if little or no short-circuiting occurred.

Two of the assumptions linked to the kinematic wave model are readily verified: a high hydraulic conductivity and a steep bed slope.

If the outflow hydrograph obtained with artificial concentration is compared to the one obtained without artificial concentration, it is seen that short-circuiting is apparently not enhanced by concentration. A similar conclusion is obtained from the behavior of the water table.

It was suggested that only a small proportion of flow, if any, can be nonlinear in the unsaturated zone under natural conditions. This is true for the Forest plot and its vicinity. It is not certain whether nonlinear flow can occur in the saturated zone of the Forest plot.

APPENDIX A

DETERMINATION OF THE STONE RATIO

1. Method to Separate Stones from Concretions by Breaking Down the Concretions

This is a method to dissolve Fe oxides but it can also be used for Al oxides. Once the cementing agents (iron and aluminum oxides) are removed, the concretions break down. The method has been adapted from Mehra and Jackson, 1960.

- Place the soil into a beaker
- Add enough citrate bicarbonate solution (8:1 ratio by volume of sodium citrate and sodium bicarbonate resp.) to cover the soil.
- Heat up the beaker to 75°C in a water bath.
- Add 1 teaspoon per 100 g of soil of sodium hydrosulfite (sodium dithionite) low in iron and purified.
- Stir slowly at first then vigorously, for about 1 min. Heat for an additional 15 min, but do not allow the temperature to rise above 80°C.
- Cool.
- Pass through a 2 mm sieve.

This method is adequate for a rough estimate.

2. Calculation of the Stone Ratio

In the B horizon, the ratio "mass of concretions, cemented aggregates, cemented sand + stones > 2 mm" to "mass of soil" was found

to be 0.49. By treating the fraction > 2 mm with a citrate bicarbonate solution and with sodium hydrosulfite (see above), the ratio "mass of stones" to "mass of fraction > 2 mm" was found to be 0.84 hence the ratio "mass of stones" to "mass of soil" is 0.41. Note that because the citrate bicarbonate treatment removed cementing agents, some of the particles in the stone fraction may have been smaller than 2 mm. The porosity for the top of the B horizon calculated by

$$1 - \frac{\text{bulk density}}{\text{particle density}}$$

is 0.63 $m^3\ m^{-3}$

The particle density is 2512 ± 254 kgm^{-3} (based on 9 samples; the number given after the ± is 2 standard deviations). This means that approximately 95% of the particle densities are between 2258 and 2766 kgm^{-3}.

The bulk density for the top of the B horizon determined by the excavation method is 931 ± 326 kgm^{-3} (based on 7 samples). This means that approximately 95% of the bulk densities are between 605 and 1257 kgm^{-3}.

Using the bulk density given above, and using for stone density the density of granite (2650 kgm^{-3}), the ratio of stones to bulk soil by volume can be found to be

$$(\text{ratio of stones by mass})\ (\frac{\text{bulk density}}{\text{density of granite}}) = 0.14$$

where

$$\text{ratio of stones by mass} = \frac{\text{mass of stones}}{\text{mass of soil}} = 0.41$$

APPENDIX B

CALCULATION OF THE MINIMUM CONCENTRATION OF IRRIGATION OBTAINED BY THE PLASTIC SHEETS

Calculation of the minimum concentration of irrigation by the plastic sheets is obtained by

minimum concentration = "minimum estimate of area of plastic sheets" divided by "maximum estimate of area of infiltration for the water flowing from the plastic sheets."

The minimum area of a plastic sheet is 55 x 75 cm^2; there are 16 plastic sheets. A maximum estimate for the area of infiltration of water flowing from one plastic sheet outflow point is 10 cm^2. There is a maximum of 4 outflow points per plastic sheet. Therefore:

$$\text{minimum concentration} = \frac{16 \times 55 \times 75 \text{ cm}^2}{16 \times 4 \times 10 \text{ cm}^2} = 100$$

For the applied irrigation rate of about 2.8×10^{-6} ms^{-1}, a concentration of 100 times yields an inflow rate of 2.8×10^{-4} ms^{-1}.

APPENDIX C

COMPARISON OF THE RECESSION WITH HEWLETT AND HIBBERT'S RECESSION: NORMALIZATION AND LIMITATIONS

In order to compare the recession obtained for the present work with the one obtained by Hewlett and Hibbert, it would be desirable to normalize the results with respect to a number of parameters. The kinematic wave model (see Note 4, Appendix H), gives the outflow rate during the recession as

$$Q = Di_o L - \frac{K \sin\omega \, D \, i_o \, t'}{n_{re}} \qquad (C\text{-}1)$$

where

D = width of the hillslope

Q = discharge (volume/time)

i_o = a constant, nonzero recharge rate per unit area parallel to the bed ($\frac{\text{volume}}{\text{area x time}}$)

K = satiated hydraulic conductivity

n_{re} = effective porosity for the recession

t' = time from stop of recharge = $t^* - t_r$

t_r = time at which recharge stopped

L = length of the saturated zone

K and n_{re} are properties of the soil. Since the effects of the soil on Q are sought, it is not desirable to normalize Q with respect to K and n_{re}. Moreover n_{re} would be difficult to obtain in practice.

Normalization with respect to i_o cannot be achieved since i_o for Hewlett and Hibbert is not known. Q for the present work has been calculated for a D of 0.91 m, which is equal to the D in Hewlett and Hibbert's work.

Also, obtaining $\frac{\partial Q}{\partial t'} \doteq \frac{\Delta Q}{\Delta t'}$ from Eq. C-1 and solving for $\Delta t'$ indicates $\Delta t'$ is proportional to $1/\sin\omega$. Hence $\Delta t'$ for the present work must be divided by 0.70 in order to be the $\Delta t'$ that would be obtained for a slope of 22°. Normalization with respect to L cannot be performed for Q since L appears only in one term. Normalization with respect to $\sin\omega$ cannot be performed for Q because $\sin\omega$ appears only in one term.

Table C-1 indicates which values of the present work given in Table 1.4.4.1 have been normalized.

Table C-1 Normalization summary for the results of the present work given in Table 1.4.4.1.

Normalized with respect to	Q	Time	$\Delta t'$
D	Yes	Yes	Yes
i_o	No	No	No
L	No	No	No
$\sin\omega$	No	No	Yes, where indicated

The comparison of the present work with Hewlett and Hibbert's should be considered with some caution since only partial normalization has been performed. Moreover, this normalization assumes the kinematic wave theory can be applied to both Hewlett and Hibbert's work and the present work.

APPENDIX D

CALCULATION OF THE POINTS USED TO PLOT FIG. 1.4.2.6, THE DETAILED HYDROGRAPH RISES

Most of the early points in Fig. 1.4.2.6 are based on two tips of the outflow tipping bucket first, then on 4 tips. The first point is given by tips one to three, tip one being the first tip after the start of irrigation, the second point by tips three to five, and so on.

Rates of outflow are plotted in the middle of the interval between the tips which is not accurate but is satisfactory for comparison purposes. Some of the points, especially later points, have been taken from the small scale hydrographs (Figs. 1.4.2.3 to 1.4.2.5).

APPENDIX E

EFFECT OF ERRORS AND LIMITATIONS IN OUTFLOW RATE

The outflow rate is subject to a number of errors and limitations. Their effect on the main results of outflow are discussed below.

1. There is an antecedent outflow smaller than 2.8×10^{-8} m^3 s^{-1} for Ex2 and smaller or equal to 1.5×10^{-7} m^3 s^{-1} for Ex3. For Ex3, the first tip is due to antecedent conditions only. The antecedent outflow does not affect the comparison of the timing of the main limb of rise (e.g. whether the main limb of rise Ex1 lags behind the main limb of rise Ex3) because a shift of 1.5×10^{-7} m^3 s^{-1} for the main limb of rise is negligible. It is expected to have a negligible effect on the shape of the main limb of rise and no effect on the time to steady state. A rate of 1.5×10^{-7} m^3 s^{-1} is negligible with respect to some of the rates occurring during the initial step of Ex3. Hence the initial step of Ex3 does occur before the early rise part of the rise of Ex2 and is not due uniquely to antecedent outflow.

2. Some spurious inflow to the channel occurred.

(i) Some inflow due to overland flow when the forest floor was hydrophobic and some inflow from water falling on the plastic plot boundaries occurred. Attempts were made to prevent overland flow due to hydrophobicity from reaching the channel and confusing the interflow data. This spurious inflow is negligible once the main limb of rise has started.

Flow over the plastic frame may have been responsible for part of the early parts of the rises but this does not change the statement that the initial steps are small for Ex1 and Ex3 and non-existant for Ex2. It is probably negligible after the main limbs of rise have started, except during the rerise of Ex3. This spurious inflow during the rerise of Ex3 does not affect the results considered.

(ii) Extraneous inflow from the water collected on the plastic plot boundaries reaching the channel by an underground route. This inflow, if it actually occurs, is presumably the same for the three experiments and is constant. Hence it should not affect the comparison between the 3 experiments. Neither should it affect the slope of the main limb of rise. It has no effect on the time to steady state. It would affect the water balance. If it participates in the outflow during the initial step, it would however not change the statement that this outflow is small.

3. Water escaping collection because the channel had not been dug far enough. This affects the water balance. It might affect the comparison between Ex2 and the other two experiments if the outflow missed is affected by concentration. Since the outflow missed is probably only a small proportion of the total outflow, chances that it is affected by concentration are smaller. It will be assumed that this error does not affect the comparison between the three experiments. It would not affect the time to steady state. It is doubtful whether it can affect significantly the shape of the main limb of rise. Similarly, it is doubtful whether it can affect the water balance significantly.

4. Uncertainty as to whether the right tipping bucket calibration has been used for Ex1 until 3.5 hours before final irrigation stop and for Ex2 until 39 hours after the start of irrigation. Uncertainty in calibration may have some effect on the hydrographs. The error in calibration however would not be large enough to be responsible for the lack of initial step and the delay of the early part of the rise for Ex2.

Errors in calibration for Ex1 and Ex2 may affect the shape of the main limb of rise. Since it is a straight line for Ex3 as well as for Ex1 and Ex2, it is likely that the straight line rise for Ex1 and Ex2 is real.

Also, it is rather unlikely that errors in calibration would by chance yield a straight line rise for both Ex1 and Ex2. Moreover, straight line main limbs of rise were also observed by Utting (1978) and by Nagpal and de Vries (1976) on Nagpal and de Vries' site.

An error in calibration may affect the slopes of the main limbs of rise, the lags of the main limbs of rise and the steady state values used for the water balance. It would have no effect on the time to steady state.

5. Drift in tipping bucket calibration occurred during the experiments. Although some drift occurred during the main limbs of rise, the tipping bucket did not fill to the rim during this period hence the error was less than 30%. Following a reasoning similar to the one made under point 4, one can reach the conclusion that the straight line rise for Ex1 and Ex2 is real. Error due to drifting may affect the lags and slopes of the main limbs of rise. It may also have reduced the

outflow rate of the initial steps although drift at this stage is rather unlikely.

6. Inconsistency between irrigation rate, steady state water table height, and steady state outflow rate was observed: the irrigation rate for Ex1 and Ex2 is higher than for Ex3, yet steady state outflow rates and steady state heights of the water table are lower for Ex1 than for Ex2 and Ex3.

However, here also, it can be concluded that the straight line main limbs of rise must be real because it is unlikely that errors yield three straight line limbs of rise by chance.

7. The tipping bucket had been prefilled with one liter for Ex3. There is doubt whether it was also prefilled for Ex1 and Ex2. This error does not affect the detailed hydrographs because it does not affect the outflow rate after the first tip. It does not affect the other outflow hydrographs either.

8. For the detailed plot, outflow rates have been plotted in the middle of the interval of the tips they correspond to, which is not quite accurate. This however cannot be the cause for the lack of initial step observed for Ex2. For both Ex1 and Ex3 there are several points before the first point of Ex2, thus the delay of the early part of the rise of Ex2 cannot come from the way the points are plotted.

9. Natural rainfall occurred now and then.

No antecedent outflow was observed before Ex1 and no rain was observed on the site during this experiment. Therefore the results of this experiment are free from the influence of natural rainfall.

No rainfall was recorded at the meterological station between Ex1

and Ex2. No rainfall was recorded on the site for at least 16 hours before the start of irrigation for Ex2. No rainfall was observed during the main limb of rise of this experiment. Therefore, if rain occurred between Ex1 and Ex2, its effect would be included in the negligible antecedent outflow.

Rainfall was observed on the site between Ex2 and Ex3. However, no rainfall was observed on the Forest plot for at least 21 hours before the start of irrigation until most of the main limb of rise has occurred for Ex3. It is therefore likely that the only effect of the rainfall that occurred prior to Ex3 is included in the very small outflow of 1.5 x 10^{-7} m^3 s^{-1} noted 9 hours before the start of irrigation.

It can therefore be concluded that natural rainfall on the plot has no influence on the shape and slope of the main limbs of rise for the three experiments. It is assumed that it did not have any influence on the early parts of the rises. Even if it did, it would decrease the proportion of outflow due to irrigation during the initial steps and hence make the statement that the system behaves as if recharge were a uniform step function even stronger.

As mentioned in Section 1.3.7, it is assumed that no subsurface flow reached the plot from uphill. Steady state outflow values may have been influenced by natural rainfall falling on the plot. This natural rainfall does not affect the water balance, though, since it is included in the irrigation rate. Similarity between the small scale recessions (Figs. 1.4.2.3 to 1.4.2.5) for the three experiments indicates that they were not influenced by natural rainfall.

APPENDIX F

CALCULATION OF AVERAGE STEADY STATE OUTFLOW RATES

Average steady state outflow rates have been calculated as

$$\frac{\Sigma x_i}{N}$$

where x_i = a data point within the steady state period on the outflow hydrograph

N = number of data points used.

APPENDIX G

DEFINITION OF POROSITIES

Because the effective or air filled porosity is used extensively in Chapter II, it is designated by n in order to simplify the notation. The porosity will be designated by n_a.

Thus (Hillel, 1971)

$$n_a = \frac{V_a + V_w}{V_t}$$

$$n = \frac{V_a}{V_t}$$

where V_a = volume of air

V_w = volume of water

V_t = bulk volume of soil

APPENDIX H

CALCULATIONS FOR USE IN CHAPTER II

Note 1 Solution of the Kinematic Wave Equation by the Method of Characteristics

Eq. 2.3.6 can be rewritten as

$$\frac{d(nT)}{dt} = i \qquad \text{H-1.1}$$

The definition of a total differential like the one given in Eq. H-1.1 means that this equation can be considered to describe the rate of change of nT with respect to t as seen by a wave or observer moving at a velocity

$$c = \frac{dx}{dt}$$

Wave or "observer" motion will now be used to solve Eq. (2.3.6) by the method of characteristics (e.g. Eagleson, 1970).

Figure H-1.1 (a) shows the plots of x versus t for observers. The plot of x versus t for one observer is called a characteristic.

Figure H-1.1(a) and H-1.1(b) are based on figures given by Eagleson for a more general case.

The following discussion and derivation of the thickness T of the saturated zone is adapted from the discussion for overland flow found in Eagleson (1970). Some of the results are found in Beven (1981). Eagleson himself followed Henderson and Wooding's (1964) and Wooding's

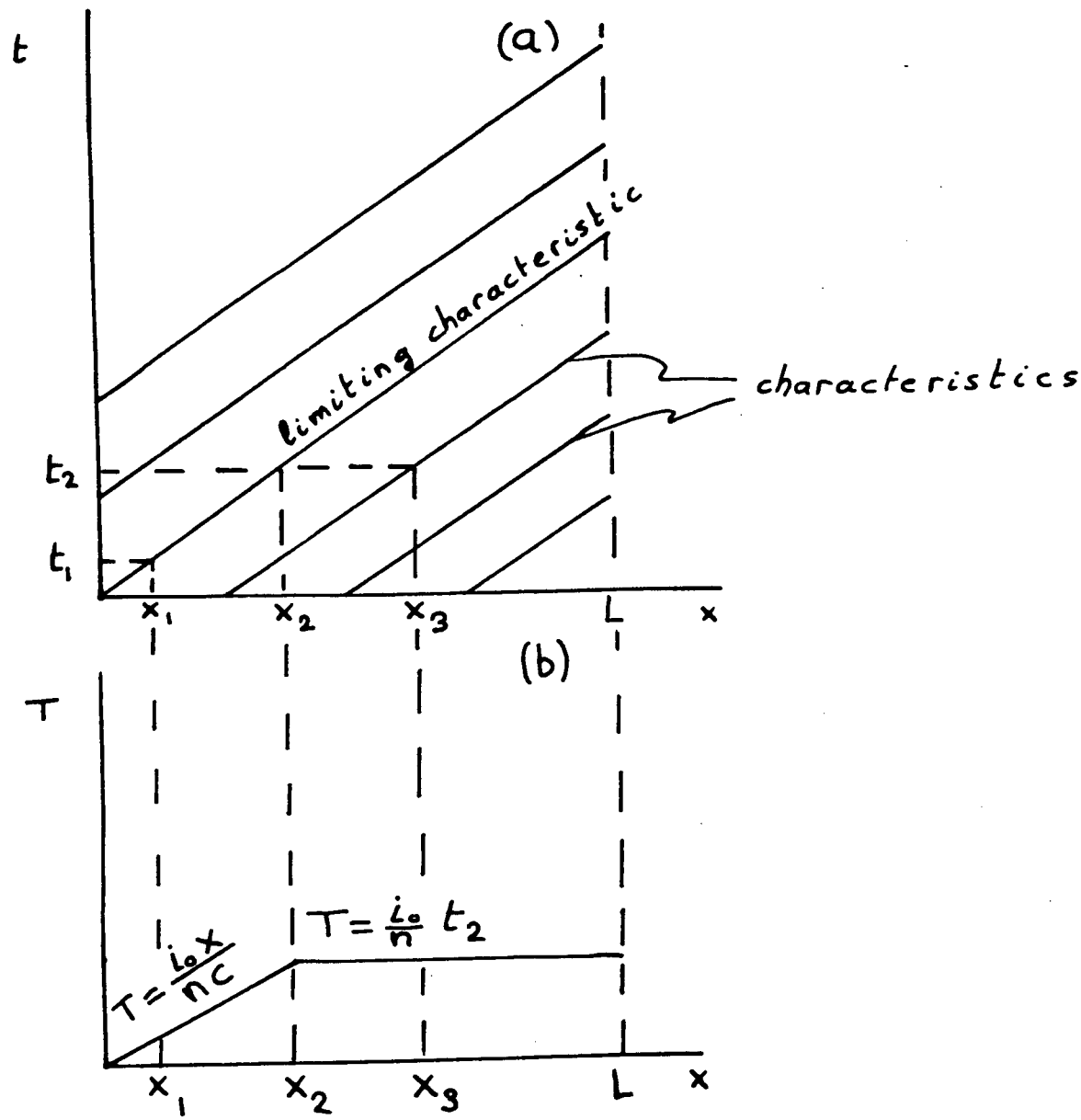

Fig. H-1.1 (a) Characteristics. (b) Water table profile at time t_2.

(1965a, b, 1966) analysis which according to Eagleson is a simplification of the methods of Lighthill and Whitham (1955) and Iwagaki (1955). The recharge rate i is equal to i_o during rise and steady state; it is zero for the recession.

(i) Rise and Steady State

If i_o is steady and uniform, Eq. H-1.1 can be integrated to yield

$$T(t^*) - T_o = \frac{i_o}{n} (t^* - t_o) \qquad \text{H-1.2}$$

where

t^* = time from the start of recharge

t_o = time at which the observer left from x_o (measured from the start of recharge)

T_o = saturated zone thickness seen by the observer at x_o and t_o.

Observers travel on the characteristics shown in Fig. H-1.1 (a) at a velocity

$$c = \frac{x - x_o}{t^* - t_o} \qquad \text{H-1.3}$$

Having K and n steady and uniform with respect to x and z renders c steady and uniform with respect to x and z.

The boundary condition $T_o = 0$ at $x = 0$ is assumed. Therefore observers leaving from $x_o = 0$ observe a saturated zone thickness $T_o = 0$ at $t^* = t_o$ and for this case, Eq. H-1.2 yields

$$T(t^*) = \frac{i_o}{n} (t^* - t_o) \qquad \text{H-1.4}$$

For the observers leaving from $x_o = 0$ at $t_o = 0$, that is, for observers travelling on the limiting characteristic,

$$T(t^*) = \frac{i_o}{n} t^* \qquad \text{H-1.5}$$

For observers leaving from $x_o = 0$ at $t_o > 0$ (Beven, 1981)

$$T(t^*) = \frac{i_o}{n} (t^* - t_o) = \frac{i_o}{n} \frac{x}{c} \qquad \text{H-1.6}$$

Thus, once the observer travelling on the limiting characteristic has reached a point x, T at this point is constant since n and c are steady, and it is given by Eq. H-1.6.

For observers leaving at $t_o = 0$ from $x_o > 0$, Eq. H-1.2 becomes (Beven, 1981)

$$T(t^*) = \frac{i_o}{n} t^* \qquad \text{H-1.7}$$

This means that, at time t*, all the observers having left at time $t_o = 0$ from a point further downhill than $x = 0$ and hence having reached a point further downhill than the observer on the limiting characteristic, see the same height of water. In other words, the water table rises parallel to the bed. Eq. H-1.7 is valid for $t^* \leq \frac{L}{c}$.

These results are depicted in Fig. H-1.1 (b). In this Fig., which shows the shape of the water table at time t_2, the observer travelling on the limiting characteristic is at x_2. Steady state has thus been reached by all points for which $x < x_2$. In particular, point x_1 reached steady state at t_1, as can be seen from Fig. H-1.1 (a). The water table height at points for which $x < x_2$ is given by Eq. H-1.6.

Fig. H-1.1 (b) shows that the water table height is the same for all the points for which $x > x_2$, in particular for x_3. For these points, the water table height at time t_2 is given by Eq. H-1.7 with $t^* = t_2$.

The discharge Q (volume/time) for a hillslope of saturated zone thickness T and width D is

$$Q = qTD \qquad \text{H-1.8}$$

Combining Eqs. 2.3.2, H-1.5 and H-1.8 yields

$$Q(t^*) = K\sin\omega\, D\frac{i_o}{n}\, t^* \qquad \text{H-1.9a}$$

at the foot of the hillslope during the rise.

The discharge is thus linear with respect to time during the rise.

When the whole hillslope has reached steady state, letting $x = L$ in Eq. H-1.6, and using Eqs. 2.3.2 and H-1.8 yields

$$Q = K\sin\omega\, D\,\frac{i_o}{n}\,\frac{L}{c} = D\, i_o\, L \qquad \text{H-1.9b}$$

where L is the length of the hillsope.

Henderson and Wooding indeed obtain $Q = D\, i_o\, L$ for overland flow. Eqs. H-1.9a and H-1.9b can be derived from equations found in Beven (1981). The hydrograph rise and steady state are also depicted in Beven's paper.

(ii) Recession

For the recession, $i = 0$ hence from Eq. H-1.1, $dT/dt = 0$ (Henderson and Wooding, 1964). It will be assumed that the recharge stops at $t = t_r$. Also, the time duration t' after recharge stopped is defined by

$$t^* - t_r = t'$$

It is also assumed that n during the recession is the same as during the rise. In Note 4, the equation with an effective porosity n_{re} during the recession is obtained.

Because $\frac{dT}{dt} = 0$, an observer leaving x_o when irrigation just stops and travelling at $c = dx/dt$ will observe a constant water depth $i_o x_o/(nc)$ from x_o to L.

This means that at a point x and at a time $t' \leq \frac{x}{c}$ after the recharge stopped,

$$T(x,\ t_r + t') = \frac{i_o x_o}{nc} \qquad \text{H-1.10}$$

where here x_o is found from

$$x - x_o = ct'$$

(The reason why t' must be $\leq \frac{x}{c}$ is that when $t' > \frac{x}{c}$, $ct' > x$ and letting $x_o = x - ct'$ in Eq. H-1.10 would yield a negative T. Physically, the observer having started from $x_o = 0$ at $t' = 0$ would have reached x and thus $T(x, t_r + t')$ would be zero). Thus, at time $t_r + t'$,

$$T(x, t_r + t') = \frac{i_o(x - ct')}{nc} = \frac{i_o x}{K\sin\omega} - \frac{i_o t'}{n} \qquad \text{H-1.11}$$

$$\text{At} \quad x = L, \; T(t_r + t') = \frac{i_o L}{K\sin\omega} - \frac{i_o t'}{n} \qquad \text{H-1.12}$$

At a time t' after recession started, all observers will be a distance ct' further downslope and as explained above, they will still see the same T as when they left. Therefore during the recession, the water table slides parallel to itself down the bed.

Using Eqs. 2.3.2, H-1.8 and H-1.12, the discharge during the recession is

$$Q(t_r + t') = i_o LD - K\sin\omega \frac{i_o D}{n} t'$$

Note 2 Problems Linked to the Evaluation of n

Estimating the effective porosity n for Eq. 2.4.1 is subject to the following problems:

(a) The water content $\theta_{in\ s.z.}$ observed in the soil just before the water table rises in it is larger than θ_{in} but may be slightly smaller than $\theta_{st.st}$. To overcome this difficulty, two estimates of n have been calculated: a maximum, obtained by using the minimum θ_{in} and a minimum, similarly obtained by using the maximum $\theta_{st.st}$.

(b) The kinematic wave model assumes that at the water table the water content increases abruptly by n whereas in reality there must be some transition zone in which the water content reaches satiation gradually. It is not clear what the effect of this transition zone is.

(c) Neutron probe data can be used to obtain the maximum unsaturated θ since all the water contents detected by the neutron probe were lower than saturated. However, the water content obtained by the neutron probe at the deepest levels (more specifically at the 110 cm depth for the upper neutron probe access tube, and at the 63 cm and 50 cm depth levels for the lower neutron probe access tube) is subject to the following errors:

First, the neutron probe does not detect soil water content at a point but an average content over a region with a 15 cm radius. Thus the water content read at the deepest levels may be too high if the access tube rests on till and if the probe detects the water retained in the till. In the case the probe did not reach the bed, the water content obtained at the deepest levels may still be too high if the probe detected a saturated zone or a transition zone above the bed.

Second, because the access tube may not have reached the bed, the reading on the neutron probe when it was in its lowest position may not correspond to the moisture content at the bottom of the B horizon. In particular the reading may be too low.

These errors may in particular affect the maximum water content used to calculate the smallest K_{eff} (at the 63 cm depth level of the lower neutron probe access tube).

Note 3 Taking the Water Balance Into account When Calculating K_{eff}

In general, the recharge rate will not be known and will have to be obtained from the rainfall rate. Since it is likely that some water is lost, the water balance must be used to obtain the recharge rate that would have yielded the observed outflow rate, had no loss taken place.

From the water balance (Chapter I, Section 1.4.6), the measured outflow rate is about 80% of the time average pooled irrigation rate. Thus the recharge rate per unit area parallel to the bed (i_o) is equal to 0.80 times the irrigation rate per unit area parallel to the bed.

Note 4 Recession with an Effective Porosity n_{re}

In Eq. 2.3.11, it was assumed that n during the recession was the same as during the rise. Q during the recession will now be derived assuming n during the recession is n_{re}, where n_{re} is equal to the porosity minus the residual water content and is assumed constant.

For the recession, Eq. 2.3.3 yields

$$n_{re} \frac{\partial T}{\partial t} + \frac{\partial (qT)}{\partial x} = 0$$

The wave velocity during the recession, c_{re} is defined by

$$c_{re} = \frac{K \sin\omega}{n_{re}} .$$

As shown in Note 1, during the recession, an observer having left x_o at $t' = 0$ and travelling downhill observes a constant height of saturated zone

$$T = \frac{i_o \, x_o}{n_{ri} \, c_{ri}}$$

where n_{ri} = effective porosity during the rise.

c_{ri} = wave velocity during the rise

$$c_{ri} = \frac{K \sin\omega}{n_{ri}} .$$

Therefore, at time $t' = \frac{x - x_o}{c_{re}}$ the height of water at x is $\frac{i_o \, x_o}{n_{ri} \, c_{ri}}$

Since $c_{re} = \frac{x - x_o}{t'}$

$$T(x, t') = \frac{i_o(x - t' \, c_{re})}{n_{ri} \, c_{ri}}$$

$$= \frac{i_o x}{K \sin\omega} - \frac{i_o t'}{n_{re}} .$$

Hence, during the recession, $Q = i_o \, LD - K \sin\omega \, D \frac{i_o \, t'}{n_{re}}$.

APPENDIX I

CALCULATIONS FOR USE IN CHAPTER III

Note 1: Calculation of $\frac{d\log f}{d\log Re}$ at q_{cr} by Eq. 3.3.15 using data obtained by de Vries (1975, 1979)

Because de Vries (1979) uses a notation slightly different from the one used here, it is necessary to express the variables used here in terms of the ones he used.

The equation used by de Vries for the nonlinear range is

$$\rho g \frac{dh}{ds} = a_d \mu q + e a_d^{1/2} \rho q^2 \qquad (I-1)$$

where

g = gravitational acceleration

μ = dynamic viscosity of the fluid

ρ = fluid density

a_d and e: constants determined by the properties of the porous medium and of the fluid (or possibly of the porous medium only).

Rewriting the corresponding equation for the present work, Eq. 3.3.2, in terms of $\rho g \frac{dh}{ds}$ yields

$$\rho g \frac{dh}{ds} = \mu \alpha_{nonlin} g q + \rho g \beta_o q^2 \qquad I-2$$

Comparison of Eq. I-1 with Eq. I-2 shows that

$$\alpha_{nonlin} = \frac{a_d}{g}$$

$$\beta_o = \frac{e\, a_d^{\frac{1}{2}}}{g}$$

$$\text{Hence} \quad \frac{\beta_o}{\alpha_{nonlin}} = \frac{\frac{e\, a_d^{1/2}}{g}}{\frac{a_d}{g}} = \frac{e}{a_d^{1/2}}$$

Table I-1 shows the calculation of

$$\frac{d\log f}{d\log Re}\bigg|_{q_{cr}} = \frac{-1}{1 + \frac{e}{\sqrt{a_d}}\frac{q_{cr}}{\nu}} \qquad \text{(I-3)}$$

using the values obtained by de Vries (1975, 1979) for 0.4 - 0.6 mm sand and 0.8 - 1.4 mm sand.

Table I-1. Calculation of $\frac{d\log f}{d\log R_e}$ from Eq. I-3 for de Vries' (1975, 1979) results.

Material	a_d (m^{-2})	e	q_{cr}(m/s)	$\nu(\frac{m^2}{s})$	$\frac{e\, q_{cr}}{\sqrt{a_d}\, \nu}$	$\frac{d\log f}{d\log Re}\Big\|_{q_{cr}}$
0.4-0.6 mm sand	9.2×10^9	0.9	3.0×10^{-3}	0.96×10^{-6}	0.029	-0.97
0.8-1.4 mm sand	1.7×10^9	0.9	3.4×10^{-3}	0.98×10^{-6}	0.076	-0.93

Note 2: Correction of q_c to take the temperature difference into account.

If 2 Reynolds numbers Re_1 and Re_2 are equal, then

$$\frac{q_1 \, L_{ch1} \, \rho_1}{\mu_1} = \frac{q_2 \, L_{ch2} \, \rho_2}{\mu_2}$$

where q has been used as characteristic velocity.

Subscript 1 will refer to de Vries' runs in 0.4 to 0.6 mm sand at 22°C. Subscript 2 will refer to the experimental flow conditions in the Forest plot presented in Table 3.4.1 (vertical infiltration and q at 2 outflow points along the channel's bank). As mentioned in Section 3.4, a temperature of 5°C will be used for the Forest and it will be assumed that $L_{ch1} = L_{ch2}$.

Also, the change in ρ is negligible for the temperatures considered.

For 5°C, $\mu = 1.5 \times 10^{-3}$ kgs^{-1}m^{-1}. The μ given by de Vries (1975) is about 0.96×10^{-3} kgs^{-1}m^{-1}. Thus $\frac{q_1}{q_2} = \frac{\mu_1}{\mu_2} = \frac{0.96}{1.5}$. q_1 is q_{ch} found by de Vries and is equal to 3×10^{-3} ms^{-1}. Hence

$$q_2 = 3 \times 10^{-3} \times \frac{1.5}{0.96} \text{ ms}^{-1}$$

$$q_2 = 4.7 \times 10^{-3} \text{ ms}^{-1}.$$

APPENDIX J

REFERENCES FOR THE APPENDICES

Beven, K. 1981. Kinematic subsurface stormflow. Water resources research, Vol. 17, No. 5: 1419-1424.

de Vries, J. 1975. Unpublished data.

de Vries, J. 1979. Prediction of non-Darcy flow in porous media. American Society of Civil Engineers, Journal of the irrigation and drainage division, Vol. 105, No. IR2, Proc. Paper 14610: 147-162.

Eagleson, P.S. 1970. Dynamic Hydrology. McGraw-Hill.

Henderson, F.M. and R.A. Wooding. 1964. Overland flow and groundwater flow from a steady rainfall of finite duration. Journal of geophysical research, Vol. 69, No. 8: 1531-1540.

Hillel, D. 1971. Soil and water: physical principles and processes. Academic Press. New York, 288 pp.

Hewlett, J.D. and A.R. Hibbert. 1963. Moisture and energy conditions within a sloping soil mass during drainage. Jour. of geophysical research, Vol. 68, No. 4: 1081-1087.

Iwagaki, Y. 1955. Fundamental studies on the runoff analysis by characteristics, Disaster Prevent. Res. Inst., Bull. 10, Kyoto University. Cited by Eagleson.

Lighthill, M.H. and G.B. Whitham. 1955. On kinematic waves. I. Flood movement in long rivers. Proc. Roy. Soc., Ser. A, Vol. 229: 281-316. Cited by Eagleson.

Mehra, O.P. and M.L. Jackson. 1960. Iron oxide removal from soils and clays by a dithionite-citrate system buffered with sodium bicarbonate. Clays and clay minerals. Vol. 5: 317-325. International series of monographs on earth science, Pergamon Press.

Nagpal, N.K. and J. de Vries. 1976. On the mechanism of water flow through a forested mountain slope soil in coastal western Canada. Unpublished material.

Utting, M.G. 1978. The generation of stormflow on a glaciated hillslope in coastal British Columbia. M.Sc. Thesis, University of British Columbia, Vancouver.

Wooding, R.A. 1965a. A hydraulic model for the catchment stream problem. I. Kinematic-wave theory. Jour. of hydrology, Vol. 3: 254-267. Cited by Eagleson.

Wooding, R.A. 1965b. A hydraulic model for the catchment-stream problem. II. Numerical solutions. Jour. of hydrology, Vol. 3: 268-282. Cited by Eagleson.

Wooding, R.A. 1966. A hydraulic model for the catchment-stream problem. III. Comparison with runoff observations. Jour. of hydrology, Vol. 4: 21-37. Cited by Eagleson.